ISSN 1949-8462 (online)

World Journal of *Cardiology*

World J Cardiol 2016 September 26; 8(9): 496-558

Published by Baishideng Publishing Group Inc

World Journal of Cardiology

A peer-reviewed, online, open-access journal of Cardiology

Editorial Board

2014-2017

The *World Journal of Cardiology* Editorial Board consists of 416 members, representing a team of worldwide experts in cardiology. They are from 46 countries, including Argentina (3), Australia (7), Austria (6), Belgium (2), Brazil (8), Canada (11), China (37), Croatia (1), Cuba (1), Cyprus (1), Czech Repoublic (2), Denmark (3), Egypt (1), Finland (3), France (3), Germany (32), Greece (10), Hungary (5), India (4), Iran (2), Ireland (1), Israel (5), Italy (63), Japan (32), Kosovo (1), Malaysia (1), Mexico (1), Morocco (1), Netherlands (9), New Zealand (1), Nigeria (2), Norway (2), Poland (8), Portugal (2), Saudi Arabia (2), Singapore (3), Slovenia (1), South Korea (9), Spain (14), Switzerland (3), Thailand (3), Turkey (13), United Arab Emirates (1), United Kingdom (20), United States (73), Uruguay (2), and Venezuela (1).

Jiu-Chang Zhong, *Shanghai*

Croatia

Viktor Culic, *Split*

Cuba

Fidel M Caceres-Loriga, *Havana*

Cyprus

Christos Eftychiou, *Nicosia*

Czech Repoublic

Pavel Osmancik, *Prague*
Jan Sochman, *Prague*

Denmark

Louise L Schierbeck, *Copenhagen NV*
Jacob Tfelt-Hansen, *Copenhagen*
Bo G Winkel, *Copenhagen*

Egypt

Mohamed E Fawzy, *Cairo*

Finland

Fausto Biancari, *Oulu*
Kjell Nikus, *Tampere*
Jani T Tikkanen, *Oulu*

France

Dominique Charron, *Paris*
Joao C Das-Neves-Pereira, *Paris*
Guillaume Leurent, *Rennes*

Germany

Helmut Acker, *Essen*
Ralf A Benndorf, *Halle* (Saale)
Niyazi Cebi, *Stade*
Emmanuel Chorianopoulos, *Heidelberg*
Ulrich H Frey, *Essen*
Alexander Ghanem, *Bonn*
Michael Gotzmann, *Bochum*
Takahiro Higuchi, *Würzburg*
Thomas W Jax, *Neuss*
Christoph J Jensen, *Essen*
Beate E Kehrel, *Muenster*
Klaus Kettering, *Frankfurt*
Korff Krause, *Hamburg*
Arnt V Kristen, *Heidelberg*
Philipp C Lurz, *Leipzig*
Thomas Muenzel, *Mainz*
Ulrich Nellessen, *Stendal*
Peter E Ong, *Stuttgart*
Guenter Pilz, *Hausham*
Tienush Rassaf, *Düsseldorf*
Bernhard Rauch, *Ludwigshafen am Rhein*
Sonja Schrepfer, *Hamburg*
Andreas Schuster, *Goettingen*
Guiscard Seebohm, *Muenster*
Hans-Jürgen Seyfarth, *Leipzig*
Erik Skobel, *Aachen*
Dirk Skowasch, *Bonn*
Gustav Steinhoff, *Rostock*
Michael Steinmetz, *Goettingen*
Theodor Tirilomis, *Goettingen*
Rainer Wessely, *Cologne*

Greece

Dimitrios Farmakis, *Athens*
Ignatios Ikonomidis, *Athens*
Theofilos M Kolettis, *Ioannina*
Antigone Lazou, *Thessaloniki*
Konstantinos Letsas, *Athens*
Kosmas I Paraskevas, *Larissa*
Elias Rentoukas, *Athens*
Georgios Tagarakis, *Thessaloniki*
Theodoros Xanthos, *Athens*
Michael Zairis, *Piraeus*

Hungary

Gergely Feher, *Pecs*
András Komócsi, *Pécs*
Béla Merkely, *Budapest*
Attila Nemes, *Szeged*
Albert Varga, *Szeged*

India

Amitesh Aggarwal, *Delhi*
Debasis Das, *Kolkata*
Yatin Mehta, *Gurgaon*
Nikhil Sikri, *Bangalore*

Iran

Farid Najafi, *Kermanshah*
Mahdi Najafi, *Tehran*

Ireland

Timothy M McGloughlin, *Abu Dhabi*

Israel

Robert Dragu, *Haifa*
Ehud Goldhammer, *Haifa*
Aviv Mager, *Petah Tikva*
David Rott, *Tel Hashomer*

Italy

Romualdo Belardinelli, *Ancona*
Matteo Bertini, *Ferrara*
Riccardo Bigi, *Milan*
Carlo Bonanno, *Vicenza*
Giuseppe Boriani, *Bologna*
Natale D Brunetti, *Foggia*
Giuseppe Bruschi, *Milan*
Alida LP Caforio, *Padova*
Corrado Carbucicchio, *Milan*
Oronzo Catalano, *Pavia*
Massimo Chello, *Rome*
Quirino Ciampi, *Benevento*
Antonio Cittadini, *Naples*
Anca I Corciu, *Pisa*
Michele Correale, *Foggia*
Michele D'Alto, *Naples*
Fabrizio D'Ascenzo, *Turin*
Giuseppe De Luca, *Novara*
Roberto De Ponti, *Varese*
Fabio Esposito, *Milan*
Pompilio Faggiano, *Brescia*
Khalil Fattouch, *Palermo*
Amalia Forte, *Naples*
Chiara Fraccaro, *Rovigo*
Mario Gaudino, *Rome*
Sandro Gelsomino, *Florence*
Massimo Iacoviello, *Bari*
Massimo Imbriaco, *Napoli*
Ciro Indolfi, *Catanzaro*
Maurizio E Landolina, *Pavia*
Chiara Lazzeri, *Florence*
Jacopo M Legramante, *Rome*
Antonio Loforte, *Bologna*
Rosalinda Madonna, *Chieti*
Olivia Manfrini, *Bologna*
Giancarlo Marenzi, *Milan*
Raffaele Marfella, *Naples*
Giovanni Mariscalco, *Varese*
Franca Di Meglio, *Naples*
Pietro A Modesti, *Florence*
Massimo Napodano, *Padua*
Daria Nurzynska, *Naples*
Claudio Passino, *Pisa*
Salvatore Patanè, *Taormina*
Francesco Perticone, *Catanzaro*
Nunzia R Petix, *Empoli*
Francesco Petrella, *Milan*
Mario Petretta, *Naples*
Carmine Pizzi, *Bologna*
Marco Pocar, *Milan*
Roberto Pola, *Rome*
Francesco Prati, *Rome*
Fabio M Pulcinelli, *Rome*
Andrea Rossi, *Verona*
Andrea Rubboli, *Bologna*
Giovanni Di Salvo, *Naples*
Giuseppe M Sangiorgi, *Rome*
Carlo Setacci, *Siena*
Imad Sheiban, *Verona*
Giuseppe Stabile, *Napoli*
Luca Testa, *Milan*

Japan

Eisuke Amiya, *Tokyo*
Ryuichiro Anan, *Miyakonojo*
Xian Wu Cheng, *Nagoya*
Ikuo Fukuda, *Aomori*
Shin-ichiro Hayashi, *Suita*
Atsushi Hirohata, *Okayama*
Toru Hosoda, *Isehara*
Kazuhiro P Izawa, *Kawasaki*
Takatoshi Kasai, *Tokyo*
Hajime Kataoka, *Oita*
Masaya Kato, *Hiroshima*
Tomoko S Kato, *Tokyo*

Atsuhiko Kawamoto, *Kobe*
Zhong-Fang Lai, *Kumamoto*
Seiichiro Matsuo, *Tokyo*
Shin-ichiro Miura, *Fukuoka*
Sachio Morimoto, *Fukuoka*
Toshiya Muramatsu, *Yokohama*
Koichi Sakabe, *Tokyo*
Hiroyuki Sakurai, *Chuo-ku*
Akira Sato, *Tsukuba*
Shinji Satoh, *Fukuoka*
Hiroshi Satoh, *Hamamatsu*
Akira Sugawara, *Sendai*
Isao Taguchi, *Tochigi*
Masamichi Takano, *Inzai*
Hiroki Teragawa, *Hiroshima*
Hiroyasu Ueda, *Osaka*
Tadayuki Uetani, *Nagoya*
Sho-ichi Yamagishi, *Kurume*
Hideya Yamamoto, *Hiroshima*
Hiroshi Yoshida, *Kashiwa*

Kosovo

Gani Bajraktari, *Prishtina*

Malaysia

Harris A Ngow, *Kuantan*

Mexico

Erick Alexanderson, *Mexico City*

Morocco

Abdenasser Drighil, *Casablanca*

Netherlands

Pierfrancesco Agostoni, *Utrecht*
Christos V Bourantas, *Rotterdam*
Jasper J Brugts, *Rotterdam*
Filippo Cademartiri, *Rotterdam*
Henricus J Duckers, *Utrecht*
Guido Krenning, *Groningen*
Frans L Moll, *Utrecht*
Martijn C Post, *Nieuwegein*
Salah AM Said, *Hengelo*

New Zealand

Barry Palmer, *Christchurch*

Nigeria

Rufus A Adedoyin, *Ile-Ife*
Okechukwu S Ogah, *Ibadan*

Norway

Jonas Hallen, *Oslo*
Serena Tonstad, *Oslo*

Poland

Maciej Banach, *Lodz*
Iwona Cicha, *Erlangen*
Grzegorz Gajos, *Krakow*
Piotr Jankowski, *Kraków*
Maciej K Kurpisz, *Poznan*
Katarzyna M Mizia-Stec, *Katowice*
Jerzy Sacha, *Opole*
Sebastian Szmit, *Warsaw*

Portugal

Rui A Providência, *Coimbra*
Fernando Ribeiro, *Aveiro*

Saudi Arabia

T Albacker, *Riyadh*
Mouaz H Al-Mallah, *Riyadh*

Singapore

Koon-Hou Mak, *Singapore*
Kian Keong Poh, *Singapore*
Samuel SW Tay, *Singapore*

Slovenia

Mitja Lainscak, *Golnik*

South Korea

Kyung-Mook Choi, *Seoul*
Young-Hoon Jeong, *Jinju-si*
Hyo-Soo Kim, *Seoul*
Cheorl-Ho Kim, *Suwon*
Seong Hwan Kim, *Ansan*
Young-Guk Ko, *Seoul*
Gi-Byoung Nam, *Seoul*
Jong-Min Song, *Seoul*
Darren R Williams, *Gwangju*

Spain

Ezequiel Alvarez, *Santiago de Compostela*
Miguel A Arias, *Toledo*
Alberto B Berenguer, *Valencia*
Alberto Dominguez-Rodriguez, *Tenerife*
Julio J Ferrer-Hita, *La Laguna*
Joaquin De Haro, *Madrid*
Raul Moreno, *Madrid*
Ivan J Nunez-Gil, *Madrid*
Jesus Millan Nuuez-Cortes, *Madrid*
Jesus Peteiro, *A Coruna*
Aurelio Quesada, *Valencia*
Manel Sabate, *Barcelona*
Rocio Toro, *Cadiz*
Jose M Valdivielso, *Lleida*

Switzerland

Paul Erne, *Zurich*
Richard Kobza, *Luzern*

Thailand

Nipon Chattipakorn, *Chiang Mai*
Rungroj Krittayaphong, *Bangkok*
Yaowapa Maneerat, *Bangkok*

Turkey

Bahri Akdeniz, *Izmir*
Ismail Biyik, *Usak*
Murat Can, *Zonguldak*
Turgay Celik, *Ankara*
Yengi U Celikyurt, *Kocaeli*
Omer F Dogan, *Adana*
Dursun Duman, *Istanbul*
Nihan Erdogan, *Istanbul*
Tevfik F Ilgenli, *Konya*
Fehmi Kacmaz, *Sanliurfa*
Kaan Kirali, *Istanbul*
Mehmet Ozaydin, *Isparta*
Murat Ozeren, *Mersin*

United Arab Emirates

Nicolas Christoforou, *Abu Dhabi*

United Kingdom

Suneil K Aggarwal, *London*
Abdallah Al-Mohammad, *Sheffield*
Umberto Benedetto, *Papworth*
Christopher J Boos, *Poole*
Geoffrey Burnstock, *London*
Halina Dobrzynski, *Manchester*
Lyndon M Evans, *Cardiff*
Matthew Ginks, *Oxford*
Cathy M Holt, *Manchester*
Jamie Y Jeremy, *Bristol*
Muhammed Z Khawaja, *London*
Babu Kunadian, *Liverpool*
Najma Latif, *Harefield*
Saagar Mahida, *leeds*
Mamas Mamas, *Manchester*
Pankaj K Mishra, *Wolverhampton*
Shahzad G Raja, *London*
Sudhir Rathore, *Camberley*
Ganesh N Shivu, *Ravenshead*
Neil A Turner, *Leeds*

United States

Ola Akinboboye, *New York*
Arshad Ali, *North Platte*
Piero Anversa, *Boston*
Ehrin J Armstrong, *Denver*
Wilbert S Aronow, *Valhalla*
Basem Azab, *Staten Island*
Alison E Baird, *Brooklyn*

WJC World Journal of Cardiology

Contents

Monthly Volume 8 Number 9 September 26, 2016

DIAGNOSTIC ADVANCES

REVIEW

ORIGINAL ARTICLE

Retrospective Study

Observational Study

World Journal of Cardiology
Volume 8 Number 9 September 26, 2016

Contents

NAME OF JOURNAL
World Journal of Cardiology

ISSN
ISSN 1949-8462 (online)

LAUNCH DATE
December 31, 2009

FREQUENCY
Monthly

EDITORIAL OFFICE
Xiu-Xia Song, Director
Fang-Fang Ji, Vice Director
World Journal of Cardiology
Baishideng Publishing Group Inc
8226 Regency Drive, Pleasanton, CA 94588, USA
Telephone: +1-925-2238242
Fax: +1-925-2238243
E-mail: editorialoffice@wjgnet.com
Help Desk: http://www.wjgnet.com/esps/helpdesk.aspx
http://www.wjgnet.com

PUBLISHER
Baishideng Publishing Group Inc
8226 Regency Drive,
Pleasanton, CA 94588, USA
Telephone: +1-925-2238242
Fax: +1-925-2238243
E-mail: bpgoffice@wjgnet.com
Help Desk: http://www.wjgnet.com/esps/helpdesk.aspx
http://www.wjgnet.com

PUBLICATION DATE
September 26, 2016

INSTRUCTIONS TO AUTHORS
http://www.wjgnet.com/bpg/gerinfo/204

ONLINE SUBMISSION
http://www.wjgnet.com/esps/

World Journal of Cardiology

Submit a Manuscript: http://www.wjgnet.com/esps/
Help Desk: http://www.wjgnet.com/esps/helpdesk.aspx
DOI: 10.4330/wjc.v8.i9.496

World J Cardiol 2016 September 26; 8(9): 496-503
ISSN 1949-8462 (online)

Intra-cardiac distribution of late gadolinium enhancement in cardiac sarcoidosis and dilated cardiomyopathy

Makoto Sano, Hiroshi Satoh, Kenichiro Suwa, Masao Saotome, Tsuyoshi Urushida, Hideki Katoh, Hideharu Hayashi, Takeji Saitoh

Makoto Sano, Hiroshi Satoh, Kenichiro Suwa, Masao Saotome, Tsuyoshi Urushida, Hideki Katoh, Hideharu Hayashi, Division of Cardiology, Internal Medicine III, Hamamatsu University School of Medicine, Hamamatsu 431-3192, Japan

Takeji Saitoh, Department of Emergency Medicine, Hamamatsu University School of Medicine, Hamamatsu 431-3192, Japan

Author contributions: Sano M, Suwa K and Saitoh T designed and performed the research; Satoh H wrote the manuscript; Saotome M, Urushida T, Katoh H and Hayashi H reviewed the manuscript.

Conflict-of-interest statement: None.

Manuscript source: Invited manuscript

Correspondence to: Hiroshi Satoh, MD, PhD, Division of Cardiology, Internal Medicine III, Hamamatsu University School of Medicine, 1-20-1 Handayama, Higashi-ward, Hamamatsu 431-3192, Japan. satoh36@hama-med.ac.jp
Telephone: +81-53-4352267
Fax: +81-53-4342910

Received: May 23, 2016
Peer-review started: May 23, 2016
First decision: June 17, 2016
Revised: July 12, 2016
Accepted: July 29, 2016
Article in press: August 1, 2016
Published online: September 26, 2016

Abstract

Cardiac involvement of sarcoid lesions is diagnosed by myocardial biopsy which is frequently false-negative, and patients with cardiac sarcoidosis (CS) who have impaired left ventricular (LV) systolic function are sometimes diagnosed with dilated cardiomyopathy (DCM). Late gadolinium enhancement (LE) in magnetic resonance imaging is now a critical finding in diagnosing CS, and the novel Japanese guideline considers myocardial LE to be a major criterion of CS. This article describes the value of LE in patients with CS who have impaired LV systolic function, particularly the diagnostic and clinical significance of LE distribution in comparison with DCM. LE existed at all LV segments and myocardial layers in patients with CS, whereas it was localized predominantly in the midwall of basal to mid septum in those with DCM. Transmural (nodular), circumferential, and subepicardial and subendocardial LE distribution were highly specific in patients with CS, whereas the prevalence of striated midwall LE were high both in patients with CS and with DCM. Since sarcoidosis patients with LE have higher incidences of heart failure symptoms, ventricular tachyarrhythmia and sudden cardiac death, the analyses of extent and distribution of LE are crucial in early diagnosis and therapeutic approach for patients with CS.

Key words: Magnetic resonance imaging; Late gadolinium enhancement; Sarcoidosis; Dilated cardiomyopathy; Diagnosis

Core tip: Late gadolinium enhancement (LE) in magnetic resonance imaging is a critical finding in the diagnosis of cardiac sarcoidosis (CS), but it is also observed in dilated cardiomyopathy (DCM). We review the significance of LE distribution in comparison with DCM. LE distributed into

all ventricular segments and myocardial layers in CS, whereas it was localized predominantly in the midwall of ventricular septum in DCM. Transmural, circumferential, and subepicardial and subendocardial LE were highly specific in CS. Since patients with LE have more adverse cardiac events, the analyses of extent and distribution of LE are crucial for diagnosis and management of CS.

Sano M, Satoh H, Suwa K, Saotome M, Urushida T, Katoh H, Hayashi H, Saitoh T. Intra-cardiac distribution of late gadolinium enhancement in cardiac sarcoidosis and dilated cardiomyopathy. *World J Cardiol* 2016; 8(9): 496-503 Available from: URL: http://www.wjgnet.com/1949-8462/full/v8/i9/496.htm DOI: http://dx.doi.org/10.4330/wjc.v8.i9.496

INTRODUCTION

Sarcoidosis is a multi-organ granulomatous disorder of undetermined aetiology. Cardiac involvement is identified clinically only in few percentage (%) of patients with systemic sarcoidosis, while post-mortem investigations have found myocardial lesions in around 60%[1]. Necropsies exhibited that cardiac involvement was mostly non-transmural and lesions were located predominantly in the basal left ventricle (LV) and subepicardial myocardium[2,3]. Patients with cardiac sarcoidosis (CS) have a poor prognosis due to congestive heart failure with impaired LV function, and sudden cardiac death associated with lethal ventricular tachycardia (VT) or conduction disturbance[4].

Although endomyocardial biopsy has been the gold standard in diagnosing CS, it has limited sensitivity and certain procedural risks[5]. Actually, the results of endomyocardial biopsy were frequently false negative because of the patchy distribution of the lesions. Therefore, patients with cardiac involvement of systemic sarcoidosis (sCS) and with isolated CS (iCS) are not always positive for endomyocardial biopsy. As a result, a certain part of patients may be diagnosed with normal or dilated cardiomyopathy (DCM), and do not receive immunosuppressive therapies. Since a corticosteroid therapy can improve long-term prognosis of CS[6,7], an earlier diagnosis of CS with non-invasive cardiac imaging is clinically significant.

The recent development of various imaging modalities including magnetic resonance imaging (MRI) and 18F-fluorodeoxyglucose-positron emission computed tomography (FDG-PET) has enabled more precise diagnosis of CS. The LV wall in most patients with CS has late gadolinium enhancement (LE) in MRI[5,8-10], and the novel guideline of Japanese Ministry of Health and Welfare (JMH) considers the presence of LE to be a major criterion in CS (Table 1)[11]. However, LE is non-specific and frequently observed in other cardiomyopathies including DCM.

We have been investigating the patterns of LE distribution in various cardiomyopathies and trying to confirm the values for differential diagnosis, clinical features, and prognosis[12-18]. Here we describe the value of LE in patients with CS, particularly the diagnostic and clinical significance of LE distribution in comparison with DCM.

Table 1 Clinical cardiac findings in Diagnostic Standard and Guideline for Sarcoidosis-2015-Japanese Society of Sarcoidosis and Other Granulomatous Disorders

(1) More than two of five major findings are satisfied
(2) One of five major findings and more than two of three minor findings are satisfied
Major findings
Advanced atrioventricular block (including complete atrioventricular block) or sustained ventricular tachycardia
Basal thinning of the interventricular septum or morphological ventricular abnormality (ventricular aneurysm, wall thinning of other ventricular region, wall thickening)
Impaired left ventricular contraction (LVEF < 50%) or regionally abnormal wall motion
Abnormal cardiac uptake in gallium-67 citrate scintigraphy or fluorine-18 fluorodeoxyglucose PET
Late myocardial enhancement in gadolinium enhanced magnetic resonance imaging
Minor findings
Non-sustained ventricular tachycardia, multifocal or frequent premature ventricular contractions, bundle branch block, axis deviation, or abnormal Q wave in electrocardiography
Defect on myocardial perfusion scintigraphy
Endomyocardial biopsy: Interstitial fibrosis or monocyte infiltration over moderate grade

LVEF: Left ventricular ejection fraction; PET: Positron emission tomography.

LE DISTRIBUTION IN CS AND DIFFERENTIAL DIAGNOSIS FROM DCM

Patient characteristics

We initially enrolled 21 patients with CS who had LE in the myocardium between 2003 and 2015. Among them, the intra-cardiac and intra-mural distribution of LE were analyzed in 14 (67%) patients (13 sCS and 1 iCS) who showed reduced LV ejection fraction (LVEF: < 50%). The clinical characteristics and LE features were compared with 30 patients with DCM who were diagnosed by the World Health Organization/International Society and Federation of Cardiology definition of cardiomyopathies[19]. The present study was performed in accordance with the Declaration of Helsinki and the protocol was approved by an institutional review board. All study participants provided informed consent.

Patients with CS included more female patients and were younger, but there were no differences in symptoms, ECG findings and medications excluding corticosteroids (Table 2). Patients with CS had less decreased LVEF and smaller LV end-systolic volume index, while LV end-diastolic volume index and LV mass index did not differ from those in DCM. The LV segment number with LE was also greater in patients with CS. Figure 1 shows LE-MRI images (left) and corresponding

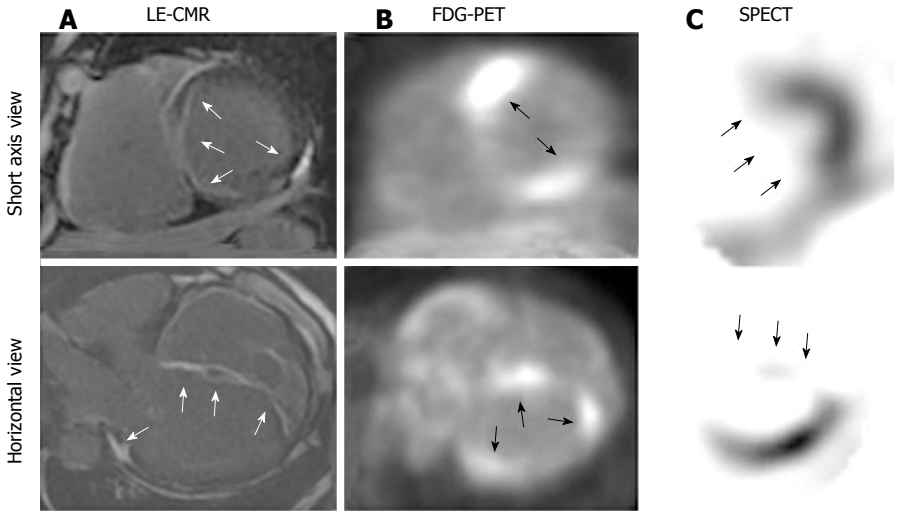

Figure 1 Non-invasive cardiac imaging in a 61-year-old male patient with cardiac involvement of systemic sarcoidosis. LE-CMR (A) shows diffuse LE in the subepicardium (RV side) and subendocardium (LV side) of basal to apical ventricular septum and patchy LE in the midwall of posterior LV (white arrows); Corresponding FDG-PET (B) demonstrates focal uptake in basal and apical ventricular septum and posterior LV wall (black arrows); ^{99m}Tc-sestamibi SPECT (C) exhibits a defect only in ventricular septum (black arrows). CMR: Cardiac magnetic resonance; FDG-PET: ^{18}F-fluorodeoxyglucose-positron emission computed tomography; LE: Late gadolinium enhancement; LV/RV: Left and right ventricles; SPECT: Single photon emission computed tomography.

FDG-PET (middle) and ^{99m}Tc-sestamibi single photon emission computed tomography (SPECT: right) in a 61-year-old patient with sCS. LE-MRI exhibits diffuse LE in the subepicardium (RV side) and subendocardium (LV side) of basal to apical ventricular septum and patchy LE in the midwall of posterior LV (white arrows). FDG-PET demonstrates focal uptake in basal and apical ventricular septum and posterior LV wall (black arrows). ^{99m}Tc-sestamibi SPECT shows a defect only in ventricular septum (black arrows).

Intra-LV and intra-mural LE distribution

The intra-LV LE distribution was analyzed using the 17-segments model[16]. Next, we visually divided the intra-mural LE distribution into subepicardial, midwall and subendocardial distribution. Then, the extent of LE in each segment was determined with a five-point scoring system (0 = no LE, 1 = 1%-25%, 2 = 26%-50%, 3 = 51%-75%, 4 = 76%-100% of transmural extent of LE). The segment with score 4 was defined as "transmural" distribution[16]. LE in patients with CS existed predominantly in the basal and mid septum, but also distributed throughout LV segments. While in patients with DCM, LE was localized mostly in the basal and mid septum[13,16]. In addition, LE distributed across all the myocardial layers in patients with CS, but was predominantly localized at the midwall in those with DCM (Figure 2). The averaged LE score in each LV segment was significantly higher in CS than that in DCM [0.95 ± 0.67 *vs* 0.42 ± 0.43, mean ± standard deviation (SD), $P < 0.05$].

Typical LE distribution profiles

Previous reports have also shown that transmural (nodular) distribution, circumferential subepicardial distribution, and subepicardial and subendocardial distribution (with spared midwall) are highly charac-

Table 2 Clinical features and magnetic resonance imaging parameters in patients with cardiac sarcoidosis and with dilated cardiomyopathy

	CS	DCM	*P* values
Number	14	30	
Sex (M/F)	M4/F10	M23/F7	0.001
Age (yr)	59.8 ± 13.5	69.2 ± 12.6	0.03
Syncope *n* (%)	2 (14.3)	6 (20.0)	0.65
Palpitation *n* (%)	7 (50.0)	17 (56.7)	0.74
NYHA	8/5/1/0	8/11/6/5	0.08
(I/II/III/IV)	(57.1%/35.7%/ 7.1%/0%)	(26.7%/36.7%/ 20%/16.7%)	
ECG findings			
PQ duration	188.4 ± 26.0	188.1 ± 40.9	0.91
1st/2nd AVB	7/1 (50.0%/7.1%)	7/0 (23.3%/0%)	0.14
QRS duration	118.6 ± 22.9	128.4 ± 36.3	0.18
Abnormal Q waves *n* (%)	6 (42.9)	3 (10.0)	0.09
RBBB/LBBB	3/5 (21.4%/35.7%)	2/15 (6.7%/50%)	0.57
VTs *n* (%)	7 (50.0)	15 (50.0)	0.74
Medications *n* (%)			
Corticosteroids	7 (50.0)	0 (0)	< 0.001
ACEI/ARB	9 (64.3)	20 (66.7)	0.73
β blockers	7 (50.0)	23 (76.7)	0.07
AADs	4 (28.6)	14 (46.7)	0.51
Diuretics	7 (50.0)	18 (60.0)	0.32
MRI			
LVEDVI (mL/m^2)	107.0 ± 45.8	135.5 ± 43.4	0.08
LVESVI (mL/m^2)	74.2 ± 44.5	106.3 ± 42.1	0.04
LVMI (g/m^2)	60.1 ± 24.9	67.1 ± 28.9	0.34
LVEF (%)	33.9 ± 11.0	22.8 ± 10.0	0.003
LE segment number	8.6 ± 4.6	5.3 ± 3.1	0.04

The categorical variables were expressed as number and percentage (%) and compared by χ^2 test. The continuous variables were expressed as means ± SD and examined by unpaired *t* test. CS: Cardiac sarcoidosis; DCM: Dilated cardiomyopathy; M/F: Male/female; NYHA: New York Heart Association; ARB: Angiotensin receptor blockers; ACEI: Angiotensin converting enzyme inhibitors; AVB: Atrioventricular block; AAD: Anti-arrhythmic drugs; MRI: Magnetic resonance imaging; LVEDVI and LVESVI: Left ventricular end-diastolic and end-systolic volume indices; LVEF: LV ejection fraction; LE: Late gadolinium enhancement; L/RBBB: Left/right bundle branch blocks; LVMI: LV mass index; VT: Ventricular tachycardia.

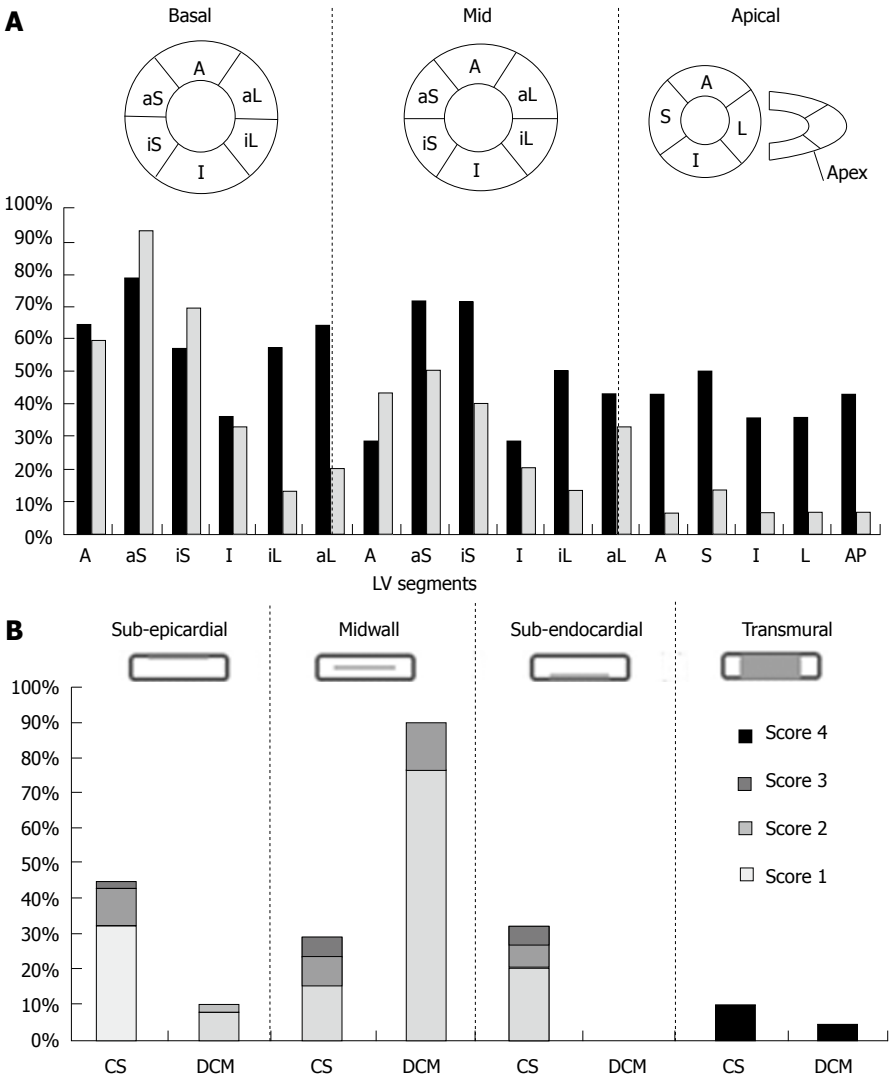

Figure 2 Intra-left ventricles (A) and intra-mural (B) late gadolinium enhancement distribution in patients with cardiac sarcoidosis and with dilated cardiomyopathy. A: Columns indicate prevalence of LE at each LV segment in patients with CS (black) and with DCM (gray). A: Anterior; aL: Antero-lateral; aS: Anterior septal; I: Inferior; iL: Infero-lateral wall in basal, mid and apical LV; AP: LV apex; B: Columns consist of prevalence of LE with scores 1 to 3 at different intra-mural distribution in patients with CS and with DCM. Score 4 indicates the transmural distribution. CS: Cardiac sarcoidosis; DCM: Dilated cardiomyopathy; LV: Left ventricles.

teristic in CS, whereas striated distribution in midwall is typical in DCM (Figure 3A)[5,10]. In our analysis, transmural (nodular), circumferential, and subepicardial and subendocardial LE distribution were highly specific in patients with CS, although the prevalence of those distribution patterns was low. In contrast, the prevalence of striated midwall LE distribution was high in both groups, but the specificity was low (Figure 3B and Table 3).

DISCUSSION

We initially demonstrated typical findings of various cardiac imaging in a patient with CS. Many reports have exhibited the correlations among LE-MRI, SPECT and FDG-PET in the evaluation of CS. The intra-mural extent of LE was quite concordant with perfusion defects in ^{201}Tl- or ^{99m}Tc-sestamibi-SPECT[9,13]. On the other hand, FDG-PET exhibits focal or focal on diffuse type of hot spots in CS[20-22]. While LE and defects in SPECT reflect irreversible fibro-granulomatous replacement, the hot spots in T2-weighted black-blood imaging (T2WBB), ^{67}Ga-SPECT and FDG-PET express active inflammatory change. The hot spots can be targeted for an endomyocardial biopsy if tissue diagnosis is required, and be adopted for an evaluation of corticosteroid therapy[21,23]. Since FDG-PET can give higher sensitivity and specificity than SPECT, we recommend the combination of LE-MRI and FDG-PET for assessing CS[20,21]. LE sometimes overlaps with hot spots in FDG-PET or T2WBB according to the disease progression or recurrence. Thus, it is important to carefully interpret findings in LE-MRI and other imaging modalities[24].

LE distributions in CS

Managing patients with reduced LV contraction who are suspected CS without histologic manifestation is a critical issue, since these cases may be diagnosed

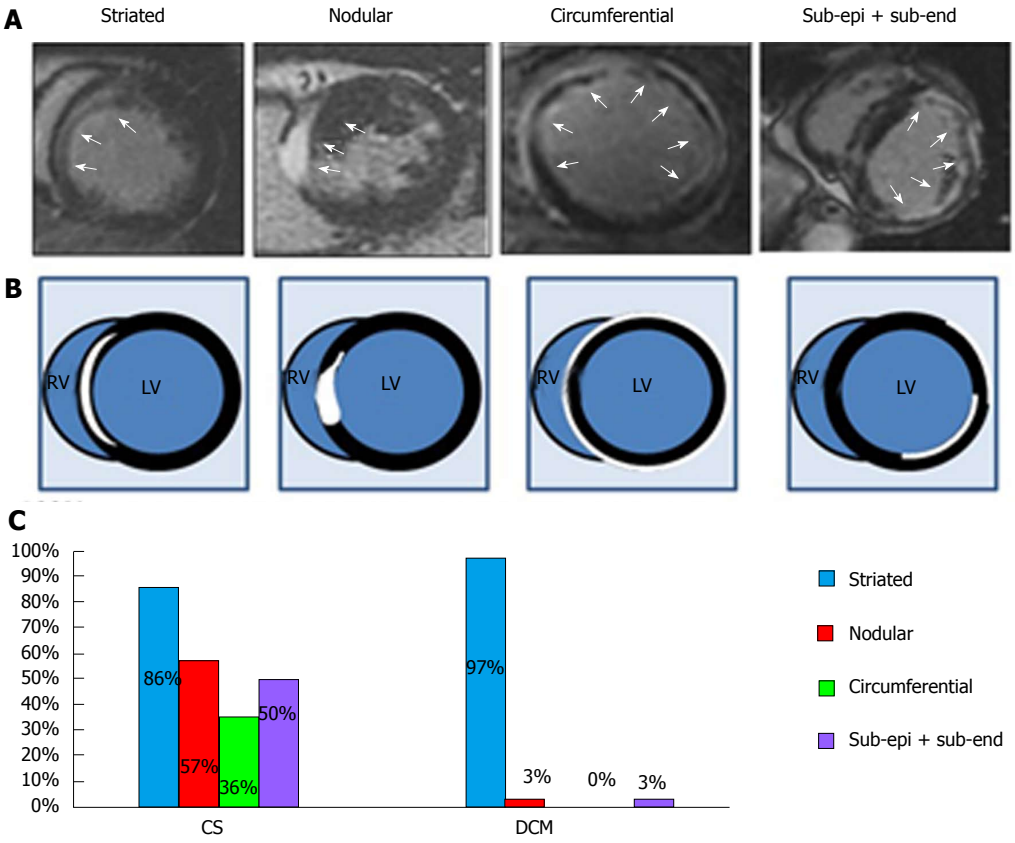

Figure 3 Typical late gadolinium enhancement distribution profiles. Characteristic patterns of LE distribution in LE-MRI (A) and the cartoons (B). Striated: Striated LE distribution in midwall; Nodular: Nodular (transmural) LE distribution; Circumferential: Subepicardial LE distribution in > 50% circumferential LV wall; Sub-epi + sub-end: Subepicardial and subendocardial LE distribution with spared midwall (white arrows); C: The prevalence of characteristic patterns of LE distribution in patients with CS and with DCM. CS: Cardiac sarcoidosis; DCM: Dilated cardiomyopathy; LE: Late gadolinium enhancement; LV/RV: Left and right ventricles; MRI: Magnetic resonance imaging.

Table 3 Diagnostic value of characteristic late gadolinium enhancement distribution patterns to differentially diagnose cardiac sarcoidosis from dilated cardiomyopathy

LE patterns	Sensitivity (%)	Specificity (%)	PPV (%)	NPV (%)
Striated	85.7	3.3	29.3	33.3
Nodular	57.1	96.7	88.9	82.9
Circumferential	35.7	96.7	83.3	76.3
Subepi + subend	50.0	96.7	87.5	80.6

PPV and NPV: Positive and negative predictive values; Sub-epi + sub-end: Subepicardial and subendocardial distribution with spared midwall; LE: Late gadolinium enhancement.

with DCM, and do not receive corticosteroid therapy[25]. Oppositely, the inclusion of the presence of LE in the novel JMH guideline (Table 1) may cause an increase in false positive patients. Although FDG-PET can be an additional tool for diagnosing CS, it is not always available in all hospitals and patients. Therefore, more detailed analyses of LE-MRI are required to differentiate CS from DCM.

Many previous studies have clarified the characteristic LE distribution in CS (Table 4). In general, LE in CS is polymorphic and heterogeneous; a classic pattern of midwall or subepicardial LE can be seen, but subendocardial or transmural LE as in patients with ischemic cardiomyopathy is also possible. LE may correspond to the location of wall thinning, wall motion abnormalities and myocardial edema[5,8,10,13,25-30]. Tezuka *et al*[25] reported that there was no difference in LE distribution between sCS and iCS.

In our analysis, transmural (nodular), circumferential, and subepicardial and subendocardial LE distribution were highly specific in patients with CS, although the prevalence of those distribution patterns was low. In contrast, the prevalence of striated midwall LE distribution was high in both groups, but the specificity was low. Although the mechanisms of these types of LE distribution remain unknown, more aggressive examination for CS such as serological tests, ^{67}Ga-SPECT and FDG-PET should be considered, when patients with reduced LVEF showed diffuse and characteristic features of LE distribution.

Clinical implications of LE

In general, LE in patients with cardiomyopathies correlates with all-cause mortality, heart failure hospitalization, and sudden cardiac death. Thus, detection of LE by LE-MRI has excellent prognostic significance and may help guide risk stratification and management in patients with various cardiomyopathies[17,31].

In sarcoidosis, previous reports showed that patients

Table 4 Reports for patterns of late gadolinium enhancement distribution and clinical relevance of late gadolinium enhancement in cardiac sarcoidosis

Ref.	Patients	LE distribution		Clinical relevance
		Intra-cardiac	Intra-mural	
Smedema *et al*[8]	12 CS	Mostly basal and lateral LV wall	Any	Diagnostic
Matoh *et al*[13]	5 sCS	Mid ventricular septum	Midwall to subepicardial	Correlations between LE area and LVEDV, LVESV and LVEF
Ichinose *et al*[10]	10 CS	Any, but mostly basal LV wall	Any, but mainly subepicardial	Correlations between sum of LE score and BNP, LVEF, LVEDV
Manis *et al*[26]	11 CS	Ventricular septum	Patchy	Diagnostic
Patel *et al*[5]	21sCS	Any, but mainly basal ventricular septum, rarely RV wall	CAD; subendo-cardial non-CAD; mid wall, subepi-cardial, patchy	Higher rate of adverse events and cardiac death
Watanabe *et al*[27]	19 CS	NA	Subepicardial, transmural	Correlations between total LE segments, and reduced LV function and duration of extra-cardiac lesions
Greulich *et al*[28]	39 sCS	Any, but mainly ventricular septum (RV side)	Patchy, intramural to transmural	Higher Hazard ratio for MACE than other clinical parameters
Yang *et al*[29]	6 sCS	Ventricular septum, LV free wall, papillary muscle	Patchy	Decreased T2 (inactive phase)
Pöyjönen *et al*[30]	8 CS	Basal ventricular septum	Multifocal	Diagnostic
Tezuka *et al*[25]	9 sCS and 4 iCS	Any, but mainly anterior ventricular septum	Any, but mainly subepicardial	No difference between sCS and iCS in LE distribution and clinical features

BNP: Serum brain natriuretic peptide level; CAD: Coronary arterial disease type; CS: Cardiac sarcoidosis; iCS: Isolated CS; LV/RV: Left/right ventricles; LVEDV/ESV: LV end-diastolic/systolic volume; LVEF: LV ejection fractionl; MACE: Major adverse cardiac events; NA: Not available; sCS: Cardiac involvement of systemic sarcoidosis.

with LE in myocardium had high prevalence of heart failure symptoms, ECG abnormalities and lethal arrhythmias[5,28]. There are significant correlations between LE burden, and LV volume and function[5,8,10,27]. Regions of granulomatous infiltration evolving into scar tissue serve as substrates for re-entrant tachyarrhythmia[32,33]. Murtagh *et al*[34] exhibited that increased LE burden and right ventricular dysfunction can identify patients at highest risk of sudden cardiac death and VT. The efficacies of implantable cardioverter defibrillator (ICD) and catheter ablation were also reported for preventing sudden cardiac death and VT storm[35,36]. Therefore, not only the presence of LE, but also the LE burden and distribution should be considered for the risk stratification and therapeutic approach for CS. Although the smaller LE burden or non-specific scarring may be associated with a benign outcome[37], patients with LE should be carefully followed up, even when they had preserved LV function because of certain risks for sudden cardiac death and VT.

Tezuka *et al*[25] mentioned that the clinical features and prognosis did not differ between patients with sCS and iCS, whereas Kandolin *et al*[38] showed poorer outcomes in patients with iCS. The total segments with LE may correlate with the duration of extra-CS[27]. LE in CS mostly reflects irreversible myocardial scarring, and previous reports failed to show a decrease in LE volume after corticosteroid therapy[5,8,29]. The serial FDG-PET imaging is valuable to evaluate the effect of corticosteroid therapy for cardiac and systemic sarcoid lesions[21,39].

Limitations

Initially, MRI is not always available in all hospitals and patients, and has a problem of cost. Patients with pulmonary congestion cannot tolerate long data acquisition time of MRI. MRI has been prohibited in patients who have had device implantation. Therefore, patients who required urgent pacemaker or ICD implantation because of atrioventricular blocks or VT were excluded from the analyses of MRI. MR conditional pacemakers can be implanted in patients who may need MRI after device implantation[40,41]. Gadolinium cannot be injected to patients with chronic renal failure, because there is a risk of nephrogenic systemic fibrosis. Finally, different determination thresholds (> 2 SD to > 5 SD) and difficult quantification of LE are also limitations.

CONCLUSION

Although LE in myocardium has become a major criterion in the novel JMH guideline for CS, the present article suggests that more diffuse and characteristic patterns of LE distribution (in combination with abnormal wall motion and morphology) may be helpful for differentiating CS from DCM in patients with reduced LVEF. Future large and longitudinal follow-up studies are necessary to define characteristic patterns of LE distribution in CS as well as those prognostic values.

REFERENCES

1 **Hunninghake GW**, Costabel U, Ando M, Baughman R, Cordier JF, du Bois R, Eklund A, Kitaichi M, Lynch J, Rizzato G, Rose C, Selroos O, Semenzato G, Sharma OP. ATS/ERS/WASOG statement on sarcoidosis. American Thoracic Society/European Respiratory Society/World Association of Sarcoidosis and other Granulomatous Disorders. *Sarcoidosis Vasc Diffuse Lung Dis* 1999; **16**: 149-173

[PMID: 10560120]
2 **Roberts WC**, McAllister HA, Ferrans VJ. Sarcoidosis of the heart. A clinicopathologic study of 35 necropsy patients (group 1) and review of 78 previously described necropsy patients (group 11). *Am J Med* 1977; **63**: 86-108 [PMID: 327806 DOI: 10.1016/0002-9343(77)90121-8]
3 **Silverman KJ**, Hutchins GM, Bulkley BH. Cardiac sarcoid: a clinicopathologic study of 84 unselected patients with systemic sarcoidosis. *Circulation* 1978; **58**: 1204-1211 [PMID: 709777 DOI: 10.1161/01.CIR.58.6.1204]
4 **Sharma OP**, Maheshwari A, Thaker K. Myocardial sarcoidosis. *Chest* 1993; **103**: 253-258 [PMID: 8417889 DOI: 10.1378/chest.103.1.253]
5 **Patel MR**, Cawley PJ, Heitner JF, Klem I, Parker MA, Jaroudi WA, Meine TJ, White JB, Elliott MD, Kim HW, Judd RM, Kim RJ. Detection of myocardial damage in patients with sarcoidosis. *Circulation* 2009; **120**: 1969-1977 [PMID: 19884472 DOI: 10.1161/CIRCULATIONAHA.109.851352]
6 **Yazaki Y**, Isobe M, Hiroe M, Morimoto S, Hiramitsu S, Nakano T, Izumi T, Sekiguchi M. Prognostic determinants of long-term survival in Japanese patients with cardiac sarcoidosis treated with prednisone. *Am J Cardiol* 2001; **88**: 1006-1010 [PMID: 11703997 DOI: 10.1016/S0002-9149(01)01978-6]
7 **Nagai T**, Nagano N, Sugano Y, Asaumi Y, Aiba T, Kanzaki H, Kusano K, Noguchi T, Yasuda S, Ogawa H, Anzai T. Effect of Corticosteroid Therapy on Long-Term Clinical Outcome and Left Ventricular Function in Patients With Cardiac Sarcoidosis. *Circ J* 2015; **79**: 1593-1600 [PMID: 25877828 DOI: 10.1253/circj.CJ-14-1275]
8 **Smedema JP**, Snoep G, van Kroonenburgh MP, van Geuns RJ, Cheriex EC, Gorgels AP, Crijns HJ. The additional value of gadolinium-enhanced MRI to standard assessment for cardiac involvement in patients with pulmonary sarcoidosis. *Chest* 2005; **128**: 1629-1637 [PMID: 16162768 DOI: 10.1378/chest.128.3.1629]
9 **Tadamura E**, Yamamuro M, Kubo S, Kanao S, Saga T, Harada M, Ohba M, Hosokawa R, Kimura T, Kita T, Togashi K. Effectiveness of delayed enhanced MRI for identification of cardiac sarcoidosis: comparison with radionuclide imaging. *AJR Am J Roentgenol* 2005; **185**: 110-115 [PMID: 15972409 DOI: 10.2214/ajr.185.1.01850110]
10 **Ichinose A**, Otani H, Oikawa M, Takase K, Saito H, Shimokawa H, Takahashi S. MRI of cardiac sarcoidosis: basal and subepicardial localization of myocardial lesions and their effect on left ventricular function. *AJR Am J Roentgenol* 2008; **191**: 862-869 [PMID: 18716120 DOI: 10.2214/AJR.07.3089]
11 **Shijubo N**, Yamaguchi T. Diagnosis Criteria and Classification of Disease Severity for Sarcoidosis in Japan (in Japanese). *Japan Society of Sarcoidosis and other Granulomatous Disorders* 2015; **35**: 3-8 [DOI: 10.7878/jjsogd.35.3]
12 **Matoh F**, Satoh H, Shiraki K, Saitoh T, Urushida T, Katoh H, Takehara Y, Sakahara H, Hayashi H. Usefulness of delayed enhancement magnetic resonance imaging to differentiate dilated phase of hypertrophic cardiomyopathy and dilated cardiomyopathy. *J Card Fail* 2007; **13**: 372-379 [PMID: 17602984 DOI: 10.1016/j.cardfail.2007.06.139]
13 **Matoh F**, Satoh H, Shiraki K, Odagiri K, Saitoh T, Urushida T, Katoh H, Takehara Y, Sakahara H, Hayashi H. The usefulness of delayed enhancement magnetic resonance imaging for diagnosis and evaluation of cardiac function in patients with cardiac sarcoidosis. *J Cardiol* 2008; **51**: 179-188 [PMID: 18522793 DOI: 10.1016/j.jjcc.2008.03.002]
14 **Satoh H**, Matoh F, Shiraki K, Saitoh T, Odagiri K, Saotome M, Urushida T, Katoh H, Takehara Y, Sakahara H, Hayashi H. Delayed enhancement on cardiac magnetic resonance and clinical, morphological, and electrocardiographical features in hypertrophic cardiomyopathy. *J Card Fail* 2009; **15**: 419-427 [PMID: 19477402 DOI: 10.1016/j.cardfail.2008.11.014]
15 **Shiraki K**, Satoh H, Saitoh T, Saotome M, Urushida T, Katoh H, Takehara Y, Sakahara H, Hayashi H. Comparison of global and regional abnormalities in 99mTc-sestamibi and cardiac magnetic resonance imaging in dilated cardiomyopathy. *J Card Fail* 2010; **16**: 641-648 [PMID: 20670843 DOI: 10.1016/j.cardfail.2010.03.004]
16 **Machii M**, Satoh H, Shiraki K, Saotome M, Urushida T, Katoh H, Takehara Y, Sakahara H, Ohtani H, Wakabayashi Y, Ukigai H, Tawarahara K, Hayashi H. Distribution of late gadolinium enhancement in end-stage hypertrophic cardiomyopathy and dilated cardiomyopathy: differential diagnosis and prediction of cardiac outcome. *Magn Reson Imaging* 2014; **32**: 118-124 [PMID: 24315973]
17 **Satoh H**, Sano M, Suwa K, Saitoh T, Nobuhara M, Saotome M, Urushida T, Katoh H, Hayashi H. Distribution of late gadolinium enhancement in various types of cardiomyopathies: Significance in differential diagnosis, clinical features and prognosis. *World J Cardiol* 2014; **6**: 585-601 [PMID: 25068019 DOI: 10.4330/wjc.v6.i7.585]
18 **Sano M**, Satoh H, Suwa K, Nobuhara M, Saitoh T, Saotome M, Urushida T, Katoh H, Shimoyama K, Suzuki D, Ogawa N, Takehara Y, Sakahara H, Hayashi H. Characteristics and clinical relevance of late gadolinium enhancement in cardiac magnetic resonance in patients with systemic sclerosis. *Heart Vessels* 2015; **30**: 779-788 [PMID: 24996373 DOI: 10.1007/s00380-014-0539-y]
19 **Richardson P**, McKenna W, Bristow M, Maisch B, Mautner B, O'Connell J, Olsen E, Thiene G, Goodwin J, Gyarfas I, Martin I, Nordet P. Report of the 1995 World Health Organization/International Society and Federation of Cardiology Task Force on the Definition and Classification of cardiomyopathies. *Circulation* 1996; **93**: 841-842 [PMID: 8598070 DOI: 10.1161/01.CIR.93.5.841]
20 **Okumura W**, Iwasaki T, Toyama T, Iso T, Arai M, Oriuchi N, Endo K, Yokoyama T, Suzuki T, Kurabayashi M. Usefulness of fasting 18F-FDG PET in identification of cardiac sarcoidosis. *J Nucl Med* 2004; **45**: 1989-1998 [PMID: 15585472]
21 **Ishimaru S**, Tsujino I, Takei T, Tsukamoto E, Sakaue S, Kamigaki M, Ito N, Ohira H, Ikeda D, Tamaki N, Nishimura M. Focal uptake on 18F-fluoro-2-deoxyglucose positron emission tomography images indicates cardiac involvement of sarcoidosis. *Eur Heart J* 2005; **26**: 1538-1543 [PMID: 15809286 DOI: 10.1093/eurheartj/ehi180]
22 **Tahara N**, Tahara A, Nitta Y, Kodama N, Mizoguchi M, Kaida H, Baba K, Ishibashi M, Hayabuchi N, Narula J, Imaizumi T. Heterogeneous myocardial FDG uptake and the disease activity in cardiac sarcoidosis. *JACC Cardiovasc Imaging* 2010; **3**: 1219-1228 [PMID: 21163450 DOI: 10.1016/j.jcmg.2010.09.015]
23 **Alberts C**, van der Schoot JB, Groen AS. 67Ga scintigraphy as an index of disease activity in pulmonary sarcoidosis. *Eur J Nucl Med* 1981; **6**: 205-212 [PMID: 7250138 DOI: 10.1007/BF00290565]
24 **Isobe M**, Tezuka D. Isolated cardiac sarcoidosis: clinical characteristics, diagnosis and treatment. *Int J Cardiol* 2015; **182**: 132-140 [PMID: 25577749 DOI: 10.1016/j.ijcard.2014.12.056]
25 **Tezuka D**, Terashima M, Kato Y, Toriihara A, Hirasawa K, Sasaoka T, Yoshikawa S, Maejima Y, Ashikaga T, Suzuki J, Hirao K, Isobe M. Clinical characteristics of definite or suspected isolated cardiac sarcoidosis: application of cardiac magnetic resonance imaging and 18F-Fluoro-2-deoxyglucose positron-emission tomography/computerized tomography. *J Card Fail* 2015; **21**: 313-322 [PMID: 25512195 DOI: 10.1016/j.cardfail.2014.12.004]
26 **Manins V**, Habersberger J, Pfluger H, Taylor AJ. Cardiac magnetic resonance imaging in the evaluation of cardiac sarcoidosis: an Australian single-centre experience. *Intern Med J* 2009; **39**: 77-82 [PMID: 18771431 DOI: 10.1111/j.1445-5994.2008.01674.x]
27 **Watanabe E**, Kimura F, Nakajima T, Hiroe M, Kasai Y, Nagata M, Kawana M, Hagiwara N. Late gadolinium enhancement in cardiac sarcoidosis: characteristic magnetic resonance findings and relationship with left ventricular function. *J Thorac Imaging* 2013; **28**: 60-66 [PMID: 23249970 DOI: 10.1097/RTI.0b013e3182761830]
28 **Greulich S**, Deluigi CC, Gloekler S, Wahl A, Zürn C, Kramer U, Nothnagel D, Bültel H, Schumm J, Grün S, Ong P, Wagner A, Schneider S, Nassenstein K, Gawaz M, Sechtem U, Bruder O, Mahrholdt H. CMR imaging predicts death and other adverse events in suspected cardiac sarcoidosis. *JACC Cardiovasc Imaging* 2013; **6**: 501-511 [PMID: 23498675 DOI: 10.1016/j.jcmg.2012.10.021]
29 **Yang Y**, Safka K, Graham JJ, Roifman I, Zia MI, Wright GA,

Balter M, Dick AJ, Connelly KA. Correlation of late gadolinium enhancement MRI and quantitative T2 measurement in cardiac sarcoidosis. *J Magn Reson Imaging* 2014; **39**: 609-616 [PMID: 23720077 DOI: 10.1002/jmri.24196]

30 **Pöyhönen P**, Holmström M, Kivistö S, Hänninen H. Late gadolinium enhancement on CMR and sustained ventricular tachycardia predict severe cardiac inflammation. *Acta Cardiol* 2014; **69**: 637-647 [PMID: 25643434]

31 **Kuruvilla S**, Adenaw N, Katwal AB, Lipinski MJ, Kramer CM, Salerno M. Late gadolinium enhancement on cardiac magnetic resonance predicts adverse cardiovascular outcomes in nonischemic cardiomyopathy: a systematic review and meta-analysis. *Circ Cardiovasc Imaging* 2014; **7**: 250-258 [PMID: 24363358 DOI: 10.1161/CIRCIMAGING.113.001144]

32 **Banba K**, Kusano KF, Nakamura K, Morita H, Ogawa A, Ohtsuka F, Ogo KO, Nishii N, Watanabe A, Nagase S, Sakuragi S, Ohe T. Relationship between arrhythmogenesis and disease activity in cardiac sarcoidosis. *Heart Rhythm* 2007; **4**: 1292-1299 [PMID: 17905334 DOI: 10.1016/j.hrthm.2007.06.006]

33 **Naruse Y**, Sekiguchi Y, Nogami A, Okada H, Yamauchi Y, Machino T, Kuroki K, Ito Y, Yamasaki H, Igarashi M, Tada H, Nitta J, Xu D, Sato A, Aonuma K. Systematic treatment approach to ventricular tachycardia in cardiac sarcoidosis. *Circ Arrhythm Electrophysiol* 2014; **7**: 407-413 [PMID: 24837644 DOI: 10.1161/CIRCEP.113.000734]

34 **Murtagh G**, Laffin LJ, Beshai JF, Maffessanti F, Bonham CA, Patel AV, Yu Z, Addetia K, Mor-Avi V, Moss JD, Hogarth DK, Sweiss NJ, Lang RM, Patel AR. Prognosis of Myocardial Damage in Sarcoidosis Patients With Preserved Left Ventricular Ejection Fraction: Risk Stratification Using Cardiovascular Magnetic Resonance. *Circ Cardiovasc Imaging* 2016; **9**: e003738 [PMID: 26763280 DOI: 10.1161/CIRCIMAGING.115.003738]

35 **Nadel J**, Lancefield T, Voskoboinik A, Taylor AJ. Late gadolinium enhancement identified with cardiac magnetic resonance imaging in sarcoidosis patients is associated with long-term ventricular arrhythmia and sudden cardiac death. *Eur Heart J Cardiovasc Imaging* 2015; **16**: 634-641 [PMID: 25617029 DOI: 10.1093/ehjci/jeu294]

36 **Kumar S**, Barbhaiya C, Nagashima K, Choi EK, Epstein LM, John RM, Maytin M, Albert CM, Miller AL, Koplan BA, Michaud GF, Tedrow UB, Stevenson WG. Ventricular tachycardia in cardiac sarcoidosis: characterization of ventricular substrate and outcomes of catheter ablation. *Circ Arrhythm Electrophysiol* 2015; **8**: 87-93 [PMID: 25527825 DOI: 10.1161/CIRCEP.114.002145]

37 **Nagai T**, Kohsaka S, Okuda S, Anzai T, Asano K, Fukuda K. Incidence and prognostic significance of myocardial late gadolinium enhancement in patients with sarcoidosis without cardiac manifestation. *Chest* 2014; **146**: 1064-1072 [PMID: 24853830 DOI: 10.1378/chest.14-0139]

38 **Kandolin R**, Lehtonen J, Airaksinen J, Vihinen T, Miettinen H, Ylitalo K, Kaikkonen K, Tuohinen S, Haataja P, Kerola T, Kokkonen J, Pelkonen M, Pietilä-Effati P, Utrianen S, Kupari M. Cardiac sarcoidosis: epidemiology, characteristics, and outcome over 25 years in a nationwide study. *Circulation* 2015; **131**: 624-632 [PMID: 25527698 DOI: 10.1161/CIRCULATIONAHA.114.011522]

39 **Osborne MT**, Hulten EA, Singh A, Waller AH, Bittencourt MS, Stewart GC, Hainer J, Murthy VL, Skali H, Dorbala S, Di Carli MF, Blankstein R. Reduction in ^{18}F-fluorodeoxyglucose uptake on serial cardiac positron emission tomography is associated with improved left ventricular ejection fraction in patients with cardiac sarcoidosis. *J Nucl Cardiol* 2014; **21**: 166-174 [PMID: 24307261 DOI: 10.1007/s12350-013-98286]

40 **Raphael CE**, Vassiliou V, Alpendurada F, Prasad SK, Pennell DJ, Mohiaddin RH. Clinical value of cardiovascular magnetic resonance in patients with MR-conditional pacemakers. *Eur Heart J Cardiovasc Imaging* 2015 Nov 20; Epub ahead of print [PMID: 26588986 DOI: 10.1093/ehjci/jev305]

41 **Kono T**, Ogimoto A, Saito M, Fujimoto K, Fujii A, Uetani T, Nagai T, Nishimura K, Inoue K, Suzuki J, Okura T, Kido T, Miyagawa M, Mochizuki T, Higaki J. Cardiac magnetic resonance imaging for assessment of steroid therapy in a patient with cardiac sarcoidosis and a magnetic resonance-conditional pacemaker. *Int J Cardiol* 2014; **176**: e89-e91 [PMID: 25150491 DOI: 10.1016/j.ijcard.2014.07.157]

P- Reviewer: Fett JD, Peteiro J, Sabate M, Teragawa H
S- Editor: Ji FF **L- Editor**: A **E- Editor**: Wu HL

World Journal of Cardiology

Submit a Manuscript: http://www.wjgnet.com/esps/
Help Desk: http://www.wjgnet.com/esps/helpdesk.aspx
DOI: 10.4330/wjc.v8.i9.504

World J Cardiol 2016 September 26; 8(9): 504-519
ISSN 1949-8462 (online)

REVIEW

Novel concepts in radiation-induced cardiovascular disease

Jason R Cuomo, Gyanendra K Sharma, Preston D Conger, Neal L Weintraub

Jason R Cuomo, Neal L Weintraub, Department of Medicine, Medical College of Georgia at Augusta University, Augusta, GA 30912, United States

Gyanendra K Sharma, Preston D Conger, Department of Medicine, Division of Cardiology, Medical College of Georgia at Augusta University, Augusta, GA 30912, United States

Author contributions: All authors equally contributed to this paper with conception and design of the study, literature review and analysis, drafting and critical revision and editing, and final approval of the final version.

Supported by The National Institutes of Health to Neal L Weintraub, Nos. HL11264, HL126949, and AR070029.

Conflict-of-interest statement: No potential conflicts of interest.

Manuscript source: Invited manuscript

Correspondence to: Neal L Weintraub, MD, Department of Medicine, Medical College of Georgia at Augusta University, 1459 Laney Walker Blvd., Augusta, GA 30912, United States. nweintraub@augusta.edu
Telephone: +1-706-7216164
Fax: +1-706-7219799

Received: April 29, 2016
Peer-review started: April 29, 2016
First decision: June 17, 2016
Revised: July 14, 2016
Accepted: July 29, 2016
Article in press: August 1, 2016
Published online: September 26, 2016

Abstract

Radiation-induced cardiovascular disease (RICVD) is the most common nonmalignant cause of morbidity and mortality among cancer survivors who have undergone mediastinal radiation therapy (RT). Cardiovascular complications include effusive or constrictive pericarditis, cardiomyopathy, valvular heart disease, and coronary/vascular disease. These are pathophysiologically distinct disease entities whose prevalence varies depending on the timing and extent of radiation exposure to the heart and great vessels. Although refinements in RT dosimetry and shielding will inevitably limit future cases of RICVD, the increasing number of long-term cancer survivors, including those treated with older higher-dose RT regimens, will ensure a steady flow of afflicted patients for the foreseeable future. Thus, there is a pressing need for enhanced understanding of the disease mechanisms, and improved detection methods and treatment strategies. Newly characterized mechanisms responsible for the establishment of chronic fibrosis, such as oxidative stress, inflammation and epigenetic modifications, are discussed and linked to potential treatments currently under study. Novel imaging modalities may serve as powerful screening tools in RICVD, and recent research and expert opinion advocating their use is introduced. Data arguing for the aggressive use of percutaneous interventions, such as transcutaneous valve replacement and drug-eluting stents, are examined and considered in the context of prior therapeutic approaches. RICVD and its treatment options are the subject of a rich and dynamic body of research, and patients who are at risk or suffering from this disease will benefit from the care of physicians with specialty expertise in the emerging field of cardio-oncology.

Key words: Radiotherapy; Radiation; Cardiovascular; Atherosclerosis; Cardiomyopathy; Pericarditis; Valvular; Hodgkin; Breast cancer; Radiation fibrosis

Core tip: Radiation-induced cardiovascular disease is a common complication of mediastinal radiotherapy and often occurs years or decades after treatment. It most commonly manifests as chronic pericarditis, cardiomyopathy, and valvular or coronary heart disease. Its pathophysiology is chiefly that of radiation fibrosis, fueled by chronic states of inflammation and oxidative stress. Conventional risk factors impose additive risk to these patients and must be addressed as early as possible. Development of more sensitive imaging modalities is enabling detection at earlier stages of the disease and creating opportunities for novel treatment strategies. Percutaneous interventions have an increasing role in the treatment of symptomatic vascular and valvular disease.

Cuomo JR, Sharma GK, Conger PD, Weintraub NL. Novel concepts in radiation-induced cardiovascular disease. *World J Cardiol* 2016; 8(9): 504-519 Available from: URL: http://www.wjgnet.com/1949-8462/full/v8/i9/504.htm DOI: http://dx.doi.org/10.4330/wjc.v8.i9.504

INTRODUCTION

Mediastinal radiotherapy (RT) has been successfully used to decrease mortality and recurrence of a number of thoracic malignancies for decades, particularly early Hodgkin's lymphoma (HL) and breast cancer. Thanks to advances in chemotherapeutics and radiation oncology, HL is now eminently curable, with 20-year survival approaching 80%[1], while 15-year breast cancer survival is nearing the same threshold[2]. Increased longevity has unintended consequences, however, including radiation-induced cardiovascular disease (RICVD). Where the heart was once thought to be insensitive to radiation, RICVD is now known to be the chief non-malignant cause of death in these patients, responsible for between one-quarter and one-third of their mortality[1,3-5]. The intervening decades have witnessed significant decreases in the amount of radiation to which patients are exposed, but injury to the pericardium, myocardium, valvular architecture, and vasculature continue to impose significant challenges to patients and clinicians entrusted with their care. Here, we will briefly review the epidemiology and basic characteristics of the cardinal types of RICVD, focusing on emerging concepts in the pathophysiology, prevention, and treatment of this disease.

EPIDEMIOLOGY AND BASIC CHARACTERISTICS

The epidemiology of RICVD is complicated by the continual improvements in radiation dosimetry and shielding that tend to reduce cardiovascular exposure and the latent effects of radiation, which take years or decades to manifest. Thus, RICD is an inherently dynamic disease process, and while clinicians continue to cope with radiation-induced comorbidities afflicted by older and higher-dose radiation regimens, data derived from patients treated decades ago will tend to overestimate incidences and morbidities, *etc.*, of newly evolving cases. Updated epidemiologic data is therefore of critical importance to inform both patients and clinicians. Several large studies have been published over the last few years that analyzed the outcomes of RT administered between one and four decades ago. In the following section, these data will be presented in reference to the four cardinal radiation-induced cardiovascular pathologies, as well as a brief overview of the gross anatomic and histopathologic derangements known to occur over the given timelines and at the described doses.

Acute and chronic pericarditis

Radiation-induced pericarditis is the earliest form of RICVD to occur following mediastinal radiation. It may occur in either of two forms, early and acute or delayed and chronic, which should be regarded from a histopathological standpoint as two distinct disease entities. As an early complication of very high dose radiation, early pericarditis is extremely rare today due to implementation of dose reducing techniques. It occurs either during RT or in the days or weeks after in response to irradiation in excess of the "tolerance dose" of the organ, which is variably described as a mean heart dose of greater than 36 or 40 Gy, or a > 50 Gy dose administered to > 30% of the heart[6-8]. The effect of these doses on histopathology is profound in the short-term. In the acute setting, the pericardium becomes porous, resulting in a neutrophilic infiltrate and collection of a high-protein exudate[9]. Nearly half of affected patients develop hemodynamically-significant effusions, although in most cases they are self-limited. The development of apparently benign pericardial effusions in the acute stage may predispose the patient to chronic pericarditis of delayed onset, however[10].

Chronic pericarditis is the most common cardiac complication of radiation therapy, observed in some 70%-90% of necropsy cases[11,12]. The effect is highly dose-dependent, with incidence increasing from < 10% to > 50% as the total dose is increased from 50 to 60 Gy[7]. The incidence of symptomatic chronic, delayed pericarditis has decreased dramatically since the 1970s, falling from 20% to 2.5% with the application of just a few of the radiation-sparing techniques that are used today[13]. Nevertheless, even the low-dose radiation to which contemporary cohorts are exposed increases the incidence of chronic pericarditis by a factor of 1.6 when comparing patients undergoing left- *vs* right-sided RT[14]. This finding suggests that through the early 2000s, breast cancer survivors were accruing excess risk of chronic pericardial disease despite modern dose-schedules.

The time to onset of symptoms in chronic pericar-

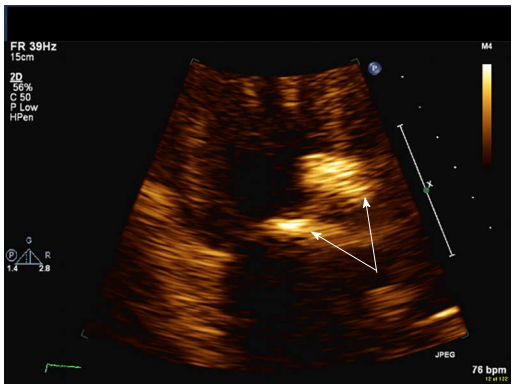

Figure 1 Severe calcification of proximal aorta and aortic leaflets (arrows) resulting in moderate aortic regurgitation and stenosis.

ditis can range from three months to over a decade, with one year being the median[8]. In the months prior to presentation, these patients will experience fibrous thickening of the pericardium and replacement of pericardial fat by collagen[11]. In nearly 20% of cases, pericardial thickening is severe enough to cause a chronic constrictive pericarditis[15], which, when it becomes symptomatic, does so much later, requiring pericardiectomy at a median of 11 years after RT according to one recent study[16].

Radiation-induced cardiomyopathy

According to the latest epidemiologic data, radiation-induced cardiomyopathy (RICM) occurs at a 40-year cumulative incidence rate of 24.8%, though most of these cases evolve following a distinct cardiac insult such as valvular disease or myocardial infarction (MI)[17]. The risk of RICM increases after 5 years, but it can evolve decades after initial RT[18]. Higher doses of radiation exposure are required to instigate this level of injury; rat hearts display a tolerance dose of 15-20 Gy[19], whereas the tolerance dose of human myocardium is approximately 40 Gy[7]. That said, asymptomatic myocardial perfusion defects have been detected as soon as 6 mo following irradiation at the much lower mean heart radiation doses used in the contemporary treatment of breast cancer[20]. In the latter study, defects were observed in about 40% of patients within two years, suggesting that RICM will continue to be a significant late adverse effect of RT in the coming decades despite reductions in radiation exposure.

Pathologically, RICM is characterized by inflammation followed by the development of a diffuse, patchy interstitial fibrosis of the myocardium, and effacement of the peri-myocyte endothelium[21]. Perfusion defects can often be detected by nuclear medicine studies in the early years following RT. They lie in the irradiated regions and do not follow the major coronary artery distributions, reinforcing the view that microvascular injury is central to this pathology[22]. As the heart becomes fibrotic it loses compliance, resulting in diastolic dysfunction[23]. Wall-motion abnormalities follow, occurring in 18% and 29% of patients in their second and third decades after RT, respectively, *vs* 5% in non-irradiated age-matched subjects in the Framingham population[24]. In the same study, a decline in left ventricular mass and wall thickness was also noted, which runs contrary to the trend seen in normal aging. Impairment of systolic function occurs last and should be considered a sign of late RICVD.

Valvular heart disease

The natural history of valvular heart disease (VHD) varies with radiation dose and, by extension, the decade in which the patient was treated. A study of HL survivors irradiated under obsolete protocols between 1965 and 1995 revealed 13- and 30-year cumulative incidences of 10% and 20%, respectively. Prior history of RT increased the risk of VHD for these patients 7-fold[18]. Unfortunately, VHD progresses in more than 30% of irradiated HL survivors throughout the second and third decades following treatment in this dose range[25]. More recently, researchers at the Netherlands Cancer Institute found a stepwise decrease in 30-year cumulative incidence of VHD corresponding to diminishing doses of RT, from 12.4% at doses greater than 40 Gy to 3.0% at doses less than 30 Gy[26]. At the lower end of this steep dose-response curve, where most treatment regimens are dosed currently, the absolute difference in 30 year VHD risk in irradiated *vs* non-irradiated patients was estimated to be 1.4%. Nevertheless, patients treated in past decades will continue to experience higher rates of VHD in the coming decades, particularly those exposed to high doses of radiation in the remote past.

With respect to the gross pathology of VHD, the earliest change appears to be the formation of valvular retractions and accompanying regurgitation preferentially involving the mitral and aortic valves, occurring within the first 10 years. The progression to fibrotic thickening and calcification of the valves occurs much later, with stenosis often appearing 20 years after RT[25]. Mitral and aortic valve regurgitation are the most common defects, and when stenosis occurs, it most commonly afflicts the aortic valve (Figures 1 and 2).

Radiation-induced coronary heart disease

Radiation-induced coronary heart disease (CHD) is currently the most active area of RICVD research. Until the 1990s, its existence was controversial, but it has been unmasked by longer survivorships and mass epidemiological studies in the ensuing decades. The disease burden it imposes is significant, in part because it can be induced by radiation doses that are well less than 10% of the tolerance dose of other cardiac tissues; thus, it more frequently complicates the course of breast cancer treatment than other forms of RICVD[7]. A large case control study of breast cancer survivors in Denmark and Sweden undertaken in 2013 found that the risk of a major CHD event begins to increase

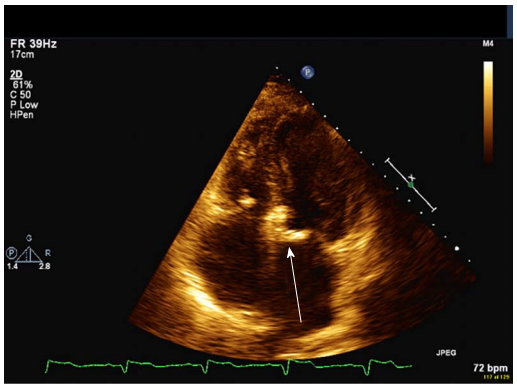

Figure 2 Apical four chamber view of mitral annular calcification (arrow).

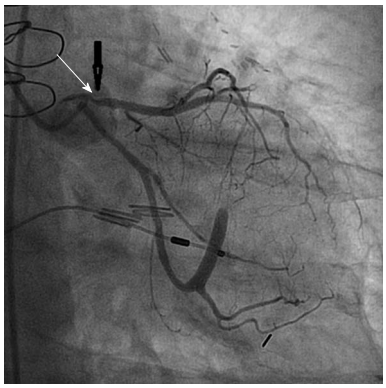

Figure 3 Severe proximal stenosis of the left anterior descending coronary artery (arrow).

within the first 5 years post-treatment and continues to significantly exceed that of the general population through at least 20 years of follow-up[27]. These patients experienced increased risk of angina pectoris, MI, and sudden cardiac death despite having been treated with a modest mean heart dose of 3.6 Gy RT between 1958 and 2001. Patients receiving radiation doses of < 2 Gy, 2-4 Gy, 5-9 Gy and > 10 Gy experienced dose-dependent excess risks of 10%, 30%, 40% and 116%, respectively, *vs* carefully matched controls. Another large study of women in Denmark and Sweden (n = 35000) comparing incidences of MI in breast cancer survivors observed an incidence ratio of 1.22 in patients undergoing left-sided *vs* right-sided RT[14]. In that study, the mean heart dose in patients with right-sided tumors was 2.7 Gy (*vs* 6.3 Gy for left-sided tumors), so the incidence ratio likely underestimates the true excess risk of RT compared with the general population. Concerning higher-dose radiotherapy, a 2015 study from the Netherlands Cancer Institute found a 40-year cumulative CHD incidence of 22.9%, amounting to a 4- to 7-fold increase in risk and 475 excess cases per 10000 person-years as compared to the general population[18].

The gross pathology of radiation-induced CHD differs from that of ordinary CHD in certain key respects. Radiation-induced coronary artery lesions tend to be longer and to preferentially involve the ostium, and they are therefore more challenging to treat percutaneously[28-30]. The left anterior descending (LAD) coronary artery is often preferentially involved because of its proximity to the radiation field (Figure 3).

This is particularly so in treatment of breast cancer where, while average heart doses are currently 1-5 Gy, the maximum LAD doses may exceed 20 Gy[31]. With respect to histopathology, these lesions tend to differ little from those of ordinary atherosclerosis and are characterized by intimal thickening, lipid accumulation, inflammation, and thrombosis[13]. They are often, however, somewhat more fibrous, with reduced lipid content, and the vessels involved tend to be more friable[23]. Other great vessels are likewise subject to radiation-induced friability, and the aorta and carotid artery have been known to rupture following RT on occasion[21]. Moreover, the carotid arteries have been noted to demonstrate early and rapid formation of unstable plaques following irradiation in rat models[7].

PATHOPHYSIOLOGY

Our basic understanding of the pathophysiology of RICVD has changed little since the seminal work of Fajardo *et al*[9,10] in the 1960s and 1970s. It has long been understood that irradiated pericardial, myocardial, endocardial, or endothelial tissue is prone to inflammation, which later results in tissue fibrosis and loss of capillaries at the microvascular level[10]. Until the early 2000s, studies in animal models and *in vitro* human tissues primarily focused on the mechanisms by which these changes occurred in the acute setting. Since the turn of the century, emphasis has shifted to the manner in which the acute inflammatory state gives way to chronic, pathological fibrosis. This section will begin with an overview of the inflammatory response, followed by a discussion of novel research into the mechanisms by which chronic and long-lasting profibrotic states become realized.

Acute inflammation

The mechanisms of tissue injury in the acute setting of radiation-induced pericarditis, valvular disease, cardiomyopathy and coronary disease are essentially the same and appear to be largely mediated by damage to the endothelium. Whether in the visceral pericardium, the highly vascular myocardium - which has a capillary density of 2800 capillaries/mm^2 as compared to 350/mm^2 in skeletal muscle[32] - or the small and medium-sized vessels that perfuse the heart, the endothelium is site of initial damage. Within minutes of irradiation, endothelial cells become hyperpermeable. By the passing of the second hour, the endothelium has begun to display membrane-bound molecules such as E- and P-selectin, which are involved in leukocyte cell rolling, and ICAM-1 and PECAM-1, which are involved in leukocyte arrest and transmigration[7].

These activities stimulate the neutrophilic response that predominates acutely, with these first-responders releasing pro-inflammatory cytokines such as tumor necrosis factor, monocyte chemotactic factor, and interleukin (IL)-8, resulting in recruitment of additional inflammatory cells[33]. While this pro-inflammatory activity of granulocytes and other immune cell types was once thought to be the chief, if not the sole cause of acute inflammation and fibrosis[34], inflammatory chemokine secretion by the endothelium itself has garnered much research interest in recent years. *In vitro* studies of cultured human microvascular endothelial cells have confirmed a radiation-induced increase in IL-6, IL-8, human fibroblast growth factor, and adhesion molecules such as ICAM-1, in the absence of immunologic cells. This suggests an immunologic and secretory functionality of the vascular endothelium that contributes to the pro-inflammatory state[35,36].

Finally, the contribution of coagulation to this acute endothelial inflammatory response merits consideration. The presence of early fibrin deposits in the capillary networks within radiation-exposed myocardium was noted in the initial studies of RICVD[37]. This is now known to result from impaired endogenous fibrinolysis, likely due in part to thrombomodulin inhibition by transforming growth factor-beta (TGF-β), and perhaps by RT itself[38]. The role of hyperacute coagulation in the eventual development of chronic fibrosis is as yet unknown. Certain coagulation factors such as thrombin, however, can induce endothelial secretion of chemokines such as IL-8 and monocyte chemoattractant peptide, which in turn promote chemotaxis of neutrophils and expression of adhesion molecules to upregulate inflammation[39,40].

Fibrosis

Fibrosis is the chief process by which chronic radiation damage occurs. At the biochemical level, fibrosis is the result of abnormal deposition of collagenous extracellular matrix (ECM) by activated myofibroblasts. The manner in which this comes about is still the subject of investigation. Cardiovascular fibrosis is a chronic but dynamic process that is propagated by pro-fibrotic cytokines, phenotypic alterations in various cell types, and the presence of chronic hypoxia and oxidative stress. Central to this process is the terminal differentiation of fibroblasts into myofibroblasts, which secrete more type Ⅰ and Ⅲ collagen, as well as alpha-smooth muscle actin, another ECM protein, than do their progenitors[41]. Stimuli that may lead to myofibroblast formation in radiation injury include pro-inflammatory cytokines, matricellular signals, and epigenetic reprogramming.

Pro-fibrotic cytokines such as platelet-derived growth factor (PDGF), IL-13, IL-4, and TGF-β are secreted in abundance by neutrophils and other immune cell types recruited to irradiated tissues. TGF-β in particular has many pro-fibrotic activities, including both the promulgation of myofibroblasts and the inhibition of collagenases[40,41]. IL-13 and IL-4 are chiefly secreted by Th2 lymphocytes and act at a variety of tissues to stimulate collagen deposition[34,42]. They have chiefly been studied in the context of hepatic and pulmonary fibrosis but are active in vascular tissues as well[43-45].

Matricellular signals also contribute to pro-fibrotic phenotypic changes. One such ECM protein that may constitute a future therapeutic target in RICVD is connective tissue growth factor (CTGF), which is induced by TGF-β and promotes differentiation of mesenchymal cells and resident fibroblasts into myofibroblasts[46-48]. Moreover, CTGF can continue to stimulate myofibroblasts to secrete ECM even after TGF-β levels have normalized, thus perpetuating fibrosis long after the initial insult has passed[49,50]. Indeed, knockdown of CTGF expression in human cardiac fibroblasts decreased fibroblast growth, and CTGF inhibition was shown to reverse fibrosis, decreasing vascular stiffness and myocardial dysfunction in rodent models, though this finding has not yet been replicated in irradiated models[51].

As terminally-differentiated cells, myofibroblasts are destined to undergo apoptosis rather than mitosis during normal wound healing. This typically results in a self-limited and acellular scar[52]. They persist in radiation-induced fibrosis, however, and a growing body of evidence links this to epigenetic reprogramming. DNA methylation is the most studied mode of epigenetic modification in radiation-induced fibrosis[53]. In murine fibroblasts, expression of the α-smooth muscle actin gene, a marker of myofibroblast differentiation, was reported to be regulated by methylation of CpG islands in the gene promoter[54]. Moreover, TGF-β-induced suppression of DNA methyltransferase expression contributed to induction of the α-smooth muscle actin gene and thus myofibroblast differentiation. In contrast, induction of α-smooth muscle actin expression during hypoxia was reported to be associated with DNA hypermethylation and upregulation of DNA methyltransferases[55]. This and other studies suggest that regulation of fibroblast differentiation *via* epigenetic DNA methylation is complex and context-specific[56,57].

Hypermethylation of genes involved in apoptosis has been observed following irradiation and is associated with decreased cell death, which could promote fibrosis[58]. Moreover, the patterns of DNA methylation predating irradiation may be a determinant of radiation fibrosis. Human dermal fibroblasts taken from patients who later developed radiation-induced fibrosis demonstrated decreased methylation of two intragenic sequences of the diacylglycerol kinase alpha gene, a regulator of fibrosis-associated signaling pathways[59]. Moreover, decreased DNA methylation at these sites correlated with future development of profibrotic fibroblast activation, highlighting the potential prognostic value of epigenetic modifications with respect to radiation-induced fibrosis. Methylation-inhibiting agents may hold promise in the treatment or prevention of RICVD and are currently in clinical trials. Aberrations in

two other modes of epigenetic modulation - microRNA activity and histone modifications - have been linked to fibrosis in various tissues, including the heart (for a detailed review, see Weigel *et al*[53]), but we know very little about their contributions to RICVD at this time.

Oxidative stress

In addition to directly inflicting cellular injury, radiation-induced oxidative stress is thought to play a key role in the transition from acute inflammation to chronic inflammation and fibrosis[60]. Reactive oxygen species (ROS) are acutely generated by the direct action of radiation and subsequently produced by both macrophages and the inflamed endothelium, which are replete with ROS-generating enzymes[61]. Macrophages produce large quantities of superoxide and nitric oxide, the latter *via* inducible nitric oxide synthase[62,63]. Superoxide and nitric oxide react to form peroxynitrite, a toxic source of free radical injury[64]. The decreased availability of nitric oxide resulting from this conversion promotes vascular dysfunction and tissue hypoxia, which further exacerbates oxidative stress[63].

Once initiated, oxidative stress propagates inflammation through several mechanisms. For example, oxidative stress promotes chemotaxis by upregulating expression of adhesion molecules such as ICAM[65] and by increasing monocyte chemotactic protein-1 and TNF-α levels[66]. Moreover, ROS increase thrombin activity by inactivating thrombomodulin, potentially promoting inflammation as previously described[67]. Though a causal link between radiation-induced oxidative stress and inflammatory cytokine production is difficult to establish, anti-oxidant studies are informative. For example, administration of alpha-lipoic acid prior to irradiation was reported to decrease local levels of IL-1, IL-6, and metalloproteinases in mice[68], while melatonin decreased levels of IL-1, TNF-α, and TGF-β[69].

ROS also promote inflammation *via* their complex interaction with NF-κB, a transcription factor responsible for such critical functions as immune regulation and cell survival. In the setting of RICVD, NF-κB activation by ROS results in increased adhesion molecule, cytokine, and chemokine production[70]. An association with fibroblast stimulation and collagen deposition has also been demonstrated. Importantly, NF-κB upregulation was detected from week 4 through week 500 post-irradiation in small vessels of the neck in humans[71], suggesting that NF-κB might be a critical element in the transition from acute inflammation to chronic fibrosis (Figure 4).

Free radicals produced by macrophages result in increased pro-fibrotic TGF-β production in irradiated animals[72]. This change is preceded by tissue hypoxia, which follows in RICVD from capillary effacement and diminished perfusion. Additionally, ROS have been reported to cleave TGF-β from its anchorage sites in the ECM, which in turn promotes myofibroblast differentiation and ECM deposition[61]. Lastly, free radicals establish a preference for the Th2 lymphocyte phenotype over the Th1 response[73,74], thus skewing the lymphocyte population towards those that preferentially secrete IL-4, IL-13, TGF-β, *etc*. These and other chemical signals act in concert to stimulate myofibroblast hyperactivity and disordered ECM deposition.

PREVENTION

The cardiovascular morbidity and mortality of RT can be forestalled through primary prevention, which consists of dose reduction and radioprotection, and secondary prevention, which consists of screening and radiomitigation. No pharmaceuticals are currently approved by the Food and Drug Administration for either purpose, although Amifostine, a scavenger of free radicals, was recently approved for the reduction of radiation-induced xerostomia[75]. This discussion will therefore focus on dose-reduction, screening, and risk modification, ending with a brief discussion of novel uses of existing pharmaceuticals, such as statins and ACE inhibitors.

The most important means of prevention is reduction in radiation exposure. Advances in radiation oncology have resulted in decreases in absolute 15-year cardiac mortality from 13% in the mid-1970s to 5.8% in the late 1980s for breast cancer survivors[76]. Meanwhile, the incidence of major CHD events in HL survivors has remained roughly unchanged during the same period despite dramatic increases in utilization of cardiotoxic chemotherapeutics[18]. Recent reviews have dealt with the techniques by which this has been achieved[77,78]. Some of these strategies involve manipulating the patient so as to exclude as much of the myocardium from the treatment field as possible; for instance, use of breast boards or prone positioning may reduce the volume of myocardium traversed by the radiation beam. Likewise, deep inspiration and inspiratory gating are two techniques by which radiation oncologists exploit the heart's tendency to fall inferiorly and posteriorly out of the radiation field. Perhaps the most important advancement is the use of intensity-modulated RT, in which 3-D CT images are used in conjunction with multileaf collimators that can be manipulated to deliver radiation beams that conform closely to the shape of the tumor. With respect to HL, reductions in radiation exposure are mainly attributable to dose fractionation, and to the shift from mantle field radiation, which encompasses much of the neck, mediastinum, and axilla, to more limited, involved fields[79]. All of these techniques presuppose superior imaging and software technologies that deliver radiation more accurately - often to within several millimeters of the desired target - and with much smaller margins than were used in the in the previous century.

Despite these improvements, excess risk of morbidity and mortality persist. It is therefore imperative that cardio-oncologic care be coordinated prior to initiation of RT for the establishment of appropriate cardiac baselines and for continued surveillance throughout the

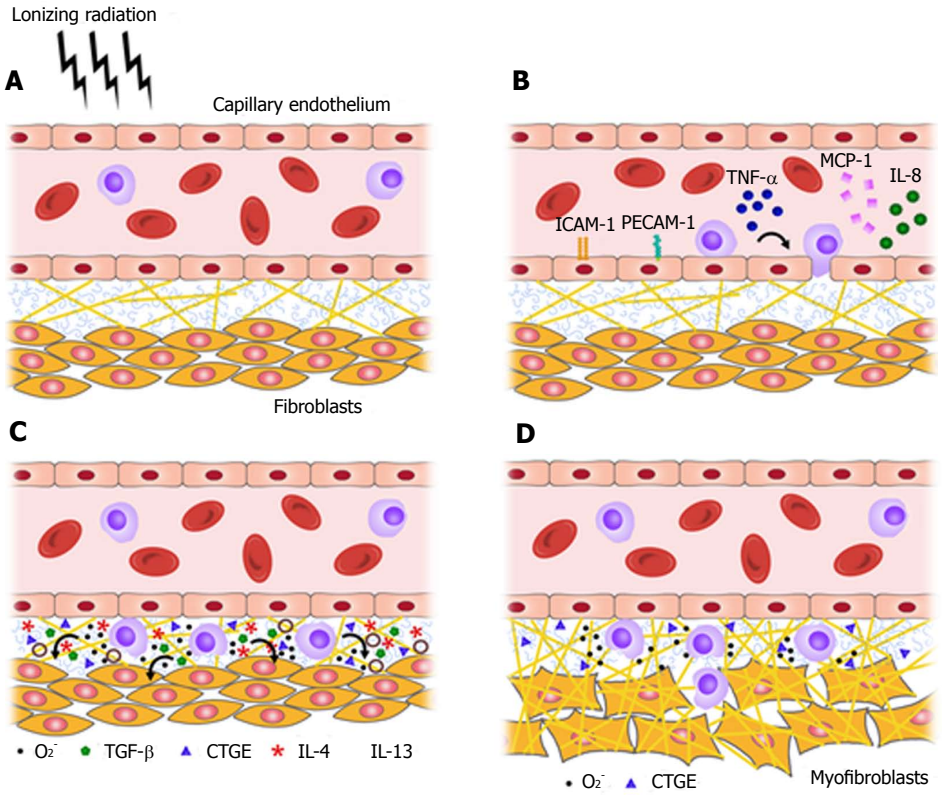

Figure 4 Radiation injury and the transition from acute inflammation to chronic fibrosis, as mediated by pro-fibrotic cytokines and reactive oxygen species. A-C: Normal tissue (A) becomes inflamed within hours of irradiation (B), and a pro-fibrotic cytokine profile predominates within days-to-weeks (C); D: Represents the chronic state of fibrosis characteristic of radiation injury. O_2^-: Reactive oxygen species; TNF-α: Tumor necrosis factor alpha; MCP-1: Monocyte chemotactic protein-1; CTGF: Connective tissue growth factor; TGF-β: Tumor growth factor beta; IL: Interleukin.

patient's lifetime. The younger the patient is at time of treatment, the more critical the need for surveillance, as both their relative risk of RICVD and their survivorship with respect to cancer are greater[18]. Cardio-oncologic care should begin with risk factor modification, as conventional CHD risk factors are particularly hazardous in this population. Indeed, traditional risk factors have been shown to more than double the relative risk of CHD events in these patients as compared to matched patients in the general population[80]. Thus, hypertension, hyperlipidemia, and diabetes mellitus should be managed aggressively, and patients should be counseled regarding smoking cessation, weight loss, and exercise where appropriate.

Screening and detection

The cardiac morbidity and mortality associated with RT can be reduced if treated early, which justifies the need for screening and early detection of RICVD[81]. Prospective data regarding cost- and risk-benefit analyses with respect to screening are lacking, however. Although evidence-based guidelines are unavailable, several expert consensus statements have been derived based on the available randomized trials and epidemiological studies. In 2014, the American College of Radiology Appropriateness Criteria Report made a case for the importance of surveillance but stopped at recommending personalization[82]. The expert panel of the National Comprehensive Cancer Network (NCCN) called for aggressive management of cardiovascular risk factors with annual blood pressure and biannual lipid screening in their expert consensus statement released in 2015. They also recommended considering a baseline stress test or echocardiogram every 10 years after treatment[83]. Some experts have proposed that irradiation should be considered an additional CHD risk factor in the presence of hypertension, hyperlipidemia, or diabetes[81].

Finally, the most rigorous set of screening recommendations came from the European Association of Cardiovascular Imaging and the American Society of Echocardiography in 2013, which recommend aggressive risk factor modification and yearly physician visits. The statement went further, however, recommending baseline echocardiography prior to RT, followed by repeat echocardiography 10 years after treatment and every five years thereafter in heart-healthy patients[84]. For patients with one or more conventional risk factors, screening echocardiography was recommended in the fifth year after treatment, and noninvasive stress testing was recommended 5-10 years after treatment and at 5-year intervals, with a preference for stress echocardiography in these patients.

The prospective data supporting these statements was largely derived from a series of studies by Heidenreich *et al*[24], who screened asymptomatic HL

survivors for RICVD. Their study of echocardiography in asymptomatic patients uncovered a 29% prevalence of significant valve disease in HL patients as compared to 3% in the general population[24]. Diastolic dysfunction was detected in 14% of the HL patients at a mean of 14 years post-RT[23]. While the cost-benefit ratio of screening for heart failure with preserved ejection fraction (EF) is uncertain due to the lack of effective treatment, a disproportionate number of patients thus afflicted also demonstrated stress-induce ischemia on subsequent stress echocardiogram or nuclear perfusion imaging (23%). Finally, Heidenreich *et al*[85] evaluated stress echocardiography and radionuclide perfusion imaging as screening tests for asymptomatic CHD after RT. They observed a 2.7% prevalence of severe, multivessel or proximal coronary stenosis, and a 7.5% prevalence of coronary stenosis greater than 50% at a mean 15 years after RT. The cohort overall had a documented 8% prevalence of coronary insufficiency or death. The generalizability of these data is limited by the high radiation doses employed in the cohort; the mean heart dose in the three trials was 43-44 Gy, which is much higher than most HL patients receive today. Nevertheless, these findings are likely pertinent to patients irradiated prior to the 1990s, or to more recently treated patients receiving mean heart doses greater than 35 Gy.

Thus, current literature supports use of transthoracic echocardiogram as the screening tool of choice to evaluate baseline left ventricular EF, diastolic function and VHD. Echocardiography is also important in the assessment of restrictive cardiomyopathy and constrictive pericarditis. Ultrasonographic technologies are constantly evolving, leading to improvements in the ability to detect subtle signs of RICVD disease *via* echocardiography. Using cardiac MRI as the gold standard, 3D echocardiography was reported to exhibit greater sensitivity than 2D echocardiography to detect left ventricular EFs less than 50% (53% *vs* 25%, respectively)[86]. Deformation imaging using speckle tracking or tissue Doppler velocities may be even more sensitive to detect subtle abnormalities in left ventricular function[87,88]. Reductions in systolic myocardial deformation were detected immediately and 2 mo after RT, in the absence of detectable reductions in EF[89]. Speckle tracking echocardiography demonstrated abnormal global longitudinal and global circumferential strain in 33% and 21.7%, respectively, of patients who underwent RT, while depressed EF was detected by 3D echocardiography in only 5.7% of patients at a median 22.6 years[90]. While no gold standard was applied, abnormal longitudinal strain was correlated with reduced quality of life and lower mean 6-min walk distances, even when it was the sole abnormal finding. Thus, while reduced EF is a late finding in RICVD, abnormal strain measurements may herald early onset disease and are increasingly being incorporated into screening protocols (Figure 5).

Though it is not a first-line screening tool, cardiac MRI is helpful in evaluation of left ventricular EF and, with the addition of myocardial tagging, may be utilized for better evaluation of constrictive pericarditis. This modality is particularly well-suited to detection of the patchy fibrosis that may be associated with micro-vascular insufficiency even in the absence of classical ostial coronary stenosis, ischemia, or infarction[91]. The pattern of late gadolinium enhanced MRI images can help differentiate between MI, diffuse myocardial fibrosis, and constrictive pericarditis as the underlying mechanism of the cardiomyopathy[92,93].

Newer screening modalities for radiation-induced vascular disease have also been evaluated, including coronary artery calcium (CAC) imaging. In a cohort of 47 HL survivors who received a mean cardiac dose of 40.6 Gy, CAC imaging demonstrated a strong association between severity of CAC and the presence of coronary artery disease verified by angiography[94]. The proportion of patients with CAC scores of zero was much lower in the HL cohort than in the general population. Another study using CT angiography in HL survivors detected nearly twice as many atherosclerotic lesions in pre-cranial blood vessels contained within the radiation field as compared with a non-irradiated control group; the percentages of calcified *vs* non-calcified lesions were similar in the HL and control groups, suggesting that atherosclerosis, but not calcification, is a radiospecific finding[95]. Interestingly, this study also found that elevated total cholesterol, measured soon after RT, correlated strongly with later incidence of coronary artery disease. While these studies suggest a role for CT in screening for vascular disease in HL survivors, their generalization is limited by the high doses of radiation to which these older cohorts were exposed. Indeed, a larger study of CAC screening in 236, 12-year breast cancer survivors who had been exposed to lower doses of radiation did not find any excess CAC, though the duration of follow-up may have been too short to detect late occurrences[96]. Thus, CT imaging may be of greater utility in detection of CHD in cancer survivors who are in their second or third decade post-RT.

Laboratory monitoring is another important component of screening for RICVD. The importance of identification and management of hyperlipidemia in cancer survivors with a history of RT is emphasized by data showing a direct correlation between the presence of hypercholesterolemia soon after RT and atherosclerosis[95,96]. Chen *et al*[97] (2009) applied a decision-analytic model to perform a cost-benefit analysis in a hypothetical cohort of HL survivors to establish the cost-effectiveness of screening intervals for hyperlipidemia. Applying an assumed relative risk of cardiac mortality of 3.2 to a theoretical cohort that otherwise differed little from that of the general population, the optimal interval for screening for hyperlipidemia was determined to be every three years. With respect to biomarker screening, elevation of troponin-I and brain natriuretic peptide have been

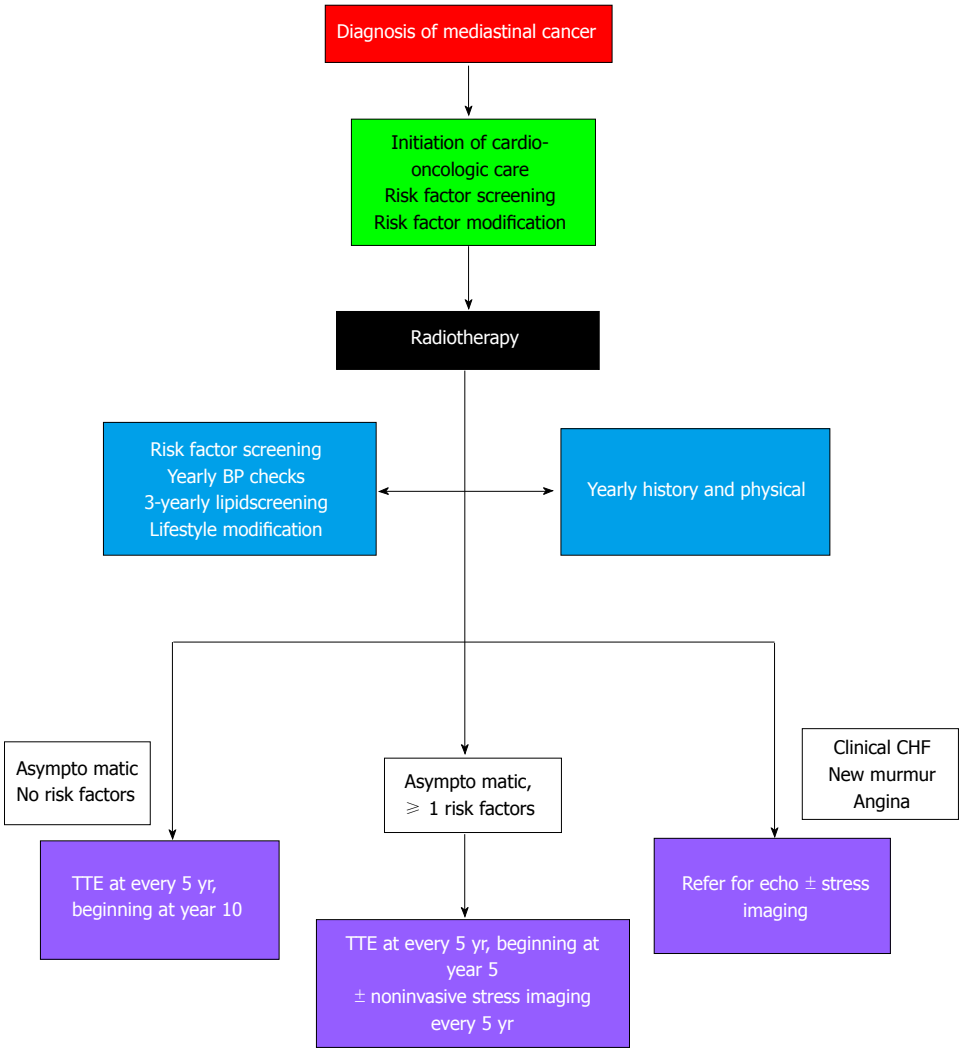

Figure 5 Proposed algorithm for cardio-oncologic screening following mediastinal radiotherapy[84]. CHF: Congestive heart failure; TTE: Transthoracic echocardiography.

demonstrated in patients during and immediately following RT in a small cohort of breast or lung cancer patients[98]. A later study found subacute elevations of high-sensitivity troponin-T following RT that were dose-dependent[99]. This study also detected echocardiographic evidence of interventricular septal thickening and prolonged diastolic deceleration time in patients who experienced a greater than 30% increase in troponin levels from baseline, suggesting that elevated high-sensitivity troponin-T correlates with subtle abnormalities of cardiac function after RT. The implications for the utility of high-sensitivity troponins in screening for future cardiac disease are unknown but may become clearer after the planned follow-up with this cohort.

Radioprotection and radiomitigation

As to the role of pharmaceuticals, several commonly prescribed agents are currently being evaluated in primary and secondary prevention after promising results were observed in animal trials. Statins have been studied extensively in rodent and *in vitro* human models and have shown promise through several of the mechanisms discussed in the Pathophysiology section. Pravastatin has been found to inhibit the activity of CTGF by modulating associated proteins such as Ras-homologous (Rho) GTPases[100]. Rho-family proteins regulate cellular responses to pro-fibrotic cytokines such as TGF-β, and to oxidative stress[46]. They also increase cell adhesion and contribute to the reorganization of the ECM[100,101]. Some of the statins' anti-fibrotic activities may also be related to attenuation of radiation-induced NF-κB activity, which depends upon activation by Rho-family GTPases[102]. Additionally, statins upregulate thrombomodulin expression in human endothelium, decreasing the pro-inflammatory activities of thrombin as described previously[103]. Lastly, atorvastatin has been found to reduce injury to and apoptosis of the vascular endothelium[104]. Notably, several trials of statins in young patients who were treated with RT are underway[105]. Although surrogate endpoints, such as detection of endothelial function and carotid intimal-medial thickness, will be employed, these studies nevertheless may begin to illuminate the role of early

statin therapy in reducing the long-term risk of RICVD.

Angiotensin converting enzyme (ACE) inhibitors are another commonly prescribed class of drug with radioprotective and radiomitigating potential. Rats treated with captopril shortly after radiation of the lung demonstrated dramatically increased survival and improved vasoreactivity, as well as decreased perivascular fibrosis and inflammatory cell infiltration[106]. Similar findings with respect to the pulmonary vasculature have been reported in rats treated with ACE inhibitors two weeks after irradiation[107]. More recently, rats treated with captopril exhibited reduced diastolic dysfunction and perivascular necrosis in the left ventricle following radiation exposure[108]. Although these data are intriguing, prospective studies evaluating the efficacy of ACE inhibitors in patients undergoing RT have not been reported.

Lastly, antioxidant approaches are the subject of much investigation. Amifostine was previously mentioned in connection with its indication for treatment of xerostomia, but in a small rodent study of RICVD, this drug was found to reduce myocardial fibrosis and impairment of aortic and coronary blood flow[75]. Melatonin is also being evaluated for this use, as it is known to act both as a scavenger of free radicals and as a stimulant of antioxidants[109,110]. It was reported to reduce the development of vasculitis, myocyte necrosis, and fibrosis following high-dose radiation in a rat model[111]. These and several other antioxidant strategies such as the use of selenium[112] show promise and warrant further exploration in animal studies.

TREATMENT

Acute and chronic pericarditis

Acute pericarditis is extremely rare thanks to reductions in the mean heart dose during RT. The clinical presentation may occur during treatment or in the following weeks. In the former instance, pericarditis is typically the result of the presence of a heavy tumor burden adjacent to or extending into the pericardium, and the subsequent tumor lysis. In both instances, the presentation is similar to that of idiopathic acute pericarditis, characterized by fever, pleuritic chest pain, and a pericardial friction rub. ECG may demonstrate low QRS voltage and diffuse ST or T wave changes. Standard transthoracic echocardiography typically demonstrates a pericardial effusion. This syndrome is usually self-limited and responds to treatment with NSAIDs and colchicine, but it may progress to tamponade physiology[37]. Pericardiocentesis is indicated in the event of hemodynamic compromise.

Radiation-induced chronic pericarditis is a more unique disease entity, in that it frequently presents as fibrinous constrictive pericarditis. The most common presentation is as an incidentally discovered asymptomatic effusion, however. This type of pericarditis rarely progresses to tamponade because of its chronicity, and the presentation is similar to that of acute pericarditis. The imaging modality of choice is echocardiography in these patients, for reasons of cost, ease of use, and reproducibility. The latter advantage is critically important in the case of recurrent effusions and symptomatic constrictive pericarditis, which may help the clinician to make appropriate referral for invasive procedures[84]. Cardiac CT and MR, on the other hand, have proven to be more sensitive in the diagnosis of constrictive pericarditis owing to better visualization of pericardial thickening and calcifications. Moreover, cardiac MR is more specific in the diagnosis of constrictive pericarditis, distinguishing it from transient constriction due to active inflammation and effusive-constrictive pericarditis. This can be useful in assessing prognosis and in determining whether or not to proceed with a high-risk pericardiectomy[93].

Recurrent symptomatic effusions may require pericardiectomy, which is also the mainstay treatment of symptomatic constrictive pericarditis. While the procedure does provide benefit to irradiated patients, these patients have poor prognoses, with a 21% perioperative mortality and a 7-year survival rate of just 27%[16,113]. In one study, zero of five patients survived beyond five years[114]. Unfortunately, these mortality rates may reflect both the technical difficulties in operating on the irradiated heart and progression of other forms of RICVD that inevitably follow from large radiation exposures.

RICM

RICM may remain asymptomatic for years before presenting as a typical clinical heart failure syndrome with shortness of breath and other symptoms of volume overload. Diastolic dysfunction is typically the earliest imaging finding in RICM, followed by abnormalities pertaining to strain and strain rate such as discussed in the screening and detection section. Therefore, this new echocardiographic modality is optimal for establishing an early diagnosis of RICM. When a reduction in EF occurs, it is often a late finding. Cardiac MR is appropriate for use in patients with poor acoustic windows and not only detects reductions in EF, but also visualizes the inciting myocardial inflammation and fibrosis[84]. Once RICM has been confirmed, treatment should be initiated per the ACC/AHA guidelines, as there are no drugs specifically approved to treat radiation-induced myocardial inflammation or fibrosis. This is also the case with respect to implantable cardioverter-defibrillator (ICD) placement, as the indications for its use have not been specifically evaluated in RICM. As to the location of ICD implantation, it has been suggested that a sub-pectoral approach may be preferred in order to avoid instrumenting the irradiated superficial tissues[5].

In patients with biventricular heart failure due to radiation-induced restrictive cardiomyopathy, cardiac transplant may be performed as a last resort. Several case series have been published in recent years detailing the outcomes of these cases. The largest was

a 2012 study of patients undergoing transplant for restrictive cardiomyopathy, which included a subgroup of 35 patients with RICM. This group demonstrated 1-, 5- and 10-year transplant survival rates of 71%, 47%, and 32%, respectively - the poorest survival rates amongst all of the subgroups[115]. A 12-subject cohort of patients transplanted for RICM reported a lower mortality, with a 5- and 10-year survival of 75% and 47%[116]. Of note, eight of these patients were transplanted for treatment of restrictive cardiomyopathy. Given the limitation in donor hearts eligible for transplantation, and the large numbers of patients currently on waiting lists, cardiac transplantation is likely to play a very limited role in patients with end-stage RICVD.

VHD

Little has been written about peculiarities of the clinical presentation of radiation-induced VHD. Echocardiographic studies have demonstrated that it typically begins as an asymptomatic regurgitation of the mitral and/or aortic valves, progressing to include aortic stenosis in 39% of patients[25]. Radiation-induced VHD is most commonly diagnosed after a long latent period[117] and in the context of clinical symptoms of heart failure[18], to which valvular insufficiency is either contributing or responsible. When VHD is suspected, *i.e.*, on the basis of a new murmur, transthoracic Doppler echocardiography is the first line of investigation, with transesophageal echocardiography reserved for when the initial evaluation is non-diagnostic[84].

The frequency of radiation-induced VHD is significantly greater than seen in the general population. In a cohort of HL patients, the standardized incidence ratio for valve surgery was found to be 9.19 when compared to the estimated expected national incidence in the United States, though this may be an overestimate, as some of these patients were irradiated under older protocols[118]. Aortic valve replacement was the most common procedure in this cohort, though mitral and tricuspid valve disease may also require intervention. Crestanello *et al*[119] reported that 32% of previously irradiated patients who underwent mitral and/or tricuspid valve repair experienced severe valve deterioration, likely because of progression of radiation-induced tissue injury. In light of these findings and the known dangers of reoperation in this cohort, the authors concluded that mitral and tricuspid valve replacement may be superior to repair in patients with RICVD.

Over the past several years, transcutaneous aortic valve replacement (TAVR) has proven equal or superior to surgical valve replacement in high-risk patients[120,121]. As valve technology and techniques for TAVR have evolved, favorable outcomes are now also being observed in intermediate risk patients. Approximately 5% of patients enrolled in recently published TAVR trials have a history of prior chest wall radiation, with initial favorable results[122]. However, long-term results are unavailable. Nevertheless, TAVR is likely to play an increasingly prominent role in treatment of patients with radiation-induced aortic disease given the associated surgical morbidity/mortality in this high-risk population.

CHD

There is currently no basis of evidence to suggest specific deviations from treatment guidelines for the medical management CHD in patients with a history of mediastinal irradiation. The increased risk of CHD in patients with a history of RT may prompt a more aggressive approach where the etiology of chest pain is in question and/or diagnostic findings are ambiguous. As always, coronary angiography is the gold standard, and clinicians should have a lower threshold to consider it in this population. On the other hand, both percutaneous interventions (PCI) and surgical revascularization are often more challenging and less effective in this population, which must be taken into account. As noted previously, coronary artery lesions tend to be proximal or ostial in this population, and may not be readily amenable to PCI. A prospective study of bare metal stent placement in HL survivors was conducted between 1993 and 2003 and revealed in-stent restenosis in 86% of irradiated patients within the first six months, with an odds ratio for this event of 21.7[123]. Moreover, revascularization of the target vessel with balloon angioplasty was required in 67% of the RT cohort at six months per coronary angiography. However, most of these patients were treated with early generation stents and single antiplatelet therapy. A larger case control study in which 36% of patients received newer drug-eluting stents, and all patients received dual antiplatelet therapy, found no difference in the rate of in-stent restenosis requiring revascularization between irradiated and non-irradiated patients[124]. Drug-eluting stents did not outperform bare metal stents in this study; nevertheless, use of newer generation drug-eluting stents is usually preferred in this population.

Surgical revascularization of the irradiated heart is often necessary, but is not without complication. Operative mortality rates of 6% have been reported, and one- and five-year actuarial survival has been estimated to be 87% and 72%, respectively[125]. Sixty-two percent of patients in the latter cohort required valve surgery concomitantly or after the initial surgery, suggesting that valvular dysfunction is a significant contributor to mortality in this population. In another, larger study of cardiothoracic surgical outcomes in irradiated patients, a dose-dependence was observed with regard to post-operative and long-term mortality data[126]. At lower doses of radiation exposure, breast cancer patients undergoing open-heart surgery were found to approach, but not reach, the levels of 4-year survival expected of the general population, while the outlook for HL patients was much worse (73%, 64% and 57% survival at 1-, 2- and 4-years, respectively). Lastly, irradiated patients often exhibit friability of the left internal mammary artery, a well-known com-

plication encountered when that vessel lies in the irradiated field, which compromises its use as a bypass conduit and diminishes the overall benefit of bypass surgery in patients with RT.

CONCLUSION

Despite advancements in radiation oncology, it appears that cancer survivors treated with breast and mediastinal radiotherapy will continue to present with complicated cardiovascular problems for the foreseeable future. Further research is needed to elucidate pro-fibrotic mechanisms and identify promising therapies that can be implemented early during the course of treatment. The phenotypic shift from fibroblast to myofibroblast is a result of the complex interplay of radiation-induced oxidative stress, inflammation, cell signaling, and epigenetic modifications, which requires further study in animal models. Medications such as ACE inhibitors and statins favorably impact many of these pathways and have shown promise in animal models of RICVD; these agents are just now beginning to be tested in patients who have undergone RT. Novel imaging approaches, such as 3D echocardiography, strain imaging, and CT/MRI scanning, are enabling the detection of early-stage RICVD, which will help to better evaluate risk and facilitate future interventional trials. Evolution of PCI (*i.e.*, transcutaneous valve replacement and drug-eluting stents) holds great potential for improving treatment of patients with RICVD, and these techniques are rapidly gaining favor given their encouraging outcomes and lower complication rates as compared to surgical interventions. Although evidence-based guidelines with respect to screening, prevention and treatment of RICVD are lacking, algorithms have been developed by experts in the field that favor a more aggressive approach than was typically pursued in prior decades. Coordination of care between oncologists, cardiologists, and primary care physicians for the purpose of early detection, risk factor modification and treatment provides the best hope of reducing the morbidity and mortality associated with RICVD.

ACKNOWLEDGMENTS

We thank Dr. Benjamin Mazer for his assistance in the creation of our figures.

REFERENCES

1 **Ng AK**, Bernardo MP, Weller E, Backstrand KH, Silver B, Marcus KC, Tarbell NJ, Friedberg J, Canellos GP, Mauch PM. Long-term survival and competing causes of death in patients with early-stage Hodgkin's disease treated at age 50 or younger. *J Clin Oncol* 2002; **20**: 2101-2108 [PMID: 11956271 DOI: 10.1200/jco.2002.08.021]

2 **American Cancer Society**. Cancer Facts & Figures 2016. Atlanta: American Cancer Society, 2016. Available from: URL: http://www.cancer.org/acs/groups/content/@research/documents/document/acspc-047079.pdf

3 **Darby SC**, McGale P, Taylor CW, Peto R. Long-term mortality from heart disease and lung cancer after radiotherapy for early breast cancer: prospective cohort study of about 300,000 women in US SEER cancer registries. *Lancet Oncol* 2005; **6**: 557-565 [PMID: 16054566 DOI: 10.1016/s1470-2045(05)70251-5]

4 **Clarke M**, Collins R, Darby S, Davies C, Elphinstone P, Evans V, Godwin J, Gray R, Hicks C, James S, MacKinnon E, McGale P, McHugh T, Peto R, Taylor C, Wang Y. Effects of radiotherapy and of differences in the extent of surgery for early breast cancer on local recurrence and 15-year survival: an overview of the randomised trials. *Lancet* 2005; **366**: 2087-2106 [PMID: 16360786]

5 **Jaworski C**, Mariani JA, Wheeler G, Kaye DM. Cardiac complications of thoracic irradiation. *J Am Coll Cardiol* 2013; **61**: 2319-2328 [PMID: 23583253 DOI: 10.1016/j.jacc.2013.01.090]

6 **Stewart FA**, Seemann I, Hoving S, Russell NS. Understanding radiation-induced cardiovascular damage and strategies for intervention. *Clin Oncol* (R Coll Radiol) 2013; **25**: 617-624 [PMID: 23876528 DOI: 10.1016/j.clon.2013.06.012]

7 **Schultz-Hector S**, Trott KR. Radiation-induced cardiovascular diseases: is the epidemiologic evidence compatible with the radiobiologic data? *Int J Radiat Oncol Biol Phys* 2007; **67**: 10-18 [PMID: 17189062]

8 **Andratschke N**, Maurer J, Molls M, Trott KR. Late radiation-induced heart disease after radiotherapy. Clinical importance, radiobiological mechanisms and strategies of prevention. *Radiother Oncol* 2011; **100**: 160-166 [PMID: 20826032 DOI: 10.1016/j.radonc.2010.08.010]

9 **Fajardo LF**, Stewart JR, Cohn KE. Morphology of radiation-induced heart disease. *Arch Pathol* 1968; **86**: 512-519 [PMID: 5681435 DOI: 10.1001/jama.1968.03150100059015]

10 **Fajardo LF**, Stewart JR. Pathogenesis of radiation-induced myocardial fibrosis. *Lab Invest* 1973; **29**: 244-257 [PMID: 4724850]

11 **Veinot JP**, Edwards WD. Pathology of radiation-induced heart disease: a surgical and autopsy study of 27 cases. *Hum Pathol* 1996; **27**: 766-773 [PMID: 8760008 DOI: 10.1016/s0046-8177(96)90447-5]

12 **Brosius FC**, Waller BF, Roberts WC. Radiation heart disease. Analysis of 16 young (aged 15 to 33 years) necropsy patients who received over 3,500 rads to the heart. *Am J Med* 1981; **70**: 519-530 [PMID: 6782873]

13 **Carmel RJ**, Kaplan HS. Mantle irradiation in Hodgkin's disease. An analysis of technique, tumor eradication, and complications. *Cancer* 1976; **37**: 2813-2825 [PMID: 949701 DOI: 10.1002/1097-0142(197606)37]

14 **McGale P**, Darby SC, Hall P, Adolfsson J, Bengtsson NO, Bennet AM, Fornander T, Gigante B, Jensen MB, Peto R, Rahimi K, Taylor CW, Ewertz M. Incidence of heart disease in 35,000 women treated with radiotherapy for breast cancer in Denmark and Sweden. *Radiother Oncol* 2011; **100**: 167-175 [PMID: 21752480 DOI: 10.1016/j.radonc.2011.06.016]

15 **Gaya AM**, Ashford RF. Cardiac complications of radiation therapy. *Clin Oncol* (R Coll Radiol) 2005; **17**: 153-159 [PMID: 15900998 DOI: 10.1016/j.clon.2004.09.016]

16 **Bertog SC**, Thambidorai SK, Parakh K, Schoenhagen P, Ozduran V, Houghtaling PL, Lytle BW, Blackstone EH, Lauer MS, Klein AL. Constrictive pericarditis: etiology and cause-specific survival after pericardiectomy. *J Am Coll Cardiol* 2004; **43**: 1445-1452 [PMID: 15093882 DOI: 10.1016/j.accreview.2004.06.051]

17 **van Nimwegen FA**, Schaapveld M, Janus CP, Krol AD, Petersen EJ, Raemaekers JM, Kok WE, Aleman BM, van Leeuwen FE. Cardiovascular disease after Hodgkin lymphoma treatment: 40-year disease risk. *JAMA Intern Med* 2015; **175**: 1007-1017 [PMID: 25915855 DOI: 10.1001/jamainternmed.2015.1180]

18 **Aleman BM**, van den Belt-Dusebout AW, De Bruin ML, van 't Veer MB, Baaijens MH, de Boer JP, Hart AA, Klokman WJ, Kuenen MA, Ouwens GM, Bartelink H, van Leeuwen FE. Late cardiotoxicity after treatment for Hodgkin lymphoma. *Blood* 2007; **109**: 1878-1886 [PMID: 17119114 DOI: 10.1016/0360-3016(85)90314-1]

19 **Lauk S**, Kiszel Z, Buschmann J, Trott KR. Radiation-induced heart disease in rats. *Int J Radiat Oncol Biol Phys* 1985; **11**: 801-808 [PMID: 3980275]

20 **Marks LB**, Yu X, Prosnitz RG, Zhou SM, Hardenbergh PH, Blazing M, Hollis D, Lind P, Tisch A, Wong TZ, Borges-Neto S. The incidence and functional consequences of RT-associated cardiac perfusion defects. *Int J Radiat Oncol Biol Phys* 2005; **63**: 214-223 [PMID: 16111592 DOI: 10.1016/j.ijrobp.2005.01.029]

21 **Heidenreich PA**, Kapoor JR. Radiation induced heart disease: systemic disorders in heart disease. *Heart* 2009; **95**: 252-258 [PMID: 19144884 DOI: 10.1136/hrt.2008.149088]

22 **Darby SC**, Cutter DJ, Boerma M, Constine LS, Fajardo LF, Kodama K, Mabuchi K, Marks LB, Mettler FA, Pierce LJ, Trott KR, Yeh ET, Shore RE. Radiation-related heart disease: current knowledge and future prospects. *Int J Radiat Oncol Biol Phys* 2010; **76**: 656-665 [PMID: 20159360 DOI: 10.1016/j.ijrobp.2009.09.064]

23 **Heidenreich PA**, Hancock SL, Vagelos RH, Lee BK, Schnittger I. Diastolic dysfunction after mediastinal irradiation. *Am Heart J* 2005; **150**: 977-982 [PMID: 16290974 DOI: 10.1016/j.ahj.2004.12.026]

24 **Heidenreich PA**, Hancock SL, Lee BK, Mariscal CS, Schnittger I. Asymptomatic cardiac disease following mediastinal irradiation. *J Am Coll Cardiol* 2003; **42**: 743-749 [PMID: 12932613 DOI: 10.1016/j.accreview.2003.10.038]

25 **Wethal T**, Lund MB, Edvardsen T, Fosså SD, Pripp AH, Holte H, Kjekshus J, Fosså A. Valvular dysfunction and left ventricular changes in Hodgkin's lymphoma survivors. A longitudinal study. *Br J Cancer* 2009; **101**: 575-581 [PMID: 19623176 DOI: 10.1038/sj.bjc.6605191]

26 **Cutter DJ**, Schaapveld M, Darby SC, Hauptmann M, van Nimwegen FA, Krol AD, Janus CP, van Leeuwen FE, Aleman BM. Risk of valvular heart disease after treatment for Hodgkin lymphoma. *J Natl Cancer Inst* 2015; **107**: pii: djv008 [PMID: 25713164 DOI: 10.1093/jnci/djv008]

27 **Darby SC**, Ewertz M, McGale P, Bennet AM, Blom-Goldman U, Brønnum D, Correa C, Cutter D, Gagliardi G, Gigante B, Jensen MB, Nisbet A, Peto R, Rahimi K, Taylor C, Hall P. Risk of ischemic heart disease in women after radiotherapy for breast cancer. *N Engl J Med* 2013; **368**: 987-998 [PMID: 23484825 DOI: 10.1056/NEJMoa1209825]

28 **Caro-Codón J**, Jiménez-Valero S, Galeote G, Sanchez-Recalde A, Moreno R. Radiation-induced coronary artery disease: Useful insights from OCT. *Int J Cardiol* 2016; **202**: 535-536 [PMID: 26451785 DOI: 10.1016/j.ijcard.2015.09.095]

29 **Imbalzano E**, Trapani G, Creazzo M, Lizio G, Saitta A. Coronary artery disease in radiotherapy. *Int J Cardiol* 2013; **168**: e125-e126 [PMID: 23993725 DOI: 10.1016/j.ijcard.2013.08.037]

30 **Orzan F**, Brusca A, Conte MR, Presbitero P, Figliomeni MC. Severe coronary artery disease after radiation therapy of the chest and mediastinum: clinical presentation and treatment. *Br Heart J* 1993; **69**: 496-500 [PMID: 8343315 DOI: 10.1136/hrt.69.6.496]

31 **Borst GR**, Sonke JJ, den Hollander S, Betgen A, Remeijer P, van Giersbergen A, Russell NS, Elkhuizen PH, Bartelink H, van Vliet-Vroegindeweij C. Clinical results of image-guided deep inspiration breath hold breast irradiation. *Int J Radiat Oncol Biol Phys* 2010; **78**: 1345-1351 [PMID: 20207496 DOI: 10.1016/j.ijrobp.2009.10.006]

32 **Taunk NK**, Haffty BG, Kostis JB, Goyal S. Radiation-induced heart disease: pathologic abnormalities and putative mechanisms. *Front Oncol* 2015; **5**: 39 [PMID: 25741474 DOI: 10.3389/fonc.2015.00039]

33 **Korpela E**, Liu SK. Endothelial perturbations and therapeutic strategies in normal tissue radiation damage. *Radiat Oncol* 2014; **9**: 266 [PMID: 25518850 DOI: 10.1186/s13014-014-0266-7]

34 **Wynn TA**. Fibrotic disease and the T(H)1/T(H)2 paradigm. *Nat Rev Immunol* 2004; **4**: 583-594 [PMID: 15286725 DOI: 10.1038/nri1412]

35 **Haubner F**, Ohmann E, Pohl F, Prantl L, Strutz J, Gassner HG. Effects of radiation on the expression of adhesion molecules and cytokines in a static model of human dermal microvascular endothelial cells. *Clin Hemorheol Microcirc* 2013; **54**: 371-379 [PMID: 23089880 DOI: 10.3233/CH-2012-1626]

36 **Khaled S**, Gupta KB, Kucik DF. Ionizing radiation increases adhesiveness of human aortic endothelial cells via a chemokine-dependent mechanism. *Radiat Res* 2012; **177**: 594-601 [PMID: 22087741 DOI: 10.1667/rr2557.1]

37 **Stewart JR**, Fajardo LF. Radiation-induced heart disease: an update. *Prog Cardiovasc Dis* 1984; **27**: 173-194 [PMID: 6387801 DOI: 10.1016/0033-0620(84)90003-3]

38 **Pathak R**, Shao L, Ghosh SP, Zhou D, Boerma M, Weiler H, Hauer-Jensen M. Thrombomodulin contributes to gamma tocotrienol-mediated lethality protection and hematopoietic cell recovery in irradiated mice. *PLoS One* 2015; **10**: e0122511 [PMID: 25860286 DOI: 10.1371/journal.pone.0122511]

39 **Danckwardt S**, Hentze MW, Kulozik AE. Pathologies at the nexus of blood coagulation and inflammation: thrombin in hemostasis, cancer, and beyond. *J Mol Med* (Berl) 2013; **91**: 1257-1271 [PMID: 23955016 DOI: 10.1007/s00109-013-1074-5]

40 **Wynn TA**. Cellular and molecular mechanisms of fibrosis. *J Pathol* 2008; **214**: 199-210 [PMID: 18161745 DOI: 10.1002/path.2277]

41 **Martin M**, Lefaix J, Delanian S. TGF-beta1 and radiation fibrosis: a master switch and a specific therapeutic target? *Int J Radiat Oncol Biol Phys* 2000; **47**: 277-290 [PMID: 10802350 DOI: 10.1016/s0360-3016(00)00435-1]

42 **May RD**, Fung M. Strategies targeting the IL-4/IL-13 axes in disease. *Cytokine* 2015; **75**: 89-116 [PMID: 26255210 DOI: 10.1016/j.cyto.2015.05.018]

43 **Büttner C**, Skupin A, Reimann T, Rieber EP, Unteregger G, Geyer P, Frank KH. Local production of interleukin-4 during radiation-induced pneumonitis and pulmonary fibrosis in rats: macrophages as a prominent source of interleukin-4. *Am J Respir Cell Mol Biol* 1997; **17**: 315-325 [PMID: 9308918 DOI: 10.1165/ajrcmb.17.3.2279]

44 **Chen J**, Wang Y, Mei Z, Zhang S, Yang J, Li X, Yao Y, Xie C. Radiation-induced lung fibrosis in a tumor-bearing mouse model is associated with enhanced Type-2 immunity. *J Radiat Res* 2016; **57**: 133-141 [PMID: 26703457 DOI: 10.1093/jrr/rrv077]

45 **Xu L**, Xiong S, Guo R, Yang Z, Wang Q, Xiao F, Wang H, Pan X, Zhu M. Transforming growth factor β3 attenuates the development of radiation-induced pulmonary fibrosis in mice by decreasing fibrocyte recruitment and regulating IFN-γ/IL-4 balance. *Immunol Lett* 2014; **162**: 27-33 [PMID: 24996042 DOI: 10.1016/j.imlet.2014.06.010]

46 **Haydont V**, Mathé D, Bourgier C, Abdelali J, Aigueperse J, Bourhis J, Vozenin-Brotons MC. Induction of CTGF by TGF-beta1 in normal and radiation enteritis human smooth muscle cells: Smad/Rho balance and therapeutic perspectives. *Radiother Oncol* 2005; **76**: 219-225 [PMID: 16046020 DOI: 10.1016/j.radonc.2005.06.029]

47 **Lee CH**, Shah B, Moioli EK, Mao JJ. CTGF directs fibroblast differentiation from human mesenchymal stem/stromal cells and defines connective tissue healing in a rodent injury model. *J Clin Invest* 2010; **120**: 3340-3349 [PMID: 20679726 DOI: 10.1172/JCI43230]

48 **Grotendorst GR**, Rahmanie H, Duncan MR. Combinatorial signaling pathways determine fibroblast proliferation and myofibroblast differentiation. *FASEB J* 2004; **18**: 469-479 [PMID: 15003992 DOI: 10.1096/fj.03-0699com]

49 **Holmes A**, Abraham DJ, Sa S, Shiwen X, Black CM, Leask A. CTGF and SMADs, maintenance of scleroderma phenotype is independent of SMAD signaling. *J Biol Chem* 2001; **276**: 10594-10601 [PMID: 11152469 DOI: 10.1074/jbc.m010149200]

50 **Vozenin-Brotons MC**, Milliat F, Sabourin JC, de Gouville AC, François A, Lasser P, Morice P, Haie-Meder C, Lusinchi A, Antoun S, Bourhis J, Mathé D, Girinsky T, Aigueperse J. Fibrogenic signals in patients with radiation enteritis are associated with increased connective tissue growth factor expression. *Int J Radiat Oncol Biol Phys* 2003; **56**: 561-572 [PMID: 12738334 DOI: 10.1016/s0360-3016(02)04601-1]

51 **Lipson KE**, Wong C, Teng Y, Spong S. CTGF is a central mediator of tissue remodeling and fibrosis and its inhibition can reverse the process of fibrosis. *Fibrogenesis Tissue Repair* 2012; **5**: S24 [PMID: 23259531 DOI: 10.1186/1755-1536-5-S1-S24]

52 **Desmoulière A**, Redard M, Darby I, Gabbiani G. Apoptosis mediates the decrease in cellularity during the transition between

granulation tissue and scar. *Am J Pathol* 1995; **146**: 56-66 [PMID: 7856739]
53 **Weigel C**, Schmezer P, Plass C, Popanda O. Epigenetics in radiation-induced fibrosis. *Oncogene* 2015; **34**: 2145-2155 [PMID: 24909163 DOI: 10.1038/onc.2014.145]
54 **Hu B**, Gharaee-Kermani M, Wu Z, Phan SH. Epigenetic regulation of myofibroblast differentiation by DNA methylation. *Am J Pathol* 2010; **177**: 21-28 [PMID: 20489138 DOI: 10.2353/ajpath.2010.090999]
55 **Watson CJ**, Collier P, Tea I, Neary R, Watson JA, Robinson C, Phelan D, Ledwidge MT, McDonald KM, McCann A, Sharaf O, Baugh JA. Hypoxia-induced epigenetic modifications are associated with cardiac tissue fibrosis and the development of a myofibroblast-like phenotype. *Hum Mol Genet* 2014; **23**: 2176-2188 [PMID: 24301681 DOI: 10.1093/hmg/ddt614]
56 **Kim YS**, Kang WS, Kwon JS, Hong MH, Jeong HY, Jeong HC, Jeong MH, Ahn Y. Protective role of 5-azacytidine on myocardial infarction is associated with modulation of macrophage phenotype and inhibition of fibrosis. *J Cell Mol Med* 2014; **18**: 1018-1027 [PMID: 24571348 DOI: 10.1111/jcmm.12248]
57 **Kim EH**, Park AK, Dong SM, Ahn JH, Park WY. Global analysis of CpG methylation reveals epigenetic control of the radiosensitivity in lung cancer cell lines. *Oncogene* 2010; **29**: 4725-4731 [PMID: 20531302 DOI: 10.1038/onc.2010.223]
58 **Antwih DA**, Gabbara KM, Lancaster WD, Ruden DM, Zielske SP. Radiation-induced epigenetic DNA methylation modification of radiation-response pathways. *Epigenetics* 2013; **8**: 839-848 [PMID: 23880508 DOI: 10.4161/epi.25498]
59 **Weigel C**, Veldwijk MR, Oakes CC, Seibold P, Slynko A, Liesenfeld DB, Rabionet M, Hanke SA, Wenz F, Sperk E, Benner A, Rösli C, Sandhoff R, Assenov Y, Plass C, Herskind C, Chang-Claude J, Schmezer P, Popanda O. Epigenetic regulation of diacylglycerol kinase alpha promotes radiation-induced fibrosis. *Nat Commun* 2016; **7**: 10893 [PMID: 26964756 DOI: 10.1038/ncomms10893]
60 **Azzam EI**, Jay-Gerin JP, Pain D. Ionizing radiation-induced metabolic oxidative stress and prolonged cell injury. *Cancer Lett* 2012; **327**: 48-60 [PMID: 22182453 DOI: 10.1016/j.canlet.2011.12.012]
61 **Yarnold J**, Brotons MC. Pathogenetic mechanisms in radiation fibrosis. *Radiother Oncol* 2010; **97**: 149-161 [PMID: 20888056 DOI: 10.1016/j.radonc.2010.09.002]
62 **Madamanchi NR**, Hakim ZS, Runge MS. Oxidative stress in atherogenesis and arterial thrombosis: the disconnect between cellular studies and clinical outcomes. *J Thromb Haemost* 2005; **3**: 254-267 [PMID: 15670030]
63 **Diet A**, Abbas K, Bouton C, Guillon B, Tomasello F, Fourquet S, Toledano MB, Drapier JC. Regulation of peroxiredoxins by nitric oxide in immunostimulated macrophages. *J Biol Chem* 2007; **282**: 36199-36205 [PMID: 17921138 DOI: 10.1074/jbc.m706420200]
64 **Csont T**, Viappiani S, Sawicka J, Slee S, Altarejos JY, Batinić-Haberle I, Schulz R. The involvement of superoxide and iNOS-derived NO in cardiac dysfunction induced by pro-inflammatory cytokines. *J Mol Cell Cardiol* 2005; **39**: 833-840 [PMID: 16171809 DOI: 10.1016/j.yjmcc.2005.07.010]
65 **Mollà M**, Gironella M, Salas A, Closa D, Biete A, Gimeno M, Coronel P, Piqué JM, Panés J. Protective effect of superoxide dismutase in radiation-induced intestinal inflammation. *Int J Radiat Oncol Biol Phys* 2005; **61**: 1159-1166 [PMID: 15752897 DOI: 10.1016/j.ijrobp.2004.11.010]
66 **Akpolat M**, Gulle K, Topcu-Tarladacalisir Y, Safi Oz Z, Bakkal BH, Arasli M, Ozel Turkcu U. Protection by L-carnitine against radiation-induced ileal mucosal injury in the rat: pattern of oxidative stress, apoptosis and cytokines. *Int J Radiat Biol* 2013; **89**: 732-740 [PMID: 23510242 DOI: 10.3109/09553002.2013.787176]
67 **Ross CC**, MacLeod SL, Plaxco JR, Froude JW, Fink LM, Wang J, Stites WE, Hauer-Jensen M. Inactivation of thrombomodulin by ionizing radiation in a cell-free system: possible implications for radiation responses in vascular endothelium. *Radiat Res* 2008; **169**: 408-416 [PMID: 18363428 DOI: 10.1667/RR1148.1]
68 **Jeong BK**, Song JH, Jeong H, Choi HS, Jung JH, Hahm JR, Woo SH, Jung MH, Choi BH, Kim JH, Kang KM. Effect of alpha-lipoic acid on radiation-induced small intestine injury in mice. *Oncotarget* 2016; **7**: 15105-15117 [PMID: 26943777 DOI: 10.18632/oncotarget.7874]
69 **Jang SS**, Kim HG, Lee JS, Han JM, Park HJ, Huh GJ, Son CG. Melatonin reduces X-ray radiation-induced lung injury in mice by modulating oxidative stress and cytokine expression. *Int J Radiat Biol* 2013; **89**: 97-105 [PMID: 23046278 DOI: 10.3109/09553002.2013.734943]
70 **Weintraub NL**, Jones WK, Manka D. Understanding radiation-induced vascular disease. *J Am Coll Cardiol* 2010; **55**: 1237-1239 [PMID: 20298931 DOI: 10.1016/j.jacc.2009.11.053]
71 **Halle M**, Gabrielsen A, Paulsson-Berne G, Gahm C, Agardh HE, Farnebo F, Tornvall P. Sustained inflammation due to nuclear factor-kappa B activation in irradiated human arteries. *J Am Coll Cardiol* 2010; **55**: 1227-1236 [PMID: 20298930 DOI: 10.1016/j.jacc.2009.10.047]
72 **Jackson IL**, Chen L, Batinic-Haberle I, Vujaskovic Z. Superoxide dismutase mimetic reduces hypoxia-induced O2*-, TGF-beta, and VEGF production by macrophages. *Free Radic Res* 2007; **41**: 8-14 [PMID: 17164174 DOI: 10.1080/10715760600913150]
73 **Gabrielli A**, Svegliati S, Moroncini G, Pomponio G, Santillo M, Avvedimento EV. Oxidative stress and the pathogenesis of scleroderma: the Murrell's hypothesis revisited. *Semin Immunopathol* 2008; **30**: 329-337 [PMID: 18548250 DOI: 10.1007/s00281-008-0125-4]
74 **Gremy O**, Benderitter M, Linard C. Acute and persisting Th2-like immune response after fractionated colorectal gamma-irradiation. *World J Gastroenterol* 2008; **14**: 7075-7085 [PMID: 19084914 DOI: 10.3748/wjg.14.7075]
75 **Kruse JJ**, Strootman EG, Wondergem J. Effects of amifostine on radiation-induced cardiac damage. *Acta Oncol* 2003; **42**: 4-9 [PMID: 12665324 DOI: 10.1080/0891060310002168]
76 **Giordano SH**, Kuo YF, Freeman JL, Buchholz TA, Hortobagyi GN, Goodwin JS. Risk of cardiac death after adjuvant radiotherapy for breast cancer. *J Natl Cancer Inst* 2005; **97**: 419-424 [PMID: 15770005 DOI: 10.1016/s1040-1741(08)70038-1]
77 **Yeboa DN**, Evans SB. Contemporary Breast Radiotherapy and Cardiac Toxicity. *Semin Radiat Oncol* 2016; **26**: 71-78 [PMID: 26617212 DOI: 10.1016/j.semradonc.2015.09.003]
78 **Ahmad SS**, Duke S, Jena R, Williams MV, Burnet NG. Advances in radiotherapy. *BMJ* 2012; **345**: e7765 [PMID: 23212681 DOI: 10.1136/bmj.e7765]
79 **Maraldo MV**, Aznar MC, Vogelius IR, Petersen PM, Specht L. Involved node radiation therapy: an effective alternative in early-stage hodgkin lymphoma. *Int J Radiat Oncol Biol Phys* 2013; **85**: 1057-1065 [PMID: 23200817 DOI: 10.1016/j.ijrobp.2012.08.041]
80 **Glanzmann C**, Kaufmann P, Jenni R, Hess OM, Huguenin P. Cardiac risk after mediastinal irradiation for Hodgkin's disease. *Radiother Oncol* 1998; **46**: 51-62 [PMID: 9488128 DOI: 10.1016/s0167-8140(97)00125-4]
81 **van Leeuwen-Segarceanu EM**, Bos WJ, Dorresteijn LD, Rensing BJ, der Heyden JA, Vogels OJ, Biesma DH. Screening Hodgkin lymphoma survivors for radiotherapy induced cardiovascular disease. *Cancer Treat Rev* 2011; **37**: 391-403 [PMID: 21333452 DOI: 10.1016/j.ctrv.2010.12.004]
82 **Ha CS**, Hodgson DC, Advani R, Dabaja BS, Dhakal S, Flowers CR, Hoppe BS, Mendenhall NP, Metzger ML, Plastaras JP, Roberts KB, Shapiro R, Smith S, Terezakis SA, Winkfield KM, Younes A, Constine LS. ACR appropriateness criteria follow-up of Hodgkin lymphoma. *J Am Coll Radiol* 2014; **11**: 1026-1033.e3 [PMID: 25278496 DOI: 10.1016/j.jacr.2014.07.038]
83 **National Comprehensive Cancer Network (NCCN)**. Clinical Practice Guidelines in Oncology. 2015. Available from: URL: http://www.nccn.org/professionals/physician_gls/pdf/hodgkins.pdf
84 **Lancellotti P**, Nkomo VT, Badano LP, Bergler-Klein J, Bogaert J, Davin L, Cosyns B, Coucke P, Dulgheru R, Edvardsen T, Gaemperli O, Galderisi M, Griffin B, Heidenreich PA, Nieman K, Plana JC, Port SC, Scherrer-Crosbie M, Schwartz RG, Sebag IA, Voigt JU, Wann S, Yang PC. Expert consensus for multi-modality imaging evaluation of cardiovascular complications of radiotherapy in

adults: a report from the European Association of Cardiovascular Imaging and the American Society of Echocardiography. *Eur Heart J Cardiovasc Imaging* 2013; **14**: 721-740 [PMID: 23847385 DOI: 10.1093/ehjci/jet123]

85 **Heidenreich PA**, Schnittger I, Strauss HW, Vagelos RH, Lee BK, Mariscal CS, Tate DJ, Horning SJ, Hoppe RT, Hancock SL. Screening for coronary artery disease after mediastinal irradiation for Hodgkin's disease. *J Clin Oncol* 2007; **25**: 43-49 [PMID: 17194904 DOI: 10.1200/jco.2006.07.0805]

86 **Armstrong GT**, Plana JC, Zhang N, Srivastava D, Green DM, Ness KK, Daniel Donovan F, Metzger ML, Arevalo A, Durand JB, Joshi V, Hudson MM, Robison LL, Flamm SD. Screening adult survivors of childhood cancer for cardiomyopathy: comparison of echocardiography and cardiac magnetic resonance imaging. *J Clin Oncol* 2012; **30**: 2876-2884 [PMID: 22802310 DOI: 10.1200/JCO.2011.40.3584]

87 **Pellerin D**, Sharma R, Elliott P, Veyrat C. Tissue Doppler, strain, and strain rate echocardiography for the assessment of left and right systolic ventricular function. *Heart* 2003; **89** Suppl 3: iii9-ii17 [PMID: 14594870 DOI: 10.1136/heart.89.suppl_3.iii9]

88 **Amundsen BH**, Helle-Valle T, Edvardsen T, Torp H, Crosby J, Lyseggen E, Støylen A, Ihlen H, Lima JA, Smiseth OA, Slørdahl SA. Noninvasive myocardial strain measurement by speckle tracking echocardiography: validation against sonomicrometry and tagged magnetic resonance imaging. *J Am Coll Cardiol* 2006; **47**: 789-793 [PMID: 16487846 DOI: 10.1016/j.jacc.2005.10.040]

89 **Erven K**, Jurcut R, Weltens C, Giusca S, Ector J, Wildiers H, Van den Bogaert W, Voigt JU. Acute radiation effects on cardiac function detected by strain rate imaging in breast cancer patients. *Int J Radiat Oncol Biol Phys* 2011; **79**: 1444-1451 [PMID: 20605341 DOI: 10.1016/j.ijrobp.2010.01.004]

90 **Armstrong GT**, Joshi VM, Ness KK, Marwick TH, Zhang N, Srivastava D, Griffin BP, Grimm RA, Thomas J, Phelan D, Collier P, Krull KR, Mulrooney DA, Green DM, Hudson MM, Robison LL, Plana JC. Comprehensive Echocardiographic Detection of Treatment-Related Cardiac Dysfunction in Adult Survivors of Childhood Cancer: Results From the St. Jude Lifetime Cohort Study. *J Am Coll Cardiol* 2015; **65**: 2511-2522 [PMID: 26065990 DOI: 10.1016/j.jacc.2015.04.013]

91 **Umezawa R**, Ota H, Takanami K, Ichinose A, Matsushita H, Saito H, Takase K, Jingu K. MRI findings of radiation-induced myocardial damage in patients with oesophageal cancer. *Clin Radiol* 2014; **69**: 1273-1279 [PMID: 25246336 DOI: 10.1016/j.crad.2014.08.010]

92 **Machann W**, Beer M, Breunig M, Störk S, Angermann C, Seufert I, Schwab F, Kölbl O, Flentje M, Vordermark D. Cardiac magnetic resonance imaging findings in 20-year survivors of mediastinal radiotherapy for Hodgkin's disease. *Int J Radiat Oncol Biol Phys* 2011; **79**: 1117-1123 [PMID: 20385449 DOI: 10.1016/j.ijrobp.2009.12.054]

93 **Aquaro GD**, Barison A, Cagnolo A, Todiere G, Lombardi M, Emdin M. Role of tissue characterization by Cardiac Magnetic Resonance in the diagnosis of constrictive pericarditis. *Int J Cardiovasc Imaging* 2015; **31**: 1021-1031 [PMID: 25827067 DOI: 10.1007/s10554-015-0648-4]

94 **Andersen R**, Wethal T, Günther A, Fosså A, Edvardsen T, Fosså SD, Kjekshus J. Relation of coronary artery calcium score to premature coronary artery disease in survivors & gt; 15 years of Hodgkin's lymphoma. *Am J Cardiol* 2010; **105**: 149-152 [PMID: 20102909 DOI: 10.1016/j.amjcard.2009.09.005]

95 **Wethal T**, Nedregaard B, Andersen R, Fosså A, Lund MB, Günther A, Kvaløy S, Fosså SD, Kjekshus J. Atherosclerotic lesions in lymphoma survivors treated with radiotherapy. *Radiother Oncol* 2014; **110**: 448-454 [PMID: 24231235 DOI: 10.1016/j.radonc.2013.10.029]

96 **Tjessem KH**, Bosse G, Fosså K, Reinertsen KV, Fosså SD, Johansen S, Fosså A. Coronary calcium score in 12-year breast cancer survivors after adjuvant radiotherapy with low to moderate heart exposure - Relationship to cardiac radiation dose and cardiovascular risk factors. *Radiother Oncol* 2015; **114**: 328-334 [PMID: 25600105 DOI: 10.1016/j.radonc.2015.01.006]

97 **Chen AB**, Punglia RS, Kuntz KM, Mauch PM, Ng AK. Cost effectiveness and screening interval of lipid screening in Hodgkin's lymphoma survivors. *J Clin Oncol* 2009; **27**: 5383-5389 [PMID: 19752333 DOI: 10.1200/JCO.2009.22.8460]

98 **Nellessen U**, Zingel M, Hecker H, Bahnsen J, Borschke D. Effects of radiation therapy on myocardial cell integrity and pump function: which role for cardiac biomarkers? *Chemotherapy* 2010; **56**: 147-152 [PMID: 20407242 DOI: 10.1159/000313528]

99 **Skyttä T**, Tuohinen S, Boman E, Virtanen V, Raatikainen P, Kellokumpu-Lehtinen PL. Troponin T-release associates with cardiac radiation doses during adjuvant left-sided breast cancer radiotherapy. *Radiat Oncol* 2015; **10**: 141 [PMID: 26159409 DOI: 10.1186/s13014-015-0436-2]

100 **Haydont V**, Bourgier C, Pocard M, Lusinchi A, Aigueperse J, Mathé D, Bourhis J, Vozenin-Brotons MC. Pravastatin Inhibits the Rho/CCN2/extracellular matrix cascade in human fibrosis explants and improves radiation-induced intestinal fibrosis in rats. *Clin Cancer Res* 2007; **13**: 5331-5340 [PMID: 17875761 DOI: 10.1158/1078-0432.ccr-07-0625]

101 **Fritz G**, Henninger C, Huelsenbeck J. Potential use of HMG-CoA reductase inhibitors (statins) as radioprotective agents. *Br Med Bull* 2011; **97**: 17-26 [PMID: 21252099 DOI: 10.1093/bmb/ldq044]

102 **Ostrau C**, Hülsenbeck J, Herzog M, Schad A, Torzewski M, Lackner KJ, Fritz G. Lovastatin attenuates ionizing radiation-induced normal tissue damage in vivo. *Radiother Oncol* 2009; **92**: 492-499 [PMID: 19615773 DOI: 10.1016/j.radonc.2009.06.020]

103 **Shi J**, Wang J, Zheng H, Ling W, Joseph J, Li D, Mehta JL, Ponnappan U, Lin P, Fink LM, Hauer-Jensen M. Statins increase thrombomodulin expression and function in human endothelial cells by a nitric oxide-dependent mechanism and counteract tumor necrosis factor alpha-induced thrombomodulin downregulation. *Blood Coagul Fibrinolysis* 2003; **14**: 575-585 [PMID: 12960612 DOI: 10.1097/00001721-200309000-00010]

104 **Ran XZ**, Ran X, Zong ZW, Liu DQ, Xiang GM, Su YP, Zheng HE. Protective effect of atorvastatin on radiation-induced vascular endothelial cell injury in vitro. *J Radiat Res* 2010; **51**: 527-533 [PMID: 20921821 DOI: 10.1269/jrr.09119]

105 **University of Minnesota - Clinical and Translational Science Institute**. Statin Therapy in Young Adult Survivors of Childhood Cancer. In: ClinicalTrials.gov [Internet]. Bethesda (MD): National Library of Medicine (US). Available from: URL: https://clinicaltrials.gov/ct2/show/NCT01733953 NLM Identifier: NCT01733953

106 **Ghosh SN**, Zhang R, Fish BL, Semenenko VA, Li XA, Moulder JE, Jacobs ER, Medhora M. Renin-Angiotensin system suppression mitigates experimental radiation pneumonitis. *Int J Radiat Oncol Biol Phys* 2009; **75**: 1528-1536 [PMID: 19931735 DOI: 10.1016/j.ijrobp.2009.07.1743]

107 **Molthen RC**, Wu Q, Fish BL, Moulder JE, Jacobs ER, Medhora MM. Mitigation of radiation induced pulmonary vascular injury by delayed treatment with captopril. *Respirology* 2012; **17**: 1261-1268 [PMID: 22882664 DOI: 10.1111/j.1440-1843.2012.02247.x]

108 **van der Veen SJ**, Ghobadi G, de Boer RA, Faber H, Cannon MV, Nagle PW, Brandenburg S, Langendijk JA, van Luijk P, Coppes RP. ACE inhibition attenuates radiation-induced cardiopulmonary damage. *Radiother Oncol* 2015; **114**: 96-103 [PMID: 25465731 DOI: 10.1016/j.radonc.2014.11.017]

109 **Mihandoost E**, Shirazi A, Mahdavi SR, Aliasgharzadeh A. Can melatonin help us in radiation oncology treatments? *Biomed Res Int* 2014; **2014**: 578137 [PMID: 24900972 DOI: 10.1155/2014/578137]

110 **Shirazi A**, Mihandoost E, Mohseni M, Ghazi-Khansari M, Rabie Mahdavi S. Radio-protective effects of melatonin against irradiation-induced oxidative damage in rat peripheral blood. *Phys Med* 2013; **29**: 65-74 [PMID: 22177584 DOI: 10.1016/j.ejmp.2011.11.00]

111 **Gürses I**, Özeren M, Serin M, Yücel N, Erkal HŞ. Histopathological evaluation of melatonin as a protective agent in heart injury induced by radiation in a rat model. *Pathol Res Pract* 2014; **210**: 863-871 [PMID: 25249491 DOI: 10.1016/j.prp.2014.08.006]

112 **Sieber F**, Muir SA, Cohen EP, Fish BL, Mäder M, Schock AM, Althouse BJ, Moulder JE. Dietary selenium for the mitigation of

radiation injury: effects of selenium dose escalation and timing of supplementation. *Radiat Res* 2011; **176**: 366-374 [PMID: 21867430 DOI: 10.1667/rr2456.1]

113 **Avgerinos D**, Rabitnokov Y, Worku B, Neragi-Miandoab S, Girardi LN. Fifteen-year experience and outcomes of pericardiectomy for constrictive pericarditis. *J Card Surg* 2014; **29**: 434-438 [PMID: 24750218 DOI: 10.1111/jocs.12344]

114 **Szabó G**, Schmack B, Bulut C, Soós P, Weymann A, Stadtfeld S, Karck M. Constrictive pericarditis: risks, aetiologies and outcomes after total pericardiectomy: 24 years of experience. *Eur J Cardiothorac Surg* 2013; **44**: 1023-1028; discussion 1028 [PMID: 23761416 DOI: 10.1093/ejcts/ezt138]

115 **DePasquale EC**, Nasir K, Jacoby DL. Outcomes of adults with restrictive cardiomyopathy after heart transplantation. *J Heart Lung Transplant* 2012; **31**: 1269-1275 [PMID: 23079066 DOI: 10.1016/j.healun.2012.09.018]

116 **Saxena P**, Joyce LD, Daly RC, Kushwaha SS, Schirger JA, Rosedahl J, Dearani JA, Kara T, Edwards BS. Cardiac transplantation for radiation-induced cardiomyopathy: the Mayo Clinic experience. *Ann Thorac Surg* 2014; **98**: 2115-2121 [PMID: 25443015 DOI: 10.1016/j.athoracsur.2014.06.056]

117 **Gujral DM**, Lloyd G, Bhattacharyya S. Radiation-induced valvular heart disease. *Heart* 2015; **pii**: heartjnl-2015-308765 [PMID: 26661320 DOI: 10.1136/heartjnl-2015-308765]

118 **Galper SL**, Yu JB, Mauch PM, Strasser JF, Silver B, Lacasce A, Marcus KJ, Stevenson MA, Chen MH, Ng AK. Clinically significant cardiac disease in patients with Hodgkin lymphoma treated with mediastinal irradiation. *Blood* 2011; **117**: 412-418 [PMID: 20858859 DOI: 10.1182/blood-2010-06-291328]

119 **Crestanello JA**, McGregor CG, Danielson GK, Daly RC, Dearani JA, Orszulak TA, Mullany CJ, Puga FJ, Zehr KJ, Schleck C, Schaff HV. Mitral and tricuspid valve repair in patients with previous mediastinal radiation therapy. *Ann Thorac Surg* 2004; **78**: 826-831; discussion 826-831 [PMID: 15337000 DOI: 10.1016/j.athoracsur.2004.04.008]

120 **Möllmann H**, Bestehorn K, Bestehorn M, Papoutsis K, Fleck E, Ertl G, Kuck KH, Hamm C. In-hospital outcome of transcatheter vs. surgical aortic valve replacement in patients with aortic valve stenosis: complete dataset of patients treated in 2013 in Germany. *Clin Res Cardiol* 2016; **105**: 553-559 [PMID: 26830097 DOI: 10.1007/s00392-016-0962-4]

121 **Adams DH**, Popma JJ, Reardon MJ, Yakubov SJ, Coselli JS, Deeb GM, Gleason TG, Buchbinder M, Hermiller J, Kleiman NS, Chetcuti S, Heiser J, Merhi W, Zorn G, Tadros P, Robinson N, Petrossian G, Hughes GC, Harrison JK, Conte J, Maini B, Mumtaz M, Chenoweth S, Oh JK. Transcatheter aortic-valve replacement with a self-expanding prosthesis. *N Engl J Med* 2014; **370**: 1790-1798 [PMID: 24678937 DOI: 10.1056/NEJMoa1400590]

122 **Beohar N**, Kirtane AJ, Blackstone E, Waksman R, Holmes D, Minha S, Alli O, Suri RM, Svensson LG, Leon M, Kodali S. Trends in Complications and Outcomes of Patients Undergoing Transfemoral Transcatheter Aortic Valve Replacement: Experience From the PARTNER Continued Access Registry. *JACC Cardiovasc Interv* 2016; **9**: 355-363 [PMID: 26803420 DOI: 10.1016/j.jcin.2015.10.050]

123 **Schömig K**, Ndrepepa G, Mehilli J, Pache J, Kastrati A, Schömig A. Thoracic radiotherapy in patients with lymphoma and restenosis after coronary stent placement. *Catheter Cardiovasc Interv* 2007; **70**: 359-365 [PMID: 17722039 DOI: 10.1002/ccd.21109]

124 **Liang JJ**, Sio TT, Slusser JP, Lennon RJ, Miller RC, Sandhu G, Prasad A. Outcomes after percutaneous coronary intervention with stents in patients treated with thoracic external beam radiation for cancer. *JACC Cardiovasc Interv* 2014; **7**: 1412-1420 [PMID: 25459527 DOI: 10.1016/j.jcin.2014.05.035]

125 **Handa N**, McGregor CG, Danielson GK, Orszulak TA, Mullany CJ, Daly RC, Dearani JA, Anderson BJ, Puga FJ. Coronary artery bypass grafting in patients with previous mediastinal radiation therapy. *J Thorac Cardiovasc Surg* 1999; **117**: 1136-1142 [PMID: 10343262 DOI: 10.1016/s0022-5223(99)70250-3]

126 **Chang AS**, Smedira NG, Chang CL, Benavides MM, Myhre U, Feng J, Blackstone EH, Lytle BW. Cardiac surgery after mediastinal radiation: extent of exposure influences outcome. *J Thorac Cardiovasc Surg* 2007; **133**: 404-413 [PMID: 17258573 DOI: 10.1016/j.jtcvs.2006.09.041]

P- Reviewer: Sergio C, Sicari R, Sun Z, Tan XR **S- Editor**: Ji FF
L- Editor: A **E- Editor**: Wu HL

World Journal of Cardiology

Submit a Manuscript: http://www.wjgnet.com/esps/
Help Desk: http://www.wjgnet.com/esps/helpdesk.aspx
DOI: 10.4330/wjc.v8.i9.520

World J Cardiol 2016 September 26; 8(9): 520-533
ISSN 1949-8462 (online)

REVIEW

Noninvasive diagnosis of vulnerable coronary plaque

Eduardo Pozo, Pilar Agudo-Quilez, Antonio Rojas-González, Teresa Alvarado, María José Olivera, Luis Jesús Jiménez-Borreguero, Fernando Alfonso

Eduardo Pozo, Pilar Agudo-Quilez, Antonio Rojas-González, Teresa Alvarado, Luis Jesús Jiménez-Borreguero, Fernando Alfonso, Cardiology Department, Hospital Universitario de La Princesa, IIS-IP, Universidad Autónoma de Madrid, 28006 Madrid, Spain

María José Olivera, Radiology Department, Hospital Universitario de La Princesa, IIS-IP, Universidad Autónoma de Madrid, 28006 Madrid, Spain

Luis Jesús Jiménez-Borreguero, Centro Nacional de Investigaciones Cardiovasculares, 28029 Madrid, Spain

Author contributions: Pozo E performed the majority of the writing and prepared the figures and tables; Agudo-Quilez P, Rojas-González A and Alvarado T assisted in the bibliographic search; Olivera MJ and Jiménez-Borreguero LJ reviewed the final version of the manuscript; Alfonso F coordinated the writing of the paper.

Conflict-of-interest statement: No conflict of interests needs to be declared by any of the authors who contributed to this manuscript.

Manuscript source: Invited manuscript

Correspondence to: Fernando Alfonso, MD, PhD, Cardiology Department, Hospital Universitario de La Princesa, IIS-IP, Universidad Autónoma de Madrid, Calle de Diego León, 62, 28006 Madrid, Spain. falf@hotmail.com
Telephone: +34-91-5202272
Fax: +34-91-5202201

Received: April 29, 2016
Peer-review started: May 3, 2016
First decision: June 17, 2016
Revised: July 8, 2016
Accepted: July 20, 2016
Article in press: July 22, 2016
Published online: September 26, 2016

Abstract

Myocardial infarction and sudden cardiac death are frequently the first manifestation of coronary artery disease. For this reason, screening of asymptomatic coronary atherosclerosis has become an attractive field of research in cardiovascular medicine. Necropsy studies have described histopathological changes associated with the development of acute coronary events. In this regard, thin-cap fibroatheroma has been identified as the main vulnerable coronary plaque feature. Hence, many imaging techniques, such as coronary computed tomography, cardiac magnetic resonance or positron emission tomography, have tried to detect noninvasively these histomorphological characteristics with different approaches. In this article, we review the role of these diagnostic tools in the detection of vulnerable coronary plaque with particular interest in their advantages and limitations as well as the clinical implications of the derived findings.

Key words: Atherosclerosis; Vulnerable coronary plaque; Diagnosis; Cardiac computed tomography; Cardiac magnetic resonance

Core tip: Noninvasive diagnosis of vulnerable coronary plaque has become of major interest in preventive cardiology. Certain histological features have been related with an increased risk of plaque rupture. Coronary computed tomography has been largely used for this aim, and some lesion characteristics have been consistently associated with acute coronary syndrome

in several studies. Moreover, a growing body of evidence suggests the potential role of cardiac magnetic resonance and positron emission tomography in high-risk lesion detection. These promising results should be put in perspective to select the high-risk population that may benefit the most from the use of coronary vulnerable plaque imaging screening.

Pozo E, Agudo-Quilez P, Rojas-González A, Alvarado T, Olivera MJ, Jiménez-Borreguero LJ, Alfonso F. Noninvasive diagnosis of vulnerable coronary plaque. *World J Cardiol* 2016; 8(9): 520-533 Available from: URL: http://www.wjgnet.com/1949-8462/full/v8/i9/520.htm DOI: http://dx.doi.org/10.4330/wjc.v8.i9.520

INTRODUCTION

Atherosclerosis constitutes the leading cause of morbidity and mortality in the developed countries, mostly secondary to acute coronary syndromes (ACS)[1]. Moreover, the progressive aging of the population forecasts an exponential growth of the prevalence of cardiovascular disease[2]. In this clinical scenario, detection of patients at risk of suffering an ACS has become one of the major goals in cardiology. Traditional cardiovascular risk factors have been extensively used for this aim. Nevertheless, they fail to anticipate the occurrence of an ACS, especially in certain populations[3,4], so myocardial infarction and sudden cardiac death (SCD) are frequent first manifestations of coronary disease. This situation has boosted the interest in subclinical detection of atherosclerosis. In this regard, quantification of calcium score with coronary computed tomography (CCT)[5] as well as ultrasound evaluation of carotid atherosclerosis[6,7] have demonstrated their utility for cardiovascular risk reclassification[8,9]. In any case, in spite of a very common detection of coronary atherosclerosis in autopsy series among young adults[10] the incidence of ACS in this population is very low[1]. Thus, the onus should be shifted onto the detection of lesions that are prone to develop a coronary event.

VULNERABLE CORONARY PLAQUE: DEFINITION, HISTOPATHOLOGICAL FEATURES AND RATIONALE FOR NONINVASIVE DIAGNOSIS

Classical studies supported that ACS were caused mainly by lesions with severe stenosis[11]; however, PROSPECT trial[12], a prospective intravascular ultrasound (IVUS) and virtual histology (VH) follow-up of non-culprit lesions after ACS, revealed that most of the events are derived from angiographically mild stenosis (< 50%). Again autopsy studies have provided relevant information regarding the atherosclerotic plaque characteristics in culprit lesions. The most frequent presentation is plaque rupture, followed by plaque erosion[13]. Rarely (2%-7% of the cases) the ACS are related with a calcified nodule morphology[14]. These lesions are unfailingly associated with a variable amount of thrombus[15]. Given that plaque rupture is the most common substrate of acute coronary events, vulnerable plaques are defined as lesions at the greatest risk of rupture, with subsequent thrombosis or rapid stenosis progression (Table 1)[16]. Therefore, they are also named high-risk or thrombosis-prone plaques.

When ruptured plaques leading to acute coronary events were studied in necropsies, they usually presented a large necrotic core with a thin overlying fibrous cap together with inflammatory cells and little calcification[17]. Moreover, unlike lesions related to stable disease, these plaques showed expansive or positive remodeling not causing significant narrowing of the coronary lumen[18]. Thus, plaques with these histomorphologic features but intact fibrous cap, named thin-cap fibroatheroma (TCFA), were assumed to be prone to rupture. This concept was evaluated in a detailed histologic analysis of atherosclerotic plaques from a large series of patients who suffered SCD[19]. This study established a relevance hierarchy of morphological features that may influence plaque rupture. In a general analysis a thin fibrous cap (< 84 μm) was able to exclude stable lesions. Interestingly, among TCFA with a cap thickness < 54 μm cross-section area stenosis was most likely < 74%. Finally, when fibrous cap thickness was not considered in the analysis, inflammation, characterized by macrophage plaque infiltration, as well as a large necrotic core emerged as typical features of potentially unstable lesions. In this regard, aforementioned PROSPECT trial[12] was able to confirm these findings *in vivo* with IVUS. In this study plaque burden $\geqslant$ 70%, minimal luminal area $\leqslant$ 4 mm^2 and TCFA characteristics on VH were independently associated with subsequent major adverse cardiovascular events (MACE) derived from non-culprit lesions.

Some considerations should be kept in mind to understand the clinical relevance of vulnerable plaque detection. All the plaque ruptures do not inevitably cause an ACS[20], whereas disruption and healing is the typical mechanism of plaque stenosis growth[21,22]. Thus, a perfect storm scenario, with confluence of plaque vulnerability, inflammatory state, platelet activation and impaired fibrinolysis, is necessary for ACS occurrence[23]. However, given that substrate presence is a *conditio sine qua non* and the other involved factors (homeostasis disbalance and thrombogenicity) are difficult to establish and/or variable in time, noninvasive detection of vulnerable plaques may be clinically relevant[24], especially in very high risk patients[25].

Hence, in this paper we review the different noninvasive diagnostic tools to evaluate vulnerable coronary plaques, with a detailed description of the relevant information they provide as well as their particular strengths and limitations (Table 2). We focus specially

Table 1 Concepts related to vulnerable coronary plaque[16]

Culprit lesion	Coronary lesion considered to be responsible for the clinical event, usually plaque complicated by intraluminal thrombosis
Thrombosed plaque	Plaque with an overlying thrombus extending into the vessel lumen either occlusive or non-occlusive
Eroded plaque	Thrombosed plaque (mainly fibrotic or proteoglycan-rich) due to loss or dysfunction of endothelial cells without associated rupture
Plaque with calcified nodule	Heavily calcified protruding plaque with loss or dysfunction of endothelial cells
Vulnerable, high-risk or thrombosis prone plaque	Plaque at increased risk of thrombosis and rapid stenosis progression TCFA: Inflamed plaque with a thin cap covering a lipid-rich necrotic core
Vulnerable patient	Patient at high-risk to experience a cardiovascular ischemic event due to a high atherosclerotic burden, high-risk plaques and/or thrombogenic blood

TCFA: Thin-cap fibroatheroma.

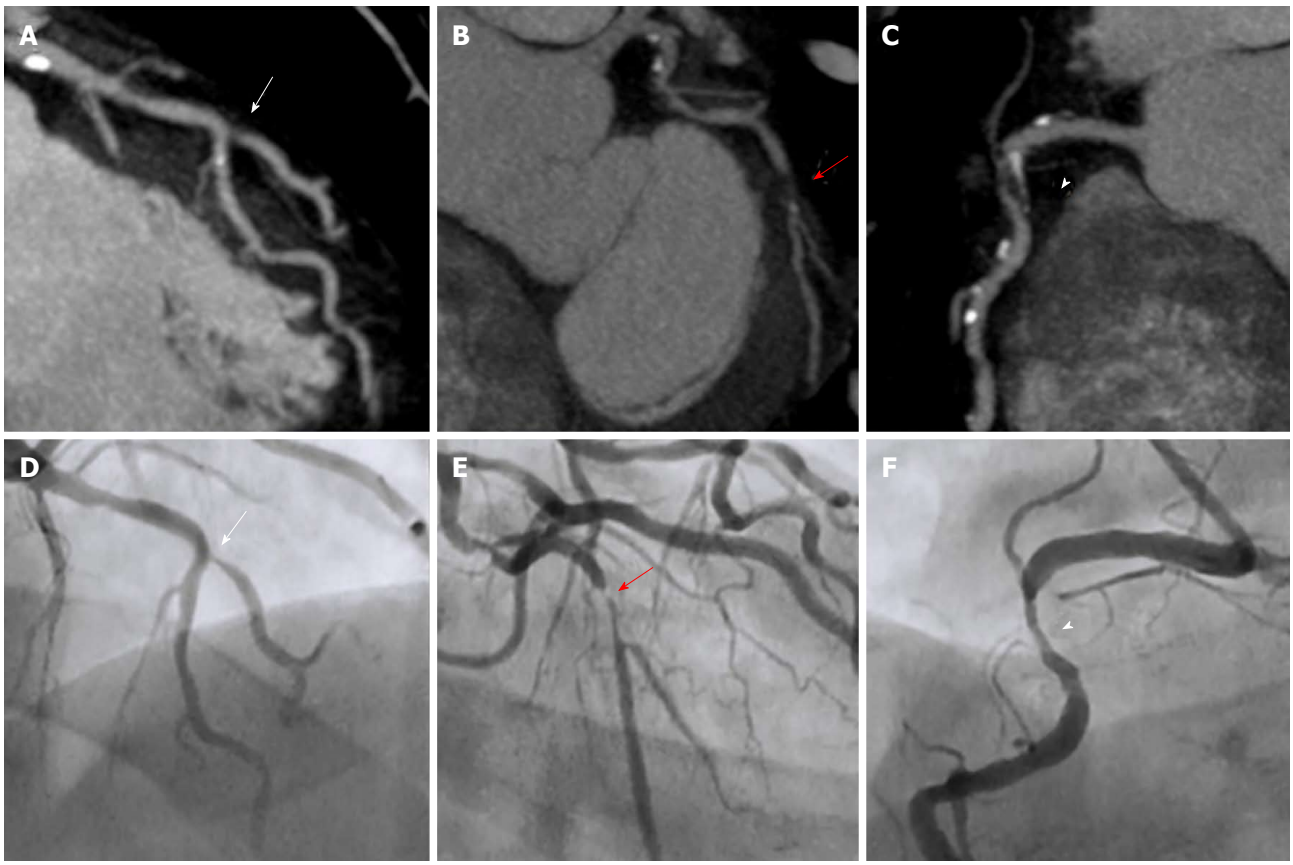

Figure 1 Coronary computed tomography stenosis evaluation compared with invasive coronary angiography. Case of a patient with 3-vessel disease. Maximum intensity projection CCT findings are shown in the upper row with the corresponding ICA projections in the lower row. (A) demonstrates a significant stenosis in the ostium of the diagonal branch (arrow) at the level of its take-off from the mid-LAD in both CCT and ICA (D); In (B) CCT shows a subtotal occlusion in the proximal LCx (red arrow) that corresponds to a critical lesion at the same level in ICA (E); In CCT image from (C) a mixed plaque is detected in proximal RCA causing a significant stenosis (arrowhead), as corroborated by ICA (F). CCT: Coronary computed tomography; ICA: Invasive coronary angiography; LAD: Left anterior descending coronary artery; LCx: Left circumflex coronary artery; RCA: Right coronary artery.

on the technique with the greatest evidence in this field, CCT, mentioning other available imaging tools with promising perspective such as cardiac magnetic resonance (CMR) imaging and positron emission tomography (PET).

CCT

CCT general information with predictive value

CCT not only provides information about the presence of significant stenoses with a high diagnostic accuracy[26] (Figure 1) but also allows a sensitive noninvasive direct evaluation of coronary atherosclerosis[27]. Coronary calcium score determination[28] as well as non-calcified plaque detection, even in the absence of significant stenosis[29-31], have demonstrated their value to predict MACE. Moreover, a large and systematic meta-analysis highlighted the relevance of luminal stenosis severity assessment with CCT[32], showing an increasing risk of the composite end-point of cardiac death or myocardial

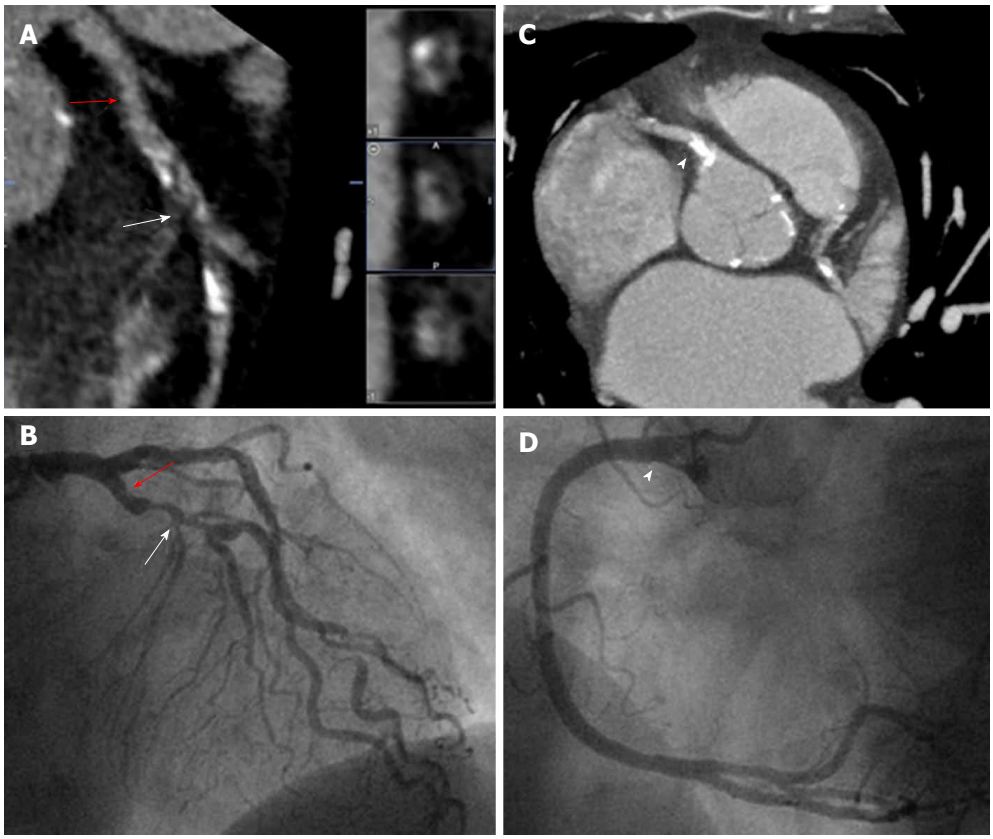

Figure 2 Coronary plaque categories by coronary computed tomography. Patient with chest pain referred for CCT. A: LAD in multiplanar reconstruction with a mixed plaque in the mid segment (arrow) that causes significant stenosis confirmed in the ICA (B, arrow). Note that there is also a nonsignificant noncalcified plaque in the proximal segment (red arrow) that is barely seen in coronariography (B, red arrow); C: A maximum intensity projection that demonstrates a severely calcified plaque in the ostial RCA (arrowhead), which does not allow luminal stenosis evaluation. However, ICA (D) confirms the absence of significant stenosis at the same level (arrowhead). CCT: Coronary computed tomography; LAD: Left anterior descending coronary artery; ICA: Invasive coronary angiography; RCA: Right coronary artery.

Table 2 Diagnostic tests for noninvasive evaluation of coronary vulnerable plaque

	CCT	CMR	PET
Plaque characterization	Plaque morphology	Plaque morphology Tissue characterization of plaque	Inflammation (FDG) Macrophage infiltration (new tracers)
Vulnerable features	Positive remodeling Low attenuation Spotty calcification Napkin-ring sign	Positive remodeling T1 hyperintensity Late gadolinium enhancement	Increased tracer uptake
Clinical relevance	Strong association with ACS Prediction of slow-flow after PCI Evaluation of response to statins	Initial data of association of T1 hyperintense plaques with slow-flow, ACS and response to statins	Differentiation between ACS and stable coronary disease
Limitations	Radiation exposure Heavy calcification Overlap in attenuation ranges Inability to detect plaque erosion	Direct relation between spatial resolution and acquisition time Susceptibility to motion artifacts	Low spatial and temporal resolution Myocardial background uptake Expensive and limited availability

CCT: Coronary computed tomography; CMR: Cardiac magnetic resonance; PET: Positron emission tomography; ACS: Acute coronary syndrome; PCI: Percutaneous coronary intervention; FDG: Fluorodeoxyglucose.

infarction for absence (0.04%), non-obstructive (1.29%) and obstructive (6.53%) coronary artery disease. It has shown a particular utility in chest pain evaluation at the emergency room[33]. There is also data supporting the capacity of CCT to evaluate coronary anatomy to determine the best revascularization strategy[34].

Coronary plaque characterization with CCT

Certainly, the most relevant information is derived from the direct evaluation of coronary plaque with CCT. By consensus[35] the lesions are classified in 3 categories: Non-calcified, calcified and mixed plaques (Figure 2). In this regard, for a further assessment of CCT

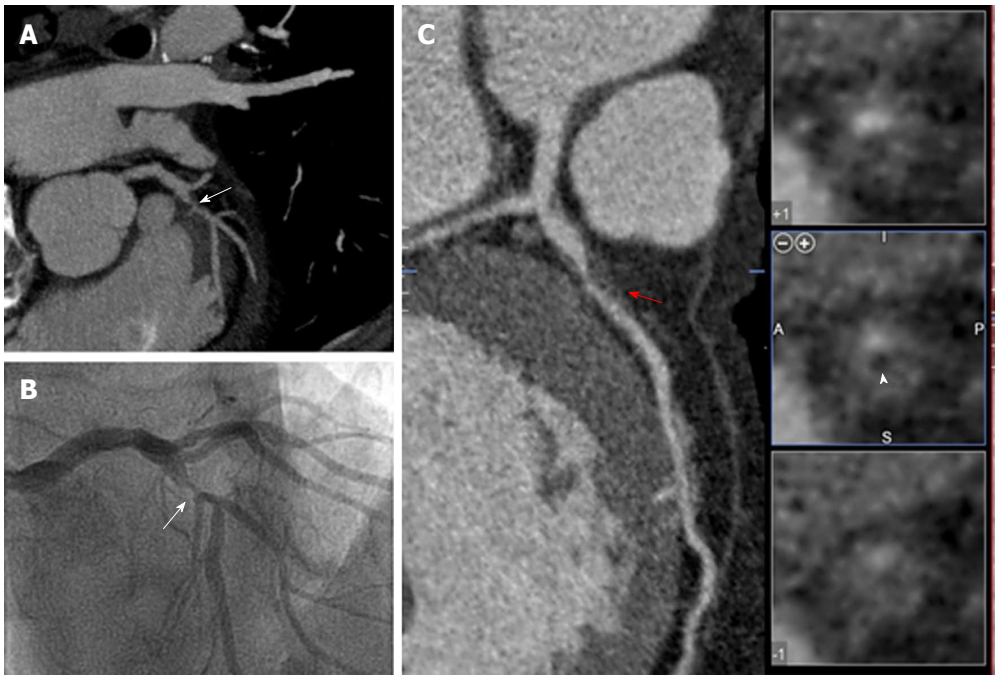

Figure 3 Vulnerable coronary plaque features by coronary computed tomography. Patient with unstable angina who underwent CCT followed by ICA. A severe stenosis (arrows) in mid-LAD just before the origin of the second diagonal was detected in CCT (A) and subsequently confirmed by ICA (B); A detailed analysis of multiplanar reconstruction of CCT (C) revealed the presence of positive remodeling (red arrow) and low attenuation (arrow head) at the level of the culprit lesion, both signs associated with vulnerable coronary plaque. CCT: Coronary computed tomography; ICA: Invasive coronary angiography; LAD: Left anterior descending coronary artery.

accuracy in coronary plaque qualitative analysis, head-to-head comparisons with VH have been performed. Pundziute *et al*[36] found a good correlation between both diagnostic tools in plaque characterization, with more fibrotic and fibro-fatty components in non-calcified plaque. Besides, the majority of TCFA in IVUS corresponded to mixed plaques in CCT. Hereof, Choi *et al*[37] established that plaques with > 10% necrotic core by VH showed significantly lower HU values in CCT. All the studies have shown a good agreement in non-calcified plaque quantification between both techniques[38-40]. However, there were contradictory results in plaque composition analysis using predefined Hounsfield unit (HU) ranges, due to overlapping in these values[38,40]. On the other hand, optical coherence tomography (OCT) has also been used as reference intravascular imaging technique. Kashiwagi *et al*[41] divided plaques in TCFA and non-TCFA according to OCT findings and studied the CCT plaque characteristics. Positive remodeling, lower attenuation values and ring-like enhancement (napkin-ring sign) on CCT were significantly more common in OCT-derived TCFA lesions. The later feature showed a good diagnostic accuracy for high-risk plaque detection and was independently associated with acute events. Moreover, napkin-ring sign has been independently associated with necrotic/lipid core area, non-core plaque area and total vessel area in post-mortem histopathological correlation[42]. However, although the presence of low attenuation and positive remodeling in CCT could identify rupture plaques in another study[43], they failed to differentiate plaque erosions leading to ACS from stable lesions. Lastly, CCT accuracy for plaque composition characterization was also evaluated with near-infrared spectroscopy (NIRS), showing a good correlation of plaque burden and non-calcified plaque area and density with cholesterol deposition in the coronary wall[27].

Thereby, even with first generation 16-rows scanners, culprit lesion characteristics could be evaluated in ACS[44]. When these lesions were compared with those in patients with stable angina, positive expansive remodeling, low attenuation (< 30 HU) non-calcified plaques and spotty calcification were detected more frequently (Figure 3). Furthermore, the combination of these three features increased the positive predictive value to 95%. These findings were corroborated with a prospective multimodal imaging protocol in acute coronary events[45]. Again lower radiological density with lower calcium score and larger remodeling index were more common in culprit lesions. Interestingly, these plaque characteristics were confirmed with IVUS and VH.

Beyond the classical tools for CCT analysis, there are new approaches with promising results in coronary plaque evaluation. Fujimoto *et al*[46] showed that the presence of delayed plaque enhancement in serial CCT acquisition was associated with high-risk plaque features. They hypothesized that this finding may be explained by plaque neovascularization and/or inflammation. In the same direction, a contrast agent formed by iodinated nanoparticles has been probed to detect macrophages in a preclinical model of atherosclerosis[47].

Prognostic relevance of plaque characterization with CCT

The hypothesis that aforementioned morphological patterns are able to identify thrombosis-prone plaques was evaluated in prospective studies. Motoyama *et al*[48] analyzed for the first time CCT plaque characteristics associated with the incidence of ACS in the follow-up. In this study, the presence of positive remodeling and/or low attenuation plaque was independently associated with ACS (HR = 22.8; $P < 0.001$) (Figure 3). Napkin-ring sign is another feature that has been associated with thrombosis-prone plaque. In a large series this sign was the strongest predictor of ACS among the vulnerable plaque characteristics[49]. On the other hand, a case-control study[50] demonstrated that when a semiautomated quantitative analysis of CCT was implemented, total and relative plaque volume and non-calcified plaque were significantly higher in patients who suffered an acute coronary event. This method of evaluation also had additive value to classical cardiovascular risk factors and conventional CCT reading for ACS prediction. Nevertheless, on top of the some methodological limitations[51], there is contradictory results in large prospective series. Among patients derived from ROMICAT Ⅱ cohort[52], acute chest pain in emergency room, presence of a least one of high risk features (positive remodeling, low attenuation, spotty calcification and napkin-ring sign) was an independent predictor of ACS, even after adjustment by clinical risk factors and > 50% or > 70% stenosis[52]. Conversely, when stable patients were evaluated, plaque feature analysis, although improved predictive accuracy, did not significantly increase model discrimination index for acute coronary events[53]. Interestingly, the relevance of high-risk plaque detection on CCT was analyzed in another important cohort from a patient-based and lesion-based perspective[54]. In the former, vulnerable plaque was independently associated with prognosis. However, presence of high-risk features failed to predict ACS in a lesion-based analysis. Additionally, when serial CCT was available, plaque progression emerged as an independent predictor of events. Putting all these data in perspective, although vulnerable plaque CCT features may predict ACS the clinical relevance of these finding still needs to be clarify.

Influence of CCT plaque characteristics in percutaneous coronary interventions outcome was evaluated as well. The incidence of slow-flow phenomenon in patients with stable coronary disease was related with the presence of circumferential plaque calcification, a higher positive remodeling index and a lower plaque density in previous CCT[55]. In fact, circumferential plaque calcification showed the strongest independent association with this complication.

Finally, when CCT was used to evaluate the response to statin therapy[56] a greater decrease of total plaque volume, due to reduction in low attenuation plaque, was detected among patients under treatment, without differences in lumen volume and remodeling index changes between the groups. Thus, CCT may play a role in evaluation of the response to lipid-lowering drugs.

Limitations of CCT in coronary plaque evaluation

Despite the promising data, CCT is far from be free of limitations in vulnerable coronary plaque analysis. First, precise definition of plaque components is hampered by inherent limited spatial resolution of this imaging technique. Thus, results of non-calcified plaque quantification may be inconsistent[39,57]. Moreover, as previously mentioned, CCT plaque characterization is restricted by the overlap in radiological attenuation ranges for the different types of lesions[58,59] (Figure 4). In this regard, dual-source CCT, whose 2 different energies provide differing attenuation of materials, have shown to improve differentiation of necrotic core and fibrous plaque *ex vivo*[60]. Nevertheless, these results worsened when applied *in vivo*[38,60]. Thus, CCT acquisition technology needs to be refined to establish a generalizable HU-based categorization for accurate evaluation of components of the coronary plaque. Second, heavily calcified plaque may obscure detailed plaque evaluation due to partial volume effect. Finally, as previously mentioned, CCT has failed to detect plaque erosion[43], which constitutes the second more frequent presentation of culprit lesions[13].

CMR

CMR not only allows a precise ventricular volume quantification[61] and myocardial tissue characterization[62,63], but also is able to detect the presence of significant (> 50%) coronary atherosclerosis with similar accuracy than CCT[64,65] (Figure 5). In any case, in CMR spatial resolution is directly proportional to scan time. Thus, the necessary high resolution for coronary imaging carries an inherent increased susceptibility to motion artifacts[66]. The most effective measure to optimize image resolution without affecting artifact susceptibility is to reduce the field of view[67], which is difficult if a whole coronary tree analysis is pursued. Apart from that, several strategies have been implemented to avoid aforementioned limitation: Techniques to accelerate image acquisition[68,69], cardiac[70] and respiratory[71] motion compensation and new sampling methods[72,73]. However, even with the last technical advances a whole-heart coronary CMR angiography still takes at least 5 min[74,75], which limits its translation to clinical practice.

Although the aforementioned limitations make the acquisition challenging, non-contrast black-blood sequences have shown a good correlation with IVUS in luminal area and coronary plaque burden determination[76,77]. Interestingly, methemoglobin produced during clot maturation has the potential of shortening T1 relaxation time, which allows coronary thrombus detection with T1-weighted sequences[78,79]. The diagnostic accuracy of this noninvasive technique was

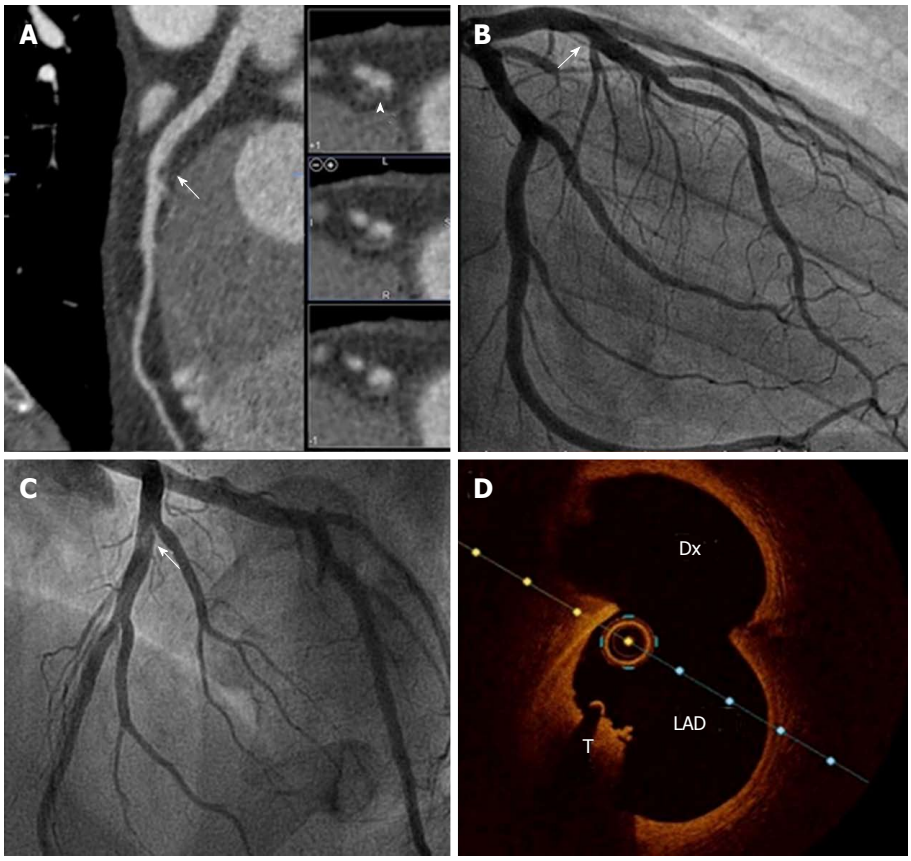

Figure 4 Coronary computed tomography characterization of plaque components. Multimodal evaluation of a mid-LAD lesion in bifurcation with a Dx branch. A: CCT multiplanar reconstruction demonstrates a nonsignificant luminal narrowing in the mid LAD (arrow), and when short axis was evaluated the lesion fulfills noncalcified plaque features (arrowhead); B and C: ICA: The same nonobstructive lesion is observed in mid-LAD (arrow), which seems hyperlucent on LAO cranial projection (C); D: OCT confirms the presence of a red intracoronary thrombus (T) in the same location. CCT: Coronary computed tomography; LAD: Left anterior descending artery; Dx: Diagonal branch; ICA: Invasive coronary angiography; OCT: Optical coherence tomography.

proven to be high when it was evaluated against invasive coronary angiography[80] and OCT[81] (Figure 6). On the other hand, in a head-to-head comparison with CCT the presence of high intensity lesions on T1 sequences was associated with features of vulnerable plaque, such as positive remodeling, low attenuation and spotty calcification[82]. Moreover, this CMR finding was also associated with prognosis: Higher incidence of slow-flow phenomenon after percutaneous coronary intervention[82], coronary events during the follow-up[83], and regression of plaque in response to statin therapy[84]. Finally, T2-weighted sequences have demonstrated their ability to detect coronary vessel wall edema, in probable relation with plaque neovascularization, in initial studies[85,86].

Targeted as well as non-targeted contrast agents have been used to evaluate coronary arteries with CMR. When nonspecific gadolinium contrast is used, the presence of hyperenhancement has been linked to the severity of coronary atherosclerosis[79]. Additionally, a progressive reduction of coronary hyperenhancement has been noted in serial CMR after acute myocardial infarction[87]. Contrarily, many targeted contrast agents, directed to specific components of the plaque, are currently under investigation. Among them some have already reached positive data for coronary evaluation in large animals and/or humans: Fibrin-specific[88-90] and elastin-specific[91] contrast agents, gadofluorine[92,93], albumin-binding[94-96] contrast agent, and iron oxide-based[97] contrast. However, due to the growing field of molecular imaging a detailed discussion of these agents exceed the scope of this review.

PET

Besides the detailed morphological characterization provided by CCT and CMR, quantification of inflammation is a key feature in vulnerable coronary plaque evaluation. In this regard, nuclear imaging techniques have been extensively used for this purpose in atherosclerosis[98,99]. PET is the preferred tool, due to its superior spatial resolution over single photon emission tomography (SPECT), and is usually combined with computed tomography for a better anatomical definition. Fluorodeoxyglucose (FDG) is the most widely used tracer in this field. However, coronary evaluation is hampered by the significant myocardial uptake of FDG. To override this limitation, free fatty myocardial metabolism was favored with a low-carbohydrate high fat preparation[100]. This strategy was initially proven to detect coronary plaque inflammation[101]. Moreover, when coronary PET was evaluated in ACS as well as in stable angina

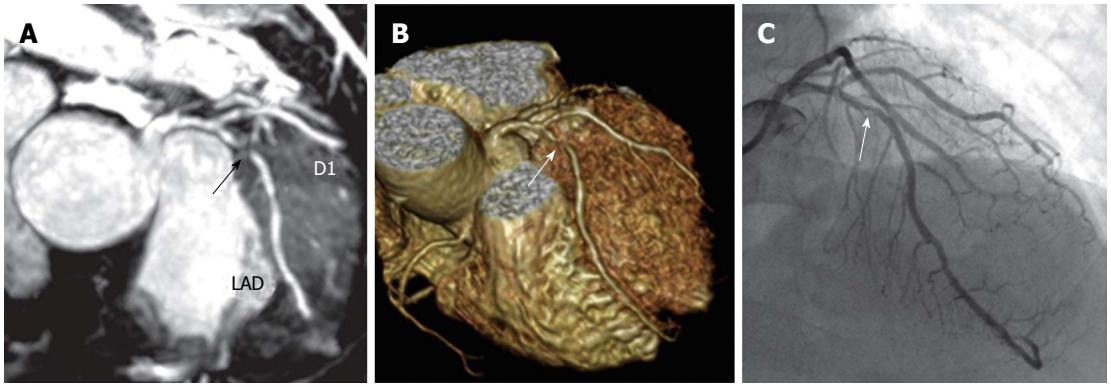

Figure 5 Unenhanced Whole-Heart coronary cardiac magnetic resonance angiography. Correlation of unenhanced whole-heart coronary CMR angiography (A, maximum intensity projection image, and B, volume-rendered image) with invasive coronary angiography (C) in a in a 50-year-old male patient with chest pain on effort. Note the presence of significant stenosis in proximal LAD (arrows). Adapted with permisssion from Nagata *et al*[75]. LAD: Left anterior descending coronary artery; D1: First diagonal branch; CMR: Cardiac magnetic resonance.

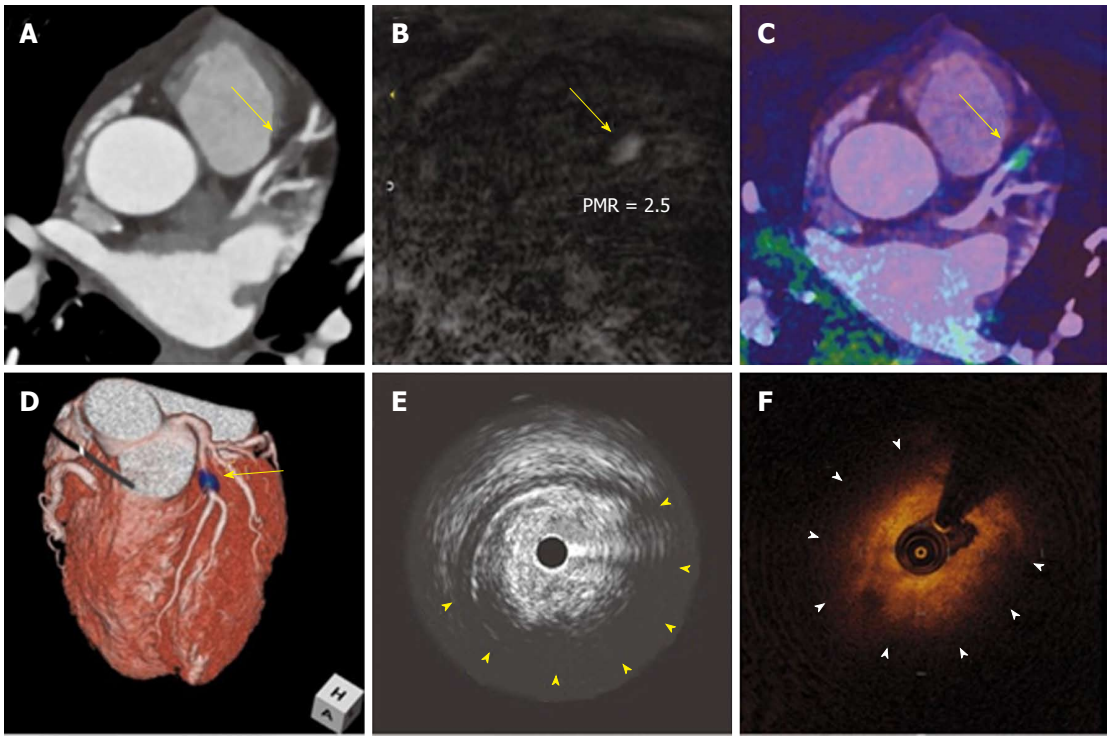

Figure 6 T1 hyperintense coronary plaques in cardiac magnetic resonance. Noninvasive and invasive coronary imaging of a significant plaque in proximal LAD. CCTA (A) showed a noncalcified plaque in LAD causing significant stenosis. When noncontrast T1-weighted CMR imaging was performed (B) a hyperintense lesion was detected. Afterwards, CMR images were fused with CCTA (C and D) and this lesion was found to correspond with the previously described coronary stenosis. Interestingly, during the subsequent coronary angiography it showed a large lipid component in IVUS (E) as well as OCT (F). Adapted with permission from Asaumi *et al*[106]. LAD: Left anterior descending coronary artery; CCTA: Coronary computed tomography; CMR: Cardiac magnetic resonance; IVUS: Intravascular ultrasound; OCT: Optical coherence tomography; PMR: Plaque to myocardium signal intensity ratio.

after stent implantation, a higher FDG uptake was noted not only in the culprit lesions but also in the left main and ascending thoracic aorta of the patients with acute coronary events (Figure 7)[102]. This suggests the presence of spread arterial wall inflammation in the former group. Conversely, Dweck *et al*[103] demonstrated the ability of the new tracer 18F-sodium fluoride to detect coronary atherosclerosis without the limitation of myocardial metabolism artifact. Increased uptake was also associated with coronary calcium score, Framingham risk score, prior cardiovascular events and angina. Lastly, new tracers targeted against other markers of inflammation such as macrophage infiltration (11C-PK11195[104] and 68Ga-DOTATATE[105]) have been successfully tested.

CONCLUSION

Noninvasive imaging tools have shown their capacity to detect features related with vulnerable coronary

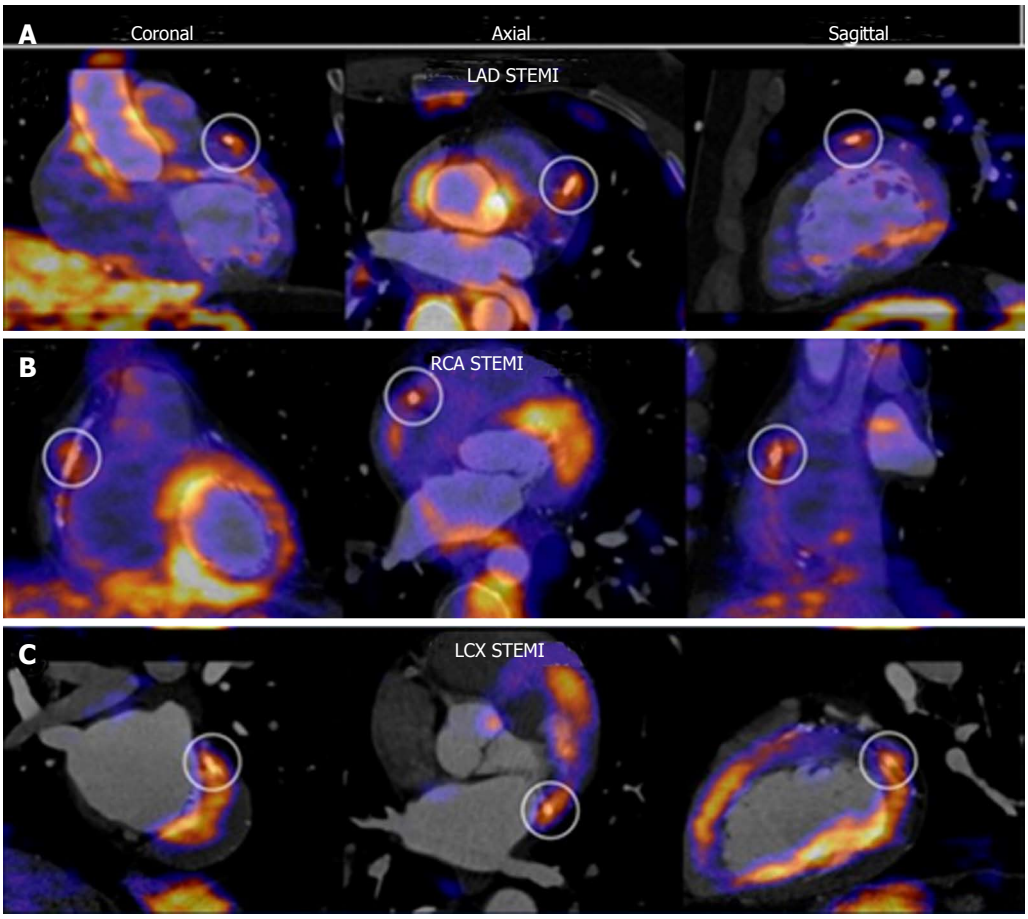

Figure 7 Fluorodeoxyglucose positron emission tomography of the coronary arteries. PET CT fusion imaging in three cases of patients with STEMI. An increased ^{18}F-FDG uptake at stent site is shown in different culprit vessels, from A to C: LAD, RCA and LCX. Adapted with permission from Cheng *et al*[107]. This research was originally published in JNM. ©by the Society of Nuclear Medicine and Molecular Imaging, Inc. FDG: Fluorodeoxyglucose; PET: Positron emission tomography; STEMI: ST elevation myocardial infarction; LAD: Left anterior descending coronary artery; RCA: Right coronary artery; LCX: Left circumflex coronary artery.

plaque. CCT has been largely tested with this aim. Certain plaque characteristics, such as positive remodeling, low attenuation, spotty calcification and napkin-ring sign, have been systematically associated with ACS occurrence. Regarding CMR, results of plaque morphology characterization are similar than CCT but the inherent acquisition limitations hampered its extension to clinical practice. Moreover this technique allows tissue characterization of the coronary plaques through T1- and T2-weighted sequences and contrast-enhanced imaging. Finally, PET has emerged as a promising molecular imaging technique being able to detect coronary inflammation and even macrophage infiltration *in vivo*. In any case, given that the presence of vulnerable plaque features is not irredeemably linked to the occurrence of an ACS, larger studies are needed to clarify the patient subgroup that may benefit from non-invasive detection of high-risk plaques. This aspect is of special interest due to the large population that may be the target of a noninvasive imaging strategy for acute coronary events prevention. In this regard, cost-effectiveness should also be evaluated carefully in the future.

REFERENCES

1 **Mozaffarian D**, Benjamin EJ, Go AS, Arnett DK, Blaha MJ, Cushman M, Das SR, de Ferranti S, Després JP, Fullerton HJ, Howard VJ, Huffman MD, Isasi CR, Jiménez MC, Judd SE, Kissela BM, Lichtman JH, Lisabeth LD, Liu S, Mackey RH, Magid DJ, McGuire DK, Mohler ER, Moy CS, Muntner P, Mussolino ME, Nasir K, Neumar RW, Nichol G, Palaniappan L, Pandey DK, Reeves MJ, Rodriguez CJ, Rosamond W, Sorlie PD, Stein J, Towfighi A, Turan TN, Virani SS, Woo D, Yeh RW, Turner MB. Executive Summary: Heart Disease and Stroke Statistics--2016 Update: A Report From the American Heart Association. *Circulation* 2016; **133**: 447-454 [PMID: 26811276 DOI: 10.1161/CIR.0000000000000366]

2 **Heidenreich PA**, Trogdon JG, Khavjou OA, Butler J, Dracup K, Ezekowitz MD, Finkelstein EA, Hong Y, Johnston SC, Khera A, Lloyd-Jones DM, Nelson SA, Nichol G, Orenstein D, Wilson PW, Woo YJ. Forecasting the future of cardiovascular disease in the United States: a policy statement from the American Heart Association. *Circulation* 2011; **123**: 933-944 [PMID: 21262990 DOI: 10.1161/CIR.0b013e31820a55f5]

3 **Berry JD**, Liu K, Folsom AR, Lewis CE, Carr JJ, Polak JF, Shea S, Sidney S, O'Leary DH, Chan C, Lloyd-Jones DM. Prevalence and progression of subclinical atherosclerosis in younger adults with low short-term but high lifetime estimated risk for cardiovascular disease: the coronary artery risk development in young adults study and multi-ethnic study of atherosclerosis.

Circulation 2009; **119**: 382-389 [PMID: 19139385 DOI: 10.1161/CIRCULATIONAHA.108.800235]
4 **Sibley C**, Blumenthal RS, Merz CN, Mosca L. Limitations of current cardiovascular disease risk assessment strategies in women. *J Womens Health* (Larchmt) 2006; **15**: 54-56 [PMID: 16417419 DOI: 10.1089/jwh.2006.15.54]
5 **Martin SS**, Blaha MJ, Blankstein R, Agatston A, Rivera JJ, Virani SS, Ouyang P, Jones SR, Blumenthal RS, Budoff MJ, Nasir K. Dyslipidemia, coronary artery calcium, and incident atherosclerotic cardiovascular disease: implications for statin therapy from the multi-ethnic study of atherosclerosis. *Circulation* 2014; **129**: 77-86 [PMID: 24141324 DOI: 10.1161/CIRCULATIONAHA.113.003625]
6 **Baber U**, Mehran R, Sartori S, Schoos MM, Sillesen H, Muntendam P, Garcia MJ, Gregson J, Pocock S, Falk E, Fuster V. Prevalence, impact, and predictive value of detecting subclinical coronary and carotid atherosclerosis in asymptomatic adults: the BioImage study. *J Am Coll Cardiol* 2015; **65**: 1065-1074 [PMID: 25790876 DOI: 10.1016/j.jacc.2015.01.017]
7 **Sillesen H**, Muntendam P, Adourian A, Entrekin R, Garcia M, Falk E, Fuster V. Carotid plaque burden as a measure of subclinical atherosclerosis: comparison with other tests for subclinical arterial disease in the High Risk Plaque BioImage study. *JACC Cardiovasc Imaging* 2012; **5**: 681-689 [PMID: 22789936 DOI: 10.1016/j.jcmg.2012.03.013]
8 **Fernández-Friera L**, Peñalvo JL, Fernández-Ortiz A, Ibañez B, López-Melgar B, Laclaustra M, Oliva B, Mocoroa A, Mendiguren J, Martínez de Vega V, García L, Molina J, Sánchez-González J, Guzmán G, Alonso-Farto JC, Guallar E, Civeira F, Sillesen H, Pocock S, Ordovás JM, Sanz G, Jiménez-Borreguero LJ, Fuster V. Prevalence, Vascular Distribution, and Multiterritorial Extent of Subclinical Atherosclerosis in a Middle-Aged Cohort: The PESA (Progression of Early Subclinical Atherosclerosis) Study. *Circulation* 2015; **131**: 2104-2113 [PMID: 25882487 DOI: 10.1161/CIRCULATIONAHA.114.014310]
9 **Naghavi M**, Falk E, Hecht HS, Jamieson MJ, Kaul S, Berman D, Fayad Z, Budoff MJ, Rumberger J, Naqvi TZ, Shaw LJ, Faergeman O, Cohn J, Bahr R, Koenig W, Demirovic J, Arking D, Herrera VL, Badimon J, Goldstein JA, Rudy Y, Airaksinen J, Schwartz RS, Riley WA, Mendes RA, Douglas P, Shah PK. From vulnerable plaque to vulnerable patient--Part III: Executive summary of the Screening for Heart Attack Prevention and Education (SHAPE) Task Force report. *Am J Cardiol* 2006; **98**: 2H-15H [PMID: 16843744 DOI: 10.1016/j.amjcard.2006.03.002]
10 **Nemetz PN**, Roger VL, Ransom JE, Bailey KR, Edwards WD, Leibson CL. Recent trends in the prevalence of coronary disease: a population-based autopsy study of nonnatural deaths. *Arch Intern Med* 2008; **168**: 264-270 [PMID: 18268166 DOI: 10.1001/archinternmed.2007.79]
11 **Ellis S**, Alderman E, Cain K, Fisher L, Sanders W, Bourassa M. Prediction of risk of anterior myocardial infarction by lesion severity and measurement method of stenoses in the left anterior descending coronary distribution: a CASS Registry Study. *J Am Coll Cardiol* 1988; **11**: 908-916 [PMID: 3128587]
12 **Stone GW**, Maehara A, Lansky AJ, de Bruyne B, Cristea E, Mintz GS, Mehran R, McPherson J, Farhat N, Marso SP, Parise H, Templin B, White R, Zhang Z, Serruys PW. A prospective natural-history study of coronary atherosclerosis. *N Engl J Med* 2011; **364**: 226-235 [PMID: 21247313 DOI: 10.1056/NEJMoa1002358]
13 **Virmani R**, Kolodgie FD, Burke AP, Farb A, Schwartz SM. Lessons from sudden coronary death: a comprehensive morphological classification scheme for atherosclerotic lesions. *Arterioscler Thromb Vasc Biol* 2000; **20**: 1262-1275 [PMID: 10807742]
14 **Virmani R**, Burke AP, Farb A, Kolodgie FD. Pathology of the vulnerable plaque. *J Am Coll Cardiol* 2006; **47**: C13-C18 [PMID: 16631505 DOI: 10.1016/j.jacc.2005.10.065]
15 **Kramer MC**, Rittersma SZ, de Winter RJ, Ladich ER, Fowler DR, Liang YH, Kutys R, Carter-Monroe N, Kolodgie FD, van der Wal AC, Virmani R. Relationship of thrombus healing to underlying plaque morphology in sudden coronary death. *J Am Coll Cardiol* 2010; **55**: 122-132 [PMID: 19818571 DOI: 10.1016/j.jacc.2009.09.007]
16 **Schaar JA**, Muller JE, Falk E, Virmani R, Fuster V, Serruys PW, Colombo A, Stefanadis C, Ward Casscells S, Moreno PR, Maseri A, van der Steen AF. Terminology for high-risk and vulnerable coronary artery plaques. Report of a meeting on the vulnerable plaque, June 17 and 18, 2003, Santorini, Greece. *Eur Heart J* 2004; **25**: 1077-1082 [PMID: 15191780 DOI: 10.1016/j.ehj.2004.01.002]
17 **Burke AP**, Farb A, Malcom GT, Liang YH, Smialek J, Virmani R. Coronary risk factors and plaque morphology in men with coronary disease who died suddenly. *N Engl J Med* 1997; **336**: 1276-1282 [PMID: 9113930 DOI: 10.1056/NEJM199705013361802]
18 **Schoenhagen P**, Ziada KM, Kapadia SR, Crowe TD, Nissen SE, Tuzcu EM. Extent and direction of arterial remodeling in stable versus unstable coronary syndromes: an intravascular ultrasound study. *Circulation* 2000; **101**: 598-603 [PMID: 10673250]
19 **Narula J**, Nakano M, Virmani R, Kolodgie FD, Petersen R, Newcomb R, Malik S, Fuster V, Finn AV. Histopathologic characteristics of atherosclerotic coronary disease and implications of the findings for the invasive and noninvasive detection of vulnerable plaques. *J Am Coll Cardiol* 2013; **61**: 1041-1051 [PMID: 23473409 DOI: 10.1016/j.jacc.2012.10.054]
20 **Takano M**, Inami S, Ishibashi F, Okamatsu K, Seimiya K, Ohba T, Sakai S, Mizuno K. Angioscopic follow-up study of coronary ruptured plaques in nonculprit lesions. *J Am Coll Cardiol* 2005; **45**: 652-658 [PMID: 15734606 DOI: 10.1016/j.jacc.2004.09.077]
21 **Burke AP**, Kolodgie FD, Farb A, Weber DK, Malcom GT, Smialek J, Virmani R. Healed plaque ruptures and sudden coronary death: evidence that subclinical rupture has a role in plaque progression. *Circulation* 2001; **103**: 934-940 [PMID: 11181466]
22 **Mann J**, Davies MJ. Mechanisms of progression in native coronary artery disease: role of healed plaque disruption. *Heart* 1999; **82**: 265-268 [PMID: 10455072]
23 **Arbab-Zadeh A**, Nakano M, Virmani R, Fuster V. Acute coronary events. *Circulation* 2012; **125**: 1147-1156 [PMID: 22392862 DOI: 10.1161/CIRCULATIONAHA.111.047431]
24 **Braunwald E**. Noninvasive detection of vulnerable coronary plaques: Locking the barn door before the horse is stolen. *J Am Coll Cardiol* 2009; **54**: 58-59 [PMID: 19555841 DOI: 10.1016/j.jacc.2009.03.040]
25 **Braunwald E**. Epilogue: what do clinicians expect from imagers? *J Am Coll Cardiol* 2006; **47**: C101-C103 [PMID: 16631504 DOI: 10.1016/j.jacc.2005.10.072]
26 **Mowatt G**, Cook JA, Hillis GS, Walker S, Fraser C, Jia X, Waugh N. 64-Slice computed tomography angiography in the diagnosis and assessment of coronary artery disease: systematic review and meta-analysis. *Heart* 2008; **94**: 1386-1393 [PMID: 18669550 DOI: 10.1136/hrt.2008.145292]
27 **Voros S**, Rinehart S, Qian Z, Joshi P, Vazquez G, Fischer C, Belur P, Hulten E, Villines TC. Coronary atherosclerosis imaging by coronary CT angiography: current status, correlation with intravascular interrogation and meta-analysis. *JACC Cardiovasc Imaging* 2011; **4**: 537-548 [PMID: 21565743 DOI: 10.1016/j.jcmg.2011.03.006]
28 **Villines TC**, Taylor AJ. Multi-ethnic study of atherosclerosis arterial age versus framingham 10-year or lifetime cardiovascular risk. *Am J Cardiol* 2012; **110**: 1627-1630 [PMID: 22921999 DOI: 10.1016/j.amjcard.2012.07.018]
29 **Lee MS**, Chun EJ, Kim KJ, Kim JA, Yoo JY, Choi SI. Asymptomatic subjects with zero coronary calcium score: coronary CT angiographic features of plaques in event-prone patients. *Int J Cardiovasc Imaging* 2013; **29** Suppl 1: 29-36 [PMID: 23754773 DOI: 10.1007/s10554-013-0257-z]
30 **Lin FY**, Shaw LJ, Dunning AM, Labounty TM, Choi JH, Weinsaft JW, Koduru S, Gomez MJ, Delago AJ, Callister TQ, Berman DS, Min JK. Mortality risk in symptomatic patients with nonobstructive coronary artery disease: a prospective 2-center study of 2,583 patients undergoing 64-detector row coronary computed tomographic angiography. *J Am Coll Cardiol* 2011; **58**: 510-519 [PMID: 21777749 DOI: 10.1016/j.jacc.2010.11.078]
31 **Yorgun H**, Canpolat U, Aytemir K, Hazırolan T, Sunman H, Ateş

AH, Sahiner L, Karahan S, Kaya EB, Tokgözoğlu L, Kabakçı G, Oto A. Prognosis of patients with mild-moderate coronary artery stenosis detected by coronary computed tomography angiography. *Int J Cardiol* 2013; **168**: 1195-1200 [PMID: 23201082 DOI: 10.1016/j.ijcard.2012.11.066]

32 **Habib PJ**, Green J, Butterfield RC, Kuntz GM, Murthy R, Kraemer DF, Percy RF, Miller AB, Strom JA. Association of cardiac events with coronary artery disease detected by 64-slice or greater coronary CT angiography: a systematic review and meta-analysis. *Int J Cardiol* 2013; **169**: 112-120 [PMID: 24090745 DOI: 10.1016/j.ijcard.2013.08.096]

33 **Alfonso F**, Salamanca J, Pozo E. Diagnóstico de síndrome coronario agudo en pacientes con dolor torácico en urgencias: ¿ cambios a la vista? *Emergencias* 2016; **28**: 6-8

34 **Pozo E**, Álvarez-Acosta L, Alonso D, Pazos-Lopez P, de Siqueira ME, Jacobi A, Narula J, Fuster V, Sanz J. Diagnostic accuracy of coronary ct for the quantification of the syntax score in patients with left main and/or 3-vessel coronary disease. Comparison with invasive angiography. *Int J Cardiol* 2015; **182**: 549-556 [PMID: 25703283 DOI: 10.1016/j.ijcard.2015.01.014]

35 **Wu FZ**, Wu MT. 2014 SCCT guidelines for the interpretation and reporting of coronary CT angiography: a report of the Society of Cardiovascular Computed Tomography Guidelines Committee. *J Cardiovasc Comput Tomogr* 2015; **9**: e3 [PMID: 25708015 DOI: 10.1016/j.jcct.2015.01.003]

36 **Pundziute G**, Schuijf JD, Jukema JW, Decramer I, Sarno G, Vanhoenacker PK, Reiber JH, Schalij MJ, Wijns W, Bax JJ. Head-to-head comparison of coronary plaque evaluation between multislice computed tomography and intravascular ultrasound radiofrequency data analysis. *JACC Cardiovasc Interv* 2008; **1**: 176-182 [PMID: 19463297 DOI: 10.1016/j.jcin.2008.01.007]

37 **Choi BJ**, Kang DK, Tahk SJ, Choi SY, Yoon MH, Lim HS, Kang SJ, Yang HM, Park JS, Zheng M, Hwang GS, Shin JH. Comparison of 64-slice multidetector computed tomography with spectral analysis of intravascular ultrasound backscatter signals for characterizations of noncalcified coronary arterial plaques. *Am J Cardiol* 2008; **102**: 988-993 [PMID: 18929698 DOI: 10.1016/j.amjcard.2008.05.060]

38 **Brodoefel H**, Burgstahler C, Heuschmid M, Reimann A, Khosa F, Kopp A, Schroeder S, Claussen CD, Clouse ME. Accuracy of dual-source CT in the characterisation of non-calcified plaque: use of a colour-coded analysis compared with virtual histology intravascular ultrasound. *Br J Radiol* 2009; **82**: 805-812 [PMID: 19332517 DOI: 10.1259/bjr/35768497]

39 **Otsuka M**, Bruining N, Van Pelt NC, Mollet NR, Ligthart JM, Vourvouri E, Hamers R, De Jaegere P, Wijns W, Van Domburg RT, Stone GW, Veldhof S, Verheye S, Dudek D, Serruys PW, Krestin GP, De Feyter PJ. Quantification of coronary plaque by 64-slice computed tomography: a comparison with quantitative intracoronary ultrasound. *Invest Radiol* 2008; **43**: 314-321 [PMID: 18424952 DOI: 10.1097/RLI.0b013e31816a88a9]

40 **Voros S**, Rinehart S, Qian Z, Vazquez G, Anderson H, Murrieta L, Wilmer C, Carlson H, Taylor K, Ballard W, Karmpaliotis D, Kalynych A, Brown C. Prospective validation of standardized, 3-dimensional, quantitative coronary computed tomographic plaque measurements using radiofrequency backscatter intravascular ultrasound as reference standard in intermediate coronary arterial lesions: results from the ATLANTA (assessment of tissue characteristics, lesion morphology, and hemodynamics by angiography with fractional flow reserve, intravascular ultrasound and virtual histology, and noninvasive computed tomography in atherosclerotic plaques) I study. *JACC Cardiovasc Interv* 2011; **4**: 198-208 [PMID: 21349459 DOI: 10.1016/j.jcin.2010.10.008]

41 **Kashiwagi M**, Tanaka A, Kitabata H, Tsujioka H, Kataiwa H, Komukai K, Tanimoto T, Takemoto K, Takarada S, Kubo T, Hirata K, Nakamura N, Mizukoshi M, Imanishi T, Akasaka T. Feasibility of noninvasive assessment of thin-cap fibroatheroma by multidetector computed tomography. *JACC Cardiovasc Imaging* 2009; **2**: 1412-1419 [PMID: 20083077 DOI: 10.1016/j.jcmg.2009.09.012]

42 **Seifarth H**, Schlett CL, Nakano M, Otsuka F, Károlyi M, Liew G, Maurovich-Horvat P, Alkadhi H, Virmani R, Hoffmann U. Histopathological correlates of the napkin-ring sign plaque in coronary CT angiography. *Atherosclerosis* 2012; **224**: 90-96 [PMID: 22771191 DOI: 10.1016/j.atherosclerosis.2012.06.021]

43 **Ozaki Y**, Okumura M, Ismail TF, Motoyama S, Naruse H, Hattori K, Kawai H, Sarai M, Takagi Y, Ishii J, Anno H, Virmani R, Serruys PW, Narula J. Coronary CT angiographic characteristics of culprit lesions in acute coronary syndromes not related to plaque rupture as defined by optical coherence tomography and angioscopy. *Eur Heart J* 2011; **32**: 2814-2823 [PMID: 21719455 DOI: 10.1093/eurheartj/ehr189]

44 **Motoyama S**, Kondo T, Sarai M, Sugiura A, Harigaya H, Sato T, Inoue K, Okumura M, Ishii J, Anno H, Virmani R, Ozaki Y, Hishida H, Narula J. Multislice computed tomographic characteristics of coronary lesions in acute coronary syndromes. *J Am Coll Cardiol* 2007; **50**: 319-326 [PMID: 17659199 DOI: 10.1016/j.jacc.2007.03.044]

45 **Hernando L**, Corros C, Gonzalo N, Hernández-Antolin R, Bañuelos C, Jiménez-Quevedo P, Bernardo E, Fernández-Ortiz A, Escaned J, Macaya C, Alfonso F. Morphological characteristics of culprit coronary lesions according to clinical presentation: insights from a multimodality imaging approach. *Int J Cardiovasc Imaging* 2013; **29**: 13-21 [PMID: 22527256 DOI: 10.1007/s10554-012-0043-3]

46 **Fujimoto S**, Kondo T, Kodama T, Takase S, Narula J. Delayed plaque enhancement by CT angiography. *JACC Cardiovasc Imaging* 2012; **5**: 1181-1182 [PMID: 23153919 DOI: 10.1016/j.jcmg.2012.01.026]

47 **Hyafil F**, Cornily JC, Feig JE, Gordon R, Vucic E, Amirbekian V, Fisher EA, Fuster V, Feldman LJ, Fayad ZA. Noninvasive detection of macrophages using a nanoparticulate contrast agent for computed tomography. *Nat Med* 2007; **13**: 636-641 [PMID: 17417649 DOI: 10.1038/nm1571]

48 **Motoyama S**, Sarai M, Harigaya H, Anno H, Inoue K, Hara T, Naruse H, Ishii J, Hishida H, Wong ND, Virmani R, Kondo T, Ozaki Y, Narula J. Computed tomographic angiography characteristics of atherosclerotic plaques subsequently resulting in acute coronary syndrome. *J Am Coll Cardiol* 2009; **54**: 49-57 [PMID: 19555840 DOI: 10.1016/j.jacc.2009.02.068]

49 **Otsuka K**, Fukuda S, Tanaka A, Nakanishi K, Taguchi H, Yoshikawa J, Shimada K, Yoshiyama M. Napkin-ring sign on coronary CT angiography for the prediction of acute coronary syndrome. *JACC Cardiovasc Imaging* 2013; **6**: 448-457 [PMID: 23498679 DOI: 10.1016/j.jcmg.2012.09.016]

50 **Versteylen MO**, Kietselaer BL, Dagnelie PC, Joosen IA, Dedic A, Raaijmakers RH, Wildberger JE, Nieman K, Crijns HJ, Niessen WJ, Daemen MJ, Hofstra L. Additive value of semiautomated quantification of coronary artery disease using cardiac computed tomographic angiography to predict future acute coronary syndrome. *J Am Coll Cardiol* 2013; **61**: 2296-2305 [PMID: 23562925 DOI: 10.1016/j.jacc.2013.02.065]

51 **Alfonso F**. Noninvasive detection of vulnerable plaques: are we there yet? *J Am Coll Cardiol* 2010; **55**: 1163; author reply 1163-1164 [PMID: 20223375 DOI: 10.1016/j.jacc.2009.07.076]

52 **Hoffmann U**, Truong QA, Schoenfeld DA, Chou ET, Woodard PK, Nagurney JT, Pope JH, Hauser TH, White CS, Weiner SG, Kalanjian S, Mullins ME, Mikati I, Peacock WF, Zakroysky P, Hayden D, Goehler A, Lee H, Gazelle GS, Wiviott SD, Fleg JL, Udelson JE. Coronary CT angiography versus standard evaluation in acute chest pain. *N Engl J Med* 2012; **367**: 299-308 [PMID: 22830462 DOI: 10.1056/NEJMoa1201161]

53 **Fujimoto S**, Kondo T, Takamura K, Baber U, Shinozaki T, Nishizaki Y, Kawaguchi Y, Matsumori R, Hiki M, Miyauchi K, Daida H, Hecht H, Stone GW, Narula J. Incremental prognostic value of coronary computed tomographic angiography high-risk plaque characteristics in newly symptomatic patients. *J Cardiol* 2016; **67**: 538-544 [PMID: 26359708 DOI: 10.1016/j.jjcc.2015.07.018]

54 **Motoyama S**, Ito H, Sarai M, Kondo T, Kawai H, Nagahara Y, Harigaya H, Kan S, Anno H, Takahashi H, Naruse H, Ishii J,

Hecht H, Shaw LJ, Ozaki Y, Narula J. Plaque Characterization by Coronary Computed Tomography Angiography and the Likelihood of Acute Coronary Events in Mid-Term Follow-Up. *J Am Coll Cardiol* 2015; **66**: 337-346 [PMID: 26205589 DOI: 10.1016/j.jacc.2015.05.069]

55 **Kodama T**, Kondo T, Oida A, Fujimoto S, Narula J. Computed tomographic angiography-verified plaque characteristics and slow-flow phenomenon during percutaneous coronary intervention. *JACC Cardiovasc Interv* 2012; **5**: 636-643 [PMID: 22721658 DOI: 10.1016/j.jcin.2012.02.016]

56 **Inoue K**, Motoyama S, Sarai M, Sato T, Harigaya H, Hara T, Sanda Y, Anno H, Kondo T, Wong ND, Narula J, Ozaki Y. Serial coronary CT angiography-verified changes in plaque characteristics as an end point: evaluation of effect of statin intervention. *JACC Cardiovasc Imaging* 2010; **3**: 691-698 [PMID: 20633846 DOI: 10.1016/j.jcmg.2010.04.011]

57 **Brodoefel H**, Reimann A, Heuschmid M, Tsiflikas I, Kopp AF, Schroeder S, Claussen CD, Clouse ME, Burgstahler C. Characterization of coronary atherosclerosis by dual-source computed tomography and HU-based color mapping: a pilot study. *Eur Radiol* 2008; **18**: 2466-2474 [PMID: 18491107 DOI: 10.1007/s00330-008-1019-5]

58 **Hur J**, Kim YJ, Lee HJ, Nam JE, Choe KO, Seo JS, Choi DH, Kim JS, Choi BW. Quantification and characterization of obstructive coronary plaques using 64-slice computed tomography: a comparison with intravascular ultrasound. *J Comput Assist Tomogr* 2009; **33**: 186-192 [PMID: 19346843 DOI: 10.1097/RCT.0b013e31817c420f]

59 **Sun J**, Zhang Z, Lu B, Yu W, Yang Y, Zhou Y, Wang Y, Fan Z. Identification and quantification of coronary atherosclerotic plaques: a comparison of 64-MDCT and intravascular ultrasound. *AJR Am J Roentgenol* 2008; **190**: 748-754 [PMID: 18287448 DOI: 10.2214/AJR.07.2763]

60 **Obaid DR**, Calvert PA, Gopalan D, Parker RA, West NE, Goddard M, Rudd JH, Bennett MR. Dual-energy computed tomography imaging to determine atherosclerotic plaque composition: a prospective study with tissue validation. *J Cardiovasc Comput Tomogr* 2014; **8**: 230-237 [PMID: 24939072 DOI: 10.1016/j.jcct.2014.04.007]

61 **Hendel RC**, Patel MR, Kramer CM, Poon M, Hendel RC, Carr JC, Gerstad NA, Gillam LD, Hodgson JM, Kim RJ, Kramer CM, Lesser JR, Martin ET, Messer JV, Redberg RF, Rubin GD, Rumsfeld JS, Taylor AJ, Weigold WG, Woodard PK, Brindis RG, Hendel RC, Douglas PS, Peterson ED, Wolk MJ, Allen JM, Patel MR. ACCF/ACR/SCCT/SCMR/ASNC/NASCI/SCAI/SIR 2006 appropriateness criteria for cardiac computed tomography and cardiac magnetic resonance imaging: a report of the American College of Cardiology Foundation Quality Strategic Directions Committee Appropriateness Criteria Working Group, American College of Radiology, Society of Cardiovascular Computed Tomography, Society for Cardiovascular Magnetic Resonance, American Society of Nuclear Cardiology, North American Society for Cardiac Imaging, Society for Cardiovascular Angiography and Interventions, and Society of Interventional Radiology. *J Am Coll Cardiol* 2006; **48**: 1475-1497 [PMID: 17010819 DOI: 10.1016/j.jacc.2006.07.003]

62 **Mahrholdt H**, Wagner A, Judd RM, Sechtem U, Kim RJ. Delayed enhancement cardiovascular magnetic resonance assessment of non-ischaemic cardiomyopathies. *Eur Heart J* 2005; **26**: 1461-1474 [PMID: 15831557 DOI: 10.1093/eurheartj/ehi258]

63 **Sharma V**, Binukrishnan S, Schoepf UJ, Ruzsics B. Myocardial tissue characterization with magnetic resonance imaging. *J Thorac Imaging* 2014; **29**: 318-330 [PMID: 24394716 DOI: 10.1097/RTI.0000000000000053]

64 **Hamdan A**, Asbach P, Wellnhofer E, Klein C, Gebker R, Kelle S, Kilian H, Huppertz A, Fleck E. A prospective study for comparison of MR and CT imaging for detection of coronary artery stenosis. *JACC Cardiovasc Imaging* 2011; **4**: 50-61 [PMID: 21232704 DOI: 10.1016/j.jcmg.2010.10.007]

65 **Yang Q**, Li K, Liu X, Bi X, Liu Z, An J, Zhang A, Jerecic R, Li D. Contrast-enhanced whole-heart coronary magnetic resonance angiography at 3.0-T: a comparative study with X-ray angiography in a single center. *J Am Coll Cardiol* 2009; **54**: 69-76 [PMID: 19555843 DOI: 10.1016/j.jacc.2009.03.016]

66 **Scott AD**, Keegan J, Firmin DN. Motion in cardiovascular MR imaging. *Radiology* 2009; **250**: 331-351 [PMID: 19188310 DOI: 10.1148/radiol.2502071998]

67 **Stuber M**, Botnar RM, Danias PG, Sodickson DK, Kissinger KV, Van Cauteren M, De Becker J, Manning WJ. Double-oblique free-breathing high resolution three-dimensional coronary magnetic resonance angiography. *J Am Coll Cardiol* 1999; **34**: 524-531 [PMID: 10440168]

68 **Lustig M**, Donoho D, Pauly JM. Sparse MRI: The application of compressed sensing for rapid MR imaging. *Magn Reson Med* 2007; **58**: 1182-1195 [PMID: 17969013 DOI: 10.1002/mrm.21391]

69 **Pruessmann KP**, Weiger M, Scheidegger MB, Boesiger P. SENSE: sensitivity encoding for fast MRI. *Magn Reson Med* 1999; **42**: 952-962 [PMID: 10542355]

70 **Fischer SE**, Wickline SA, Lorenz CH. Novel real-time R-wave detection algorithm based on the vectorcardiogram for accurate gated magnetic resonance acquisitions. *Magn Reson Med* 1999; **42**: 361-370 [PMID: 10440961]

71 **Henningsson M**, Koken P, Stehning C, Razavi R, Prieto C, Botnar RM. Whole-heart coronary MR angiography with 2D self-navigated image reconstruction. *Magn Reson Med* 2012; **67**: 437-445 [PMID: 21656563 DOI: 10.1002/mrm.23027]

72 **Meyer CH**, Hu BS, Nishimura DG, Macovski A. Fast spiral coronary artery imaging. *Magn Reson Med* 1992; **28**: 202-213 [PMID: 1461123]

73 **Stehning C**, Börnert P, Nehrke K, Eggers H, Stuber M. Free-breathing whole-heart coronary MRA with 3D radial SSFP and self-navigated image reconstruction. *Magn Reson Med* 2005; **54**: 476-480 [PMID: 16032682 DOI: 10.1002/mrm.20557]

74 **Hu P**, Chan J, Ngo LH, Smink J, Goddu B, Kissinger KV, Goepfert L, Hauser TH, Rofsky NM, Manning WJ, Nezafat R. Contrast-enhanced whole-heart coronary MRI with bolus infusion of gadobenate dimeglumine at 1.5 T. *Magn Reson Med* 2011; **65**: 392-398 [PMID: 21264933 DOI: 10.1002/mrm.22706]

75 **Nagata M**, Kato S, Kitagawa K, Ishida N, Nakajima H, Nakamori S, Ishida M, Miyahara M, Ito M, Sakuma H. Diagnostic accuracy of 1.5-T unenhanced whole-heart coronary MR angiography performed with 32-channel cardiac coils: initial single-center experience. *Radiology* 2011; **259**: 384-392 [PMID: 21406635 DOI: 10.1148/radiol.11101323]

76 **Gerretsen S**, Kessels AG, Nelemans PJ, Dijkstra J, Reiber JH, van der Geest RJ, Katoh M, Waltenberger J, van Engelshoven JM, Botnar RM, Kooi ME, Leiner T. Detection of coronary plaques using MR coronary vessel wall imaging: validation of findings with intravascular ultrasound. *Eur Radiol* 2013; **23**: 115-124 [PMID: 22782568 DOI: 10.1007/s00330-012-2576-1]

77 **He Y**, Zhang Z, Dai Q, Zhou Y, Yang Y, Yu W, An J, Jin L, Jerecic R, Yuan C, Li D. Accuracy of MRI to identify the coronary artery plaque: a comparative study with intravascular ultrasound. *J Magn Reson Imaging* 2012; **35**: 72-78 [PMID: 21989946 DOI: 10.1002/jmri.22652]

78 **Botnar RM**. Coronary plaque characterization by T(1)-weighted cardiac magnetic resonance. *JACC Cardiovasc Imaging* 2009; **2**: 729-730 [PMID: 19520343 DOI: 10.1016/j.jcmg.2009.04.002]

79 **Yeon SB**, Sabir A, Clouse M, Martinezclark PO, Peters DC, Hauser TH, Gibson CM, Nezafat R, Maintz D, Manning WJ, Botnar RM. Delayed-enhancement cardiovascular magnetic resonance coronary artery wall imaging: comparison with multislice computed tomography and quantitative coronary angiography. *J Am Coll Cardiol* 2007; **50**: 441-447 [PMID: 17662397 DOI: 10.1016/j.jacc.2007.03.052]

80 **Jansen CH**, Perera D, Makowski MR, Wiethoff AJ, Phinikaridou A, Razavi RM, Marber MS, Greil GF, Nagel E, Maintz D, Redwood S, Botnar RM. Detection of intracoronary thrombus by magnetic resonance imaging in patients with acute myocardial infarction. *Circulation* 2011; **124**: 416-424 [PMID: 21747055 DOI: 10.1161/CIRCULATIONAHA.110.965442]

81 **Ehara S**, Hasegawa T, Nakata S, Matsumoto K, Nishimura S, Iguchi T, Kataoka T, Yoshikawa J, Yoshiyama M. Hyperintense plaque identified by magnetic resonance imaging relates to intracoronary thrombus as detected by optical coherence tomography in patients with angina pectoris. *Eur Heart J Cardiovasc Imaging* 2012; **13**: 394-399 [PMID: 22277117 DOI: 10.1093/ehjci/jer305]

82 **Kawasaki T**, Koga S, Koga N, Noguchi T, Tanaka H, Koga H, Serikawa T, Orita Y, Ikeda S, Mito T, Goto Y, Shintani Y, Tanaka A, Fukuyama T. Characterization of hyperintense plaque with noncontrast T(1)-weighted cardiac magnetic resonance coronary plaque imaging: comparison with multislice computed tomography and intravascular ultrasound. *JACC Cardiovasc Imaging* 2009; **2**: 720-728 [PMID: 19520342 DOI: 10.1016/j.jcmg.2009.01.016]

83 **Noguchi T**, Kawasaki T, Tanaka A, Yasuda S, Goto Y, Ishihara M, Nishimura K, Miyamoto Y, Node K, Koga N. High-intensity signals in coronary plaques on noncontrast T1-weighted magnetic resonance imaging as a novel determinant of coronary events. *J Am Coll Cardiol* 2014; **63**: 989-999 [PMID: 24345595 DOI: 10.1016/j.jacc.2013.11.034]

84 **Noguchi T**, Tanaka A, Kawasaki T, Goto Y, Morita Y, Asaumi Y, Nakao K, Fujiwara R, Nishimura K, Miyamoto Y, Ishihara M, Ogawa H, Koga N, Narula J, Yasuda S. Effect of Intensive Statin Therapy on Coronary High-Intensity Plaques Detected by Noncontrast T1-Weighted Imaging: The AQUAMARINE Pilot Study. *J Am Coll Cardiol* 2015; **66**: 245-256 [PMID: 26184618 DOI: 10.1016/j.jacc.2015.05.056]

85 **Kim WY**, Christiansen EH, Thrysøe SA, Al-Mashhadi RH, Bøtker HE, Bøttcher M, Holm NR, Falk E. First in vivo demonstration of coronary edema in culprit lesion of patient with acute coronary syndrome by cardiovascular magnetic resonance. *Circ Cardiovasc Imaging* 2011; **4**: 344-346 [PMID: 21586745 DOI: 10.1161/CIRCIMAGING.110.963074]

86 **Pedersen SF**, Thrysøe SA, Paaske WP, Thim T, Falk E, Ringgaard S, Kim WY. Determination of edema in porcine coronary arteries by T2 weighted cardiovascular magnetic resonance. *J Cardiovasc Magn Reson* 2011; **13**: 52 [PMID: 21936914 DOI: 10.1186/1532-429X-13-52]

87 **Ibrahim T**, Makowski MR, Jankauskas A, Maintz D, Karch M, Schachoff S, Manning WJ, Schömig A, Schwaiger M, Botnar RM. Serial contrast-enhanced cardiac magnetic resonance imaging demonstrates regression of hyperenhancement within the coronary artery wall in patients after acute myocardial infarction. *JACC Cardiovasc Imaging* 2009; **2**: 580-588 [PMID: 19442944 DOI: 10.1016/j.jcmg.2008.12.029]

88 **Botnar RM**, Perez AS, Witte S, Wiethoff AJ, Laredo J, Hamilton J, Quist W, Parsons EC, Vaidya A, Kolodziej A, Barrett JA, Graham PB, Weisskoff RM, Manning WJ, Johnstone MT. In vivo molecular imaging of acute and subacute thrombosis using a fibrin-binding magnetic resonance imaging contrast agent. *Circulation* 2004; **109**: 2023-2029 [PMID: 15066940 DOI: 10.1161/01.CIR.0000127034.50006.C0]

89 **Flacke S**, Fischer S, Scott MJ, Fuhrhop RJ, Allen JS, McLean M, Winter P, Sicard GA, Gaffney PJ, Wickline SA, Lanza GM. Novel MRI contrast agent for molecular imaging of fibrin: implications for detecting vulnerable plaques. *Circulation* 2001; **104**: 1280-1285 [PMID: 11551880]

90 **Spuentrup E**, Botnar RM, Wiethoff AJ, Ibrahim T, Kelle S, Katoh M, Ozgun M, Nagel E, Vymazal J, Graham PB, Günther RW, Maintz D. MR imaging of thrombi using EP-2104R, a fibrin-specific contrast agent: initial results in patients. *Eur Radiol* 2008; **18**: 1995-2005 [PMID: 18425519 DOI: 10.1007/s00330-008-0965-2]

91 **Makowski MR**, Wiethoff AJ, Blume U, Cuello F, Warley A, Jansen CH, Nagel E, Razavi R, Onthank DC, Cesati RR, Marber MS, Schaeffter T, Smith A, Robinson SP, Botnar RM. Assessment of atherosclerotic plaque burden with an elastin-specific magnetic resonance contrast agent. *Nat Med* 2011; **17**: 383-388 [PMID: 21336283 DOI: 10.1038/nm.2310]

92 **Sirol M**, Itskovich VV, Mani V, Aguinaldo JG, Fallon JT, Misselwitz B, Weinmann HJ, Fuster V, Toussaint JF, Fayad ZA. Lipid-rich atherosclerotic plaques detected by gadofluorine-enhanced in vivo magnetic resonance imaging. *Circulation* 2004; **109**: 2890-2896 [PMID: 15184290 DOI: 10.1161/01.CIR.0000129310.17277.E7]

93 **Ronald JA**, Chen Y, Belisle AJ, Hamilton AM, Rogers KA, Hegele RA, Misselwitz B, Rutt BK. Comparison of gadofluorine-M and Gd-DTPA for noninvasive staging of atherosclerotic plaque stability using MRI. *Circ Cardiovasc Imaging* 2009; **2**: 226-234 [PMID: 19808597 DOI: 10.1161/CIRCIMAGING.108.826826]

94 **Lobbes MB**, Heeneman S, Passos VL, Welten R, Kwee RM, van der Geest RJ, Wiethoff AJ, Caravan P, Misselwitz B, Daemen MJ, van Engelshoven JM, Leiner T, Kooi ME. Gadofosveset-enhanced magnetic resonance imaging of human carotid atherosclerotic plaques: a proof-of-concept study. *Invest Radiol* 2010; **45**: 275-281 [PMID: 20351652 DOI: 10.1097/RLI.0b013e3181d5466b]

95 **Pedersen SF**, Thrysøe SA, Paaske WP, Thim T, Falk E, Ringgaard S, Kim WY. CMR assessment of endothelial damage and angiogenesis in porcine coronary arteries using gadofosveset. *J Cardiovasc Magn Reson* 2011; **13**: 10 [PMID: 21269470 DOI: 10.1186/1532-429X-13-10]

96 **Phinikaridou A**, Andia ME, Protti A, Indermuehle A, Shah A, Smith A, Warley A, Botnar RM. Noninvasive magnetic resonance imaging evaluation of endothelial permeability in murine atherosclerosis using an albumin-binding contrast agent. *Circulation* 2012; **126**: 707-719 [PMID: 22753191 DOI: 10.1161/CIRCULATIONAHA.112.092098]

97 **Alam SR**, Shah AS, Richards J, Lang NN, Barnes G, Joshi N, MacGillivray T, McKillop G, Mirsadraee S, Payne J, Fox KA, Henriksen P, Newby DE, Semple SI. Ultrasmall superparamagnetic particles of iron oxide in patients with acute myocardial infarction: early clinical experience. *Circ Cardiovasc Imaging* 2012; **5**: 559-565 [PMID: 22875883 DOI: 10.1161/CIRCIMAGING.112.974907]

98 **Rudd JH**, Hyafil F, Fayad ZA. Inflammation imaging in atherosclerosis. *Arterioscler Thromb Vasc Biol* 2009; **29**: 1009-1016 [PMID: 19304673 DOI: 10.1161/ATVBAHA.108.165563]

99 **Sanz J**, Fayad ZA. Imaging of atherosclerotic cardiovascular disease. *Nature* 2008; **451**: 953-957 [PMID: 18288186 DOI: 10.1038/nature06803]

100 **Wykrzykowska J**, Lehman S, Williams G, Parker JA, Palmer MR, Varkey S, Kolodny G, Laham R. Imaging of inflamed and vulnerable plaque in coronary arteries with 18F-FDG PET/CT in patients with suppression of myocardial uptake using a low-carbohydrate, high-fat preparation. *J Nucl Med* 2009; **50**: 563-568 [PMID: 19289431 DOI: 10.2967/jnumed.108.055616]

101 **Alexanderson E**, Slomka P, Cheng V, Meave A, Saldaña Y, García-Rojas L, Berman D. Fusion of positron emission tomography and coronary computed tomographic angiography identifies fluorine 18 fluorodeoxyglucose uptake in the left main coronary artery soft plaque. *J Nucl Cardiol* 2008; **15**: 841-843 [PMID: 18984461 DOI: 10.1007/BF03007367]

102 **Rogers IS**, Nasir K, Figueroa AL, Cury RC, Hoffmann U, Vermylen DA, Brady TJ, Tawakol A. Feasibility of FDG imaging of the coronary arteries: comparison between acute coronary syndrome and stable angina. *JACC Cardiovasc Imaging* 2010; **3**: 388-397 [PMID: 20394901 DOI: 10.1016/j.jcmg.2010.01.004]

103 **Dweck MR**, Chow MW, Joshi NV, Williams MC, Jones C, Fletcher AM, Richardson H, White A, McKillop G, van Beek EJ, Boon NA, Rudd JH, Newby DE. Coronary arterial 18F-sodium fluoride uptake: a novel marker of plaque biology. *J Am Coll Cardiol* 2012; **59**: 1539-1548 [PMID: 22516444 DOI: 10.1016/j.jacc.2011.12.037]

104 **Gaemperli O**, Shalhoub J, Owen DR, Lamare F, Johansson S, Fouladi N, Davies AH, Rimoldi OE, Camici PG. Imaging intraplaque inflammation in carotid atherosclerosis with 11C-PK11195 positron emission tomography/computed tomography. *Eur Heart J* 2012; **33**: 1902-1910 [PMID: 21933781 DOI: 10.1093/eurheartj/ehr367]

105 **Rominger A**, Saam T, Vogl E, Ubleis C, la Fougère C, Förster S, Haug A, Cumming P, Reiser MF, Nikolaou K, Bartenstein P, Hacker M. In vivo imaging of macrophage activity in the coronary arteries using 68Ga-DOTATATE PET/CT: correlation with coronary calcium burden and risk factors. *J Nucl Med* 2010; **51**: 193-197 [PMID: 20080898 DOI: 10.2967/jnumed.109.070672]

106 **Asaumi Y**, Noguchi T, Morita Y, Matsuyama TA, Otsuka F,

Fujiwara R, Kanaya T, Nagai T, Higashi M, Kusano K, Anzai T, Ishibashi-Ueda H, Ogawa H, Yasuda S. Non-contrast T1-weighted magnetic resonance imaging at 3.0 Tesla in a patient undergoing elective percutaneous coronary intervention – clinical and pathological significance of high-intensity plaque. *Circ J* 2015; **79**: 218-220 [PMID: 25342532 DOI: 10.1253/circj.CJ-14-0897]

107 **Cheng VY**, Slomka PJ, Le Meunier L, Tamarappoo BK, Nakazato R, Dey D, Berman DS. Coronary arterial 18F-FDG uptake by fusion of PET and coronary CT angiography at sites of percutaneous stenting for acute myocardial infarction and stable coronary artery disease. *J Nucl Med* 2012; **53**: 575-583 [PMID: 22419753 DOI: 10.2967/jnumed.111.097550]

P- Reviewer: Dominguez-Rodriguez A, Kusmic C, Puddu PE, Siegel C
S- Editor: Ji FF **L- Editor**: A **E- Editor**: Wu HL

World Journal of Cardiology

Submit a Manuscript: http://www.wjgnet.com/esps/
Help Desk: http://www.wjgnet.com/esps/helpdesk.aspx
DOI: 10.4330/wjc.v8.i9.534

World J Cardiol 2016 September 26; 8(9): 534-546
ISSN 1949-8462 (online)

REVIEW

Role of radionuclide imaging for diagnosis of device and prosthetic valve infections

Jean-François Sarrazin, François Philippon, Mikaël Trottier, Michel Tessier

Jean-François Sarrazin, François Philippon, Department of Cardiology, Institut Universitaire de Cardiologie et Pneumologie de Québec, Laval University, Québec, QC G1V 4G5, Canada

Mikaël Trottier, Michel Tessier, Department of Nuclear Medicine, Institut Universitaire de Cardiologie et Pneumologie de Québec, Laval University, Québec, QC G1V 4G5, Canada

Author contributions: Sarrazin JF, Philippon F, Trottier M and Tessier M drafted the article or made critical revisions to the manuscript and gave their final approval of the version of the article to be published.

Conflict-of-interest statement: No conflicts of interest.

Manuscript source: Invited manuscript

Correspondence to: Jean-François Sarrazin, MD, FRCPC, FACC, FHRS, Department of Cardiology, Institut Universitaire de Cardiologie et Pneumologie de Québec, Laval University, 2725 chemin Sainte-Foy, Quebec, QC G1V 4G5, Canada. jean-francois.sarrazin@criucpq.ulaval.ca
Telephone: +1-418-6564598
Fax: +1-418-6564581

Received: April 24, 2016
Peer-review started: April 25, 2016
First decision: June 6, 2016
Revised: July 7, 2016
Accepted: July 20, 2016
Article in press: July 22, 2016
Published online: September 26, 2016

Abstract

Cardiovascular implantable electronic device (CIED) infection and prosthetic valve endocarditis (PVE) remain a diagnostic challenge. Cardiac imaging plays an important role in the diagnosis and management of patients with CIED infection or PVE. Over the past few years, cardiac radionuclide imaging has gained a key role in the diagnosis of these patients, and in assessing the need for surgery, mainly in the most difficult cases. Both ^{18}F-fluorodeoxyglucose positron emission tomography/computed tomography (^{18}F-FDG PET/CT) and radiolabelled white blood cell single-photon emission computed tomography/computed tomography (WBC SPECT/CT) have been studied in these situations. In their 2015 guidelines for the management of infective endocarditis, the European Society of Cardiology incorporated cardiac nuclear imaging as part of their diagnostic algorithm for PVE, but not CIED infection since the data were judged insufficient at the moment. This article reviews the actual knowledge and recent studies on the use of ^{18}F-FDG PET/CT and WBC SPECT/CT in the context of CIED infection and PVE, and describes the technical aspects of cardiac radionuclide imaging. It also discusses their accepted and potential indications for the diagnosis and management of CIED infection and PVE, the limitations of these tests, and potential areas of future research.

Key words: Device; Endocarditis; Fluorodeoxyglucose; Imaging; Infection; Leukocytes; Positron emission tomography/computed tomography; Prosthetic valve; Radionuclide; Scintigraphy

Core tip: Cardiovascular implantable electronic device infection and prosthetic valve endocarditis remain a diagnostic challenge. This review article describes the evolving role of cardiac radionuclide imaging in the diagnosis and management of cardiac infections. It focuses on recent published studies, indications and limitations of both ^{18}F-fluorodeoxyglucose positron emission tomography/computed tomography and

radiolabelled white blood cell single-photon emission computed tomography/computed tomography.

Sarrazin JF, Philippon F, Trottier M, Tessier M. Role of radionuclide imaging for diagnosis of device and prosthetic valve infections. *World J Cardiol* 2016; 8(9): 534-546 Available from: URL: http://www.wjgnet.com/1949-8462/full/v8/i9/534.htm DOI: http://dx.doi.org/10.4330/wjc.v8.i9.534

INTRODUCTION

Cardiovascular implantable electronic device (CIED) infection and prosthetic valve endocarditis (PVE) carry significant morbidity and mortality as well as substantial financial burden to the society[1]. In some cases, establishing the diagnosis might be challenging since cultures are not always positive and they do not necessarily imply that the device/leads or heart valves are infected. Since device/lead extraction and repeat cardiac surgery are associated with significant risks, it is important to confirm the diagnosis and to plan the appropriate treatment. Cardiac imaging plays an important role in the pre-operative evaluation of patients with CIED infection and PVE. Radionuclide imaging has evolved over the past few years as an additional tool to confirm or exclude prosthetic infection and to guide the most appropriate clinical management, either complete removal or conservative treatment. In their 2015 guidelines for the management of infective endocarditis (IE), the European Society of Cardiology (ESC) addressed the use of nuclear medicine imaging for the diagnosis of IE[1]. The main objectives are to position ^{18}F-fluorodeoxyglucose positron emission tomography/computed tomography (^{18}F-FDG PET/CT) and white blood cell single-photon emission computed tomography/computed tomography (WBC SPECT/CT) imaging in clinical practice and to review the actual knowledge and recent studies as well as to address areas of future research.

CLINICAL PRESENTATION AND DIAGNOSIS OF CARDIAC INFECTIONS

CIED infection and PVE remain a diagnostic challenge. The clinical presentation can be highly variable because of multiple potential causative microorganisms, the presence of documented heart disease, cardiac devices or prosthetic valves, different modes of presentation, and sometimes non-specific symptoms at the time of initial presentation. The modified Duke criteria are considered the gold standard for the diagnosis of endocarditis[2,3]. However, the early diagnostic accuracy is often suboptimal with several patients being misclassified[4]. This is true mainly in patients with CIED infection and PVE. The early diagnosis of IE is imperative since postponement of antibiotic therapy and/or surgery can lead to a poor outcome[5,6].

A high level of expertise is required and it often includes cardiologists, nuclear medicine specialists, electrophysiologists, cardiac surgeons and infectious disease specialists. The concept of a "Heart Team approach" or "Endocarditis Team" has been proposed to improve the diagnosis and management of CIED infection and PVE. The use of a multidisciplinary task force with a well-defined protocol has been shown to decrease the 1-year mortality of patients with IE from 18.5% to 8.2%[7].

In addition, cardiac imaging plays an essential role in the diagnosis and management of IE. In recent guidelines, transthoracic echocardiography (TTE) and transesophageal echocardiography (TEE) remain the initial recommended imaging techniques for the diagnosis of IE (class I indication, level of evidence B)[1]. Some echocardiographic information is included as major criteria for the diagnosis of IE. The sensitivity for the identification of vegetations with TTE is 75% for native valves, but may be lower in patients with poor echogenicity or prosthetic valves or very small vegetations[8]. On the other hand, the sensitivity of TEE is superior at 85%-90%. However, a negative echocardiography does not rule out IE, and it has been recommended to repeat the TEE 3 to 5 d later or sooner when there is a high suspicion of IE or a change in the clinical status (class I, level of evidence B)[9]. In addition, non-infective vegetations such as strands or thrombi on valvular prosthesis or leads can lead to a false diagnosis of IE in up to 15% of cases[4]. These findings highlight the limitations of echocardiography and the potential benefits of other imaging techniques in such instances.

Investigation of patients with IE can also include other imaging techniques, such as multislice computed tomography for detection of abscesses or pseudoaneurysms, magnetic resonance imaging for detection of cerebral lesions, ^{18}F-FDG PET/CT, and radiolabelled WBC hybrid SPECT/CT imaging.

USE OF CARDIAC NUCLEAR IMAGING IN CARDIAC INFECTIONS

PET imaging has been used for cancer diagnosis and staging and to detect infection in orthopaedic prostheses. In cardiology, it is used to evaluate myocardial viability, ischemia and to identify infection associated with vascular grafts, CIED and prosthetic valves.

With the combination of radionuclide imaging to CT scan (hybrid technology), nuclear imaging has provided significant supplementary information in patients with suspected IE. Two radionuclide imaging techniques are presently used in the diagnosis of CIED infection and PVE: (1) radiolabelled WBC SPECT/CT using either ^{111}In-oxine or ^{99m}Tc-hexamethylpropyleneamine oxime (HMPAO); and (2) ^{18}F-FDG PET/CT.

WBC SPECT/CT imaging uses autologous radio-

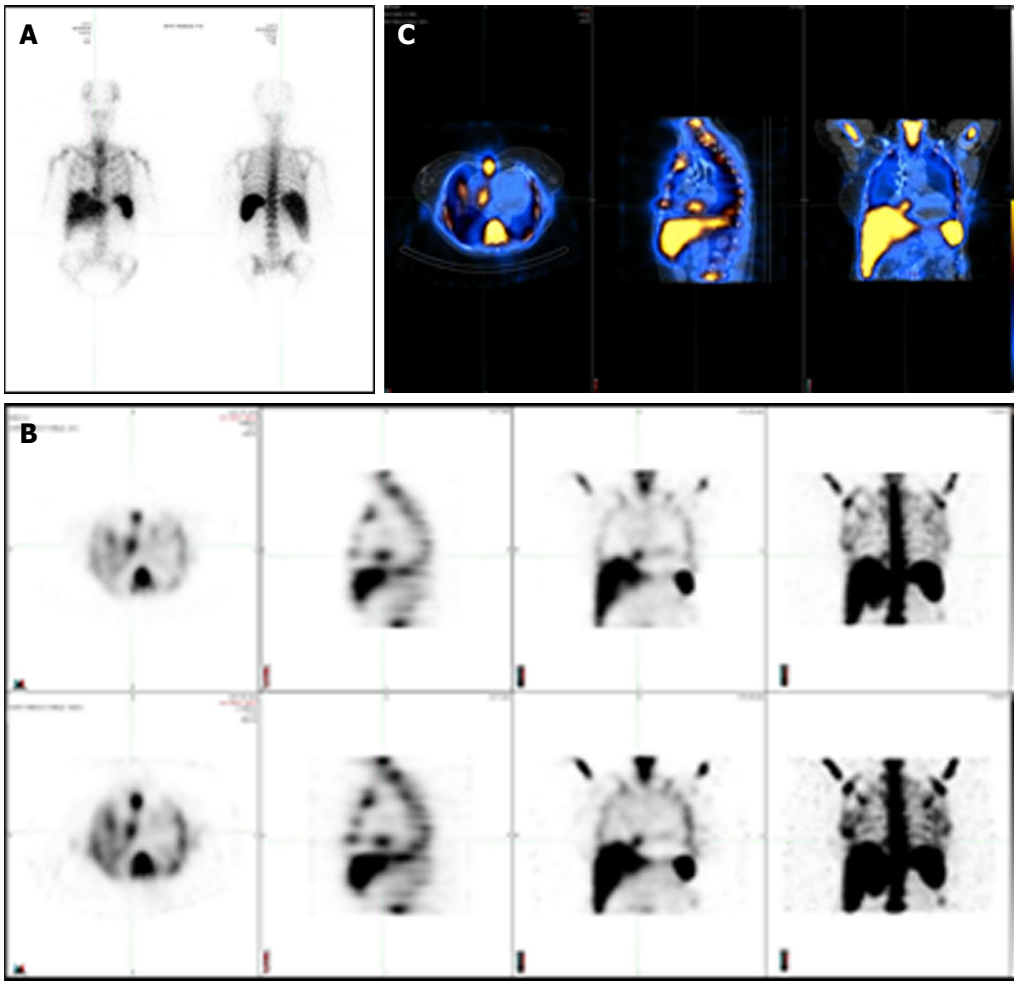

Figure 1 Different modalities in cardiac nuclear imaging. A: Planar scintigraphy with a single two-dimensional image; B: Single photon emission computed tomography (SPECT) displayed as transverse, sagittal, coronal and MIP attenuation corrected (top row) and uncorrected images (bottom row); C: Hybrid SPECT/CT with precisely registered CT image.

labelled leukocytes (^{111}In-oxine or ^{99m}Tc-HMPAO) that are injected intravenously back to the patient to look for infection in the body by imaging gamma rays. The accumulation of radiolabelled leukocytes is time-dependent between initial and late images. Planar images are obtained from different angulations with subsequent SPECT acquisition, 3D reconstruction and fusion with low-dose CT for further anatomical localization and attenuation correction. Figure 1 shows the differences between planar scintigraphy, conventional SPECT imaging and hybrid SPECT/CT. The sensitivity of this test depends on neutrophil granulocytes accumulation and is higher during acute infection. Studies have shown that cells participating in infection and inflammation, mainly neutrophils and macrophages, are able to express a great amount of glucose transporters, mainly GLUT1 or GLUT3 as well as hexokinase activity[10-14]. WBC SPECT/CT using ^{99m}Tc-HMPAO is performed 4 h following injection of radiolabelled leukocytes, although images at 24 h are possible but with loss of some image quality, whereas WBC SPECT/CT using ^{111}In-oxine allows imaging up to 72 h with potentially better sensitivity (typically performed at 4, 24 and sometimes 48 h). This is based on the half-life of each radioactive isotope, being 6 h for ^{99m}Tc and 67 h for ^{111}In. WBC SPECT/CT allows a higher specificity for the identification of active infection. However, leukocytes radiolabelling is more time-consuming. It also associated with manipulation of blood products.

^{18}F-FDG PET/CT is a well-known non-invasive imaging technique that allows 3D calculation of metabolic activity within the body obtained from the emission of positrons subsequent to the disintegration of a radioactive compound. ^{18}F-FDG is a glucose analogue, which is incorporated and retained within cells with a high metabolic activity, such as inflammatory cells. It is usually performed approximately 1 h after the injection of ^{18}F-FDG. This tracer is actively incorporated by leukocytes, macrophages and CD4$^+$ T-lymphocytes located at areas of infection *via* glucose transporters, primarily GLUT 1 and GLUT3, which are insulin sensitive and present in the myocardium[12-14]. Inside the cells, ^{18}F-FDG is phosphorylated and remains intracellular without further transformation.

Each technique has advantages and weaknesses for the identification of active infection in cases of

Table 1 Advantages and limitations of ^{18}F-fluorodeoxyglucose positron emission tomography/computed tomography and white blood cell single-photon emission computed tomography/computed tomography for the diagnosis of device infection and prosthetic valve endocarditis

Advantages	Limitations
^{18}F-FDG PET/CT	
Excellent spatial resolution	Moderate radiation exposure (8-30 mSv depending on the study performed)
Short acquisition time	Not available in several centers
High sensitivity for the detection of hypermetabolic activity	Physiological uptake of ^{18}F-FDG in the myocardium might prevent adequate detection of cardiac infection
Detection of peripheral events	Recent surgery may demonstrate residual inflammatory changes without evidence of infection
Detection of other sources of fever or bacteremia in patients with CIED	Possible uptakes can be found in active thrombi, cardiac tumours or metastasis, and foreign body reactions
Detection of CIED infection and PVE in cases of a negative TEE	Possible false-negative test in patients with small vegetations or prolonged antibiotic therapy
	Less useful for infectious brain embolisms because of high glucose metabolism in the brain
WBC SPECT/CT	
High specificity for the presence of active infection	Time-consuming
	It involves blood products handling
	Cases of false-negative study seen with Candida and Enterococcus infection

CIED: Cardiovascular implantable electronic device; ^{18}F-FDG PET/CT: 18F-fluorodeoxyglucose positron emission tomography/computed tomography; PVE: Prosthetic valve endocarditis; TEE: Transesophageal echocardiography; WBC SPECT/CT: Radiolabelled white blood cell single-photon emission computed tomography/computed tomography.

presumed PVE (Table 1). ^{18}F-FDG PET/CT has the convenience of a shorter procedure time and a high sensitivity for the identification of hypermetabolic areas. It also has an excellent spatial resolution. However, it does not discriminate enough between infection and inflammation, mainly in the first few months postoperatively. Also, evaluation of ^{18}F-FDG uptakes around cardiac valves can be more difficult if residual physiological myocardial uptake is present. For this reason, it is recommended to prepare the patient with the Atkins diet, which is a low-carbohydrate diet[15]. It is also suggested injecting a heparin bolus before administration of ^{18}F-FDG. Unfractionated heparin increases plasma free fatty acids *via* activation of lipoprotein and hepatic lipases[16]. This can lead to a reduction in glucose consumption within the normal myocardium

Technical aspects

In the literature, there are significant variations in the ^{18}F-FDG PET/CT protocols used. Normally, ^{18}F-FDG PET/CT is performed after a fasting period of 8 to 12 h. Eating foods rich in fat but very low in carbohydrates the evening prior to the exam is suggested in order to decrease the physiological uptake of ^{18}F-FDG within the myocardium[17]. Patients should avoid bread, cereals, pasta, potatoes, rice, beans, fruit juice, chewing gum and drinking alcohol. Unfractionated heparin (50 IU/kg) can also be administered intravenously 15 min prior to ^{18}F-FDG injection in an attempt to reduce more the physiological uptake. PET imaging is usually performed 1 h after the injection of 4-5 MBq/kg of ^{18}F-FDG. Simultaneously, a whole-body low-dose CT without intravenous contrast is carried out for correction of attenuation and anatomic localization. The capillary glucose is measured, and patients receive an insulin injection if the fasting glucose is above 7.7 mmol/L or 140 mg/dL. The analysis is then performed using dedicated softwares. Both attenuation-corrected and non-attenuation-corrected images are reviewed in order to recognize potential artefacts that could be related to close proximity of objects of high density, such as device generator or prosthesis. A visual analysis is first performed to identify sites of hypermetabolic or abnormal ^{18}F-FDG uptakes in close proximity to prosthetic valves and device generator/leads with further confirmation in the uncorrected images. In patients with CIED, focal uptake can be further classified based on the location (pocket infection, lead infection or both). Then, semi-quantitative analyses are done to measure the maximal standardized uptake value (SUV_{max}). However, it is important to recognize that these values have to be used with caution, since they can be falsely elevated due to the attenuation correction when measured in close proximity to a metallic object. For this reason, a semi-quantitative count ratio on non-attenuation-corrected images is likely superior to SUV_{max} (compared to an organ of reference, *i.e.*, lung, mediastinum or liver parenchyma). In addition, whole-body acquisition allows for the detection of silent embolic events and extracardiac abnormal uptakes.

Autologous radiolabelled WBC scintigraphy with ^{111}In-oxine was introduced in the mid-1970s. Over the years, it has been mainly substituted by ^{99m}Tc-HMPAO, which has more advantageous physical characteristics, cost, availability, and lower radiation burden[18]. ^{99m}Tc has a shorter imaging time because of a half-life of 6 h compared to 67 h for Indium. However, Indium is often preferred for the detection of CIED infection and PVE since it allows acquisitions over a longer period of time (up to 72 h).

There are several methods for labelling WBC, but the main principles and technique are similar. Around 40-60 mL of venous blood is taken from the patient and then combined to 10 mL of acid-citrate-dextrose anticoagulant solution. This syringe is then put in an upright position for 1 to 2 h to facilitate erythrocyte sedimentation by gravity. After erythrocytes have been removed, blood centrifugation is then performed to separate leukocytes from platelets. HMPAO is labelled with ^{99m}Tc and incubated for 15 min with leukocytes. The routine dose of ^{111}In labelled leukocytes is 10-20 MBq (0.3-0.5 mCi) while the quantity of ^{99m}Tc-HMPAO labelled

leukocytes is 185-370 MBq (5-10 mCi). Radiolabelled leukocytes are separated from HMPAO by centrifugation. The majority of labelled leukocytes are neutrophils. For this reason, the procedure is mainly useful for identification of a neutrophil-mediated process, such as a bacterial infection. A labelling efficiency of at least 40% should be achieved. Radiolabelled leukocytes are tested by the trypan blue exclusion test for viability. The cells are then resuspended in plasma before reinjection into the patient. For ^{99m}Tc-HMPAO labelled leukocytes, the scintigraphy is performed 4 and 24 h (delayed images) after injection, and sometimes 48 h or rarely 72 h for ^{111}In labelled leukocytes. Images are acquired using a SPECT/CT system. Scintigraphy is considered positive when an area of labelled WBC uptake superior to background activity is identified in the involved area and when the signal increases over time.

DEVICE INFECTION

CIED infection is associated with significant morbidity and mortality. Device infection prevalence is increasing in parallel with broader indications for ICD implantation and cardiac resynchronization, the presence of more comorbidities, and the growing number of implants in the world[19]. It is known however that the infection burden increases more than the increase in device implantations. This is probably related to more comorbidities and change in pathogens[20]. Cardiac device infections can present as a superficial or deep generator pocket infection or cardiac-device-related IE with involvement of the leads and/or extension to cardiac valves. It should be initially suspected in patients with CIED who consult for unexplained fever. Deep pocket infection and/or lead infection require complete system extraction. However, superficial infection not in contact with the device can be treated with antibiotic therapy alone. The diagnosis is sometimes quite obvious in the presence of significant pocket redness or pus, bacteremia or lead vegetation on TEE. Unfortunately, several cases are more complicated to assess. Since device and lead extraction can be associated with significant morbidity (major complications = 1.5%-2%) and mortality (0.8%) even in an experienced center, a definite diagnosis is important[21]. On the other hand, CIED infection can be overestimated with echocardiography since non-infectious accretions can be found in up to 21% by TTE and 28% by TEE in CIED patients without infection[22]. These patients can have fever or bacteremia for another reason. Thus, another form of imaging is proposed before proceeding to extraction/surgery.

Studies using ^{18}F-FDG PET/CT

The first report of cardiac infection detected by ^{18}F-FDG PET was published in 2006[23]. Afterwards, 2 small pilot studies were published on device infection and ^{18}F-FDG PET/CT. Bensimhon *et al*[24] evaluated the diagnostic value of ^{18}F-FDG PET/CT in 21 patients with presumed device infection, which were compared to 14 patients without infection. ^{18}F-FDG PET/CT had a sensitivity and specificity of 80% and 100%, respectively for diagnosis of infection. Patients with false negative studies for lead infection had received antibiotics for a longer period of time prior to the ^{18}F-FDG PET/CT (20 d *vs* 3.2 d; $P < 0.01$). The sensitivity was lower for the diagnosis of lead infection (60% compared to 100% for pocket infection). Ploux *et al*[25] investigated the role of ^{18}F-FDG PET/CT in 10 patients with CIED and fever of unknown origin. These patients were compared to a control group of 40 patients. ^{18}F-FDG PET/CT showed increased ^{18}F-FDG uptakes along the leads in 6 out 10 patients who had initial comprehensive negative investigation. Subsequently, these patients had complete extraction of the implanted material and lead cultures were positive on all 6 patients. This showed the promising value of ^{18}F-FDG PET/CT in difficult CIED cases.

In 2012, our group evaluated the usefulness of ^{18}F-FDG PET/CT for the identification of CIED infection[26]. We compared 3 groups: 42 patients with suspected CIED infection, 12 patients with recent device implantation (between 4 and 8 wk postoperatively) but no clinical signs of infection, and 12 patients with devices implanted for more than 6 mo and also no device infection. We showed an excellent correlation between sites of ^{18}F-FDG uptakes on ^{18}F-FDG PET/CT and clinical findings on TEE or at the time of extraction. ^{18}F-FDG PET/CT using a qualitative visual score had a sensitivity and specificity for diagnosis of CIED infection of 89% and 86%, respectively. We also demonstrated that ^{18}F-FDG PET/CT could identify patients with superficial infection without direct involvement of the generator or leads that could be treated only with antibiotics. Negative ^{18}F-FDG PET/CT identified a group of patients that had an excellent outcome without device extraction. Finally, we were able to identify a semi-quantitative ratio between the maximal uptake and normal lung parenchyma uptake, which was useful in differentiating between CIED infection and residual normal post-operative changes; a ratio of 1.5 had the best combination of sensitivity and specificity. Based on this information, we suggested an algorithm using ^{18}F-FDG PET/CT for the evaluation of CIED infection (Figure 2). An important clinical aspect of ^{18}F-FDG PET/CT is its high negative predictive value.

Since, Cautela *et al*[27] demonstrated that ^{18}F-FDG PET/CT had a high accuracy for the diagnosis of skin and pocket CIED infection (sensitivity 86.7% and specificity 100%), but a lower sensitivity of only 30.8% and a specificity of 62.5% for lead or cardiac involvement. Many patients with a false-negative test were already on antibiotics. The size of the vegetations might also have influenced the results. It cannot be excluded that some patients with lead extraction had a non-infectious cause for the vegetations seen on the lead. Finally, a possible limitation of this study is suboptimal patient preparation in order to partially explain the lower sensitivity observed for lead or cardiac involvement. It is of the utmost importance to make

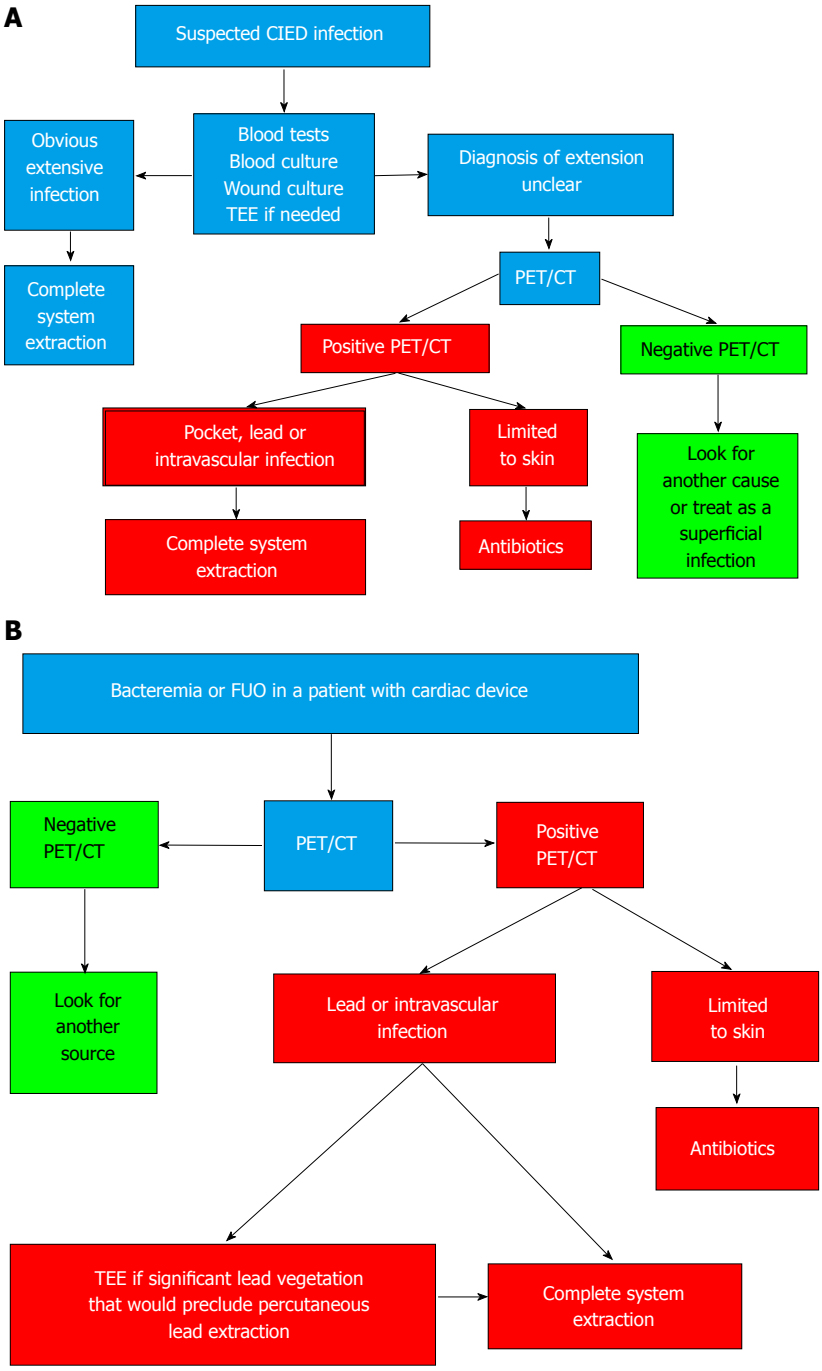

Figure 2 Proposed algorithms incorporating ^{18}F-fluorodeoxyglucose positron emission tomography/computed tomography in the evaluation and management of patients with possible device infection. A: Initial CIED infection suspicion; B: Patients with cardiac device and bacteremia or fever of unknown origin (FUO) (Reprinted from Sarrazin JF, Philippon F, Tessier M, Guimond J, Molin F, Champagne J, Nault I, Blier L, Nadeau M, Charbonneau L, Trottier M, O'Hara G. Usefulness of fluorine-18 positron emission tomography/computed tomography for identification of cardiovascular implantable electronic device infections. *J Am Coll Cardiol* 2012; 59: 1616-1625, with permission from Elsevier). CIED: Cardiovascular implantable electronic device; PET/CT: Positron emission tomography/computed tomography; TEE: Transesophageal echocardiography.

sure that physiologic myocardial uptake is suppressed to be able to realize an optimal evaluation. Ideally, every patient should be prepared with the Atkins diet and receive a heparin bolus before ^{18}F-FDG injection. Ahmed *et al*[28] demonstrated that ^{18}F-FDG PET/CT had a high diagnostic accuracy for the detection of patient with pocket infection that eventually required extraction. They find that the optimal semi-quantitative ratio cut-off value for the early identification of patients with pocket infection was > 2.0, giving a sensitivity of 97% and a specificity of 98%.

Figure 3 shows a positive ^{18}F-FDG PET/CT in a patient with a deep pocket infection, while Figure 4 shows another positive ^{18}F-FDG PET/CT but in a patient with a lead infection. Note how the physiologic myocardial uptake is well suppressed in this case.

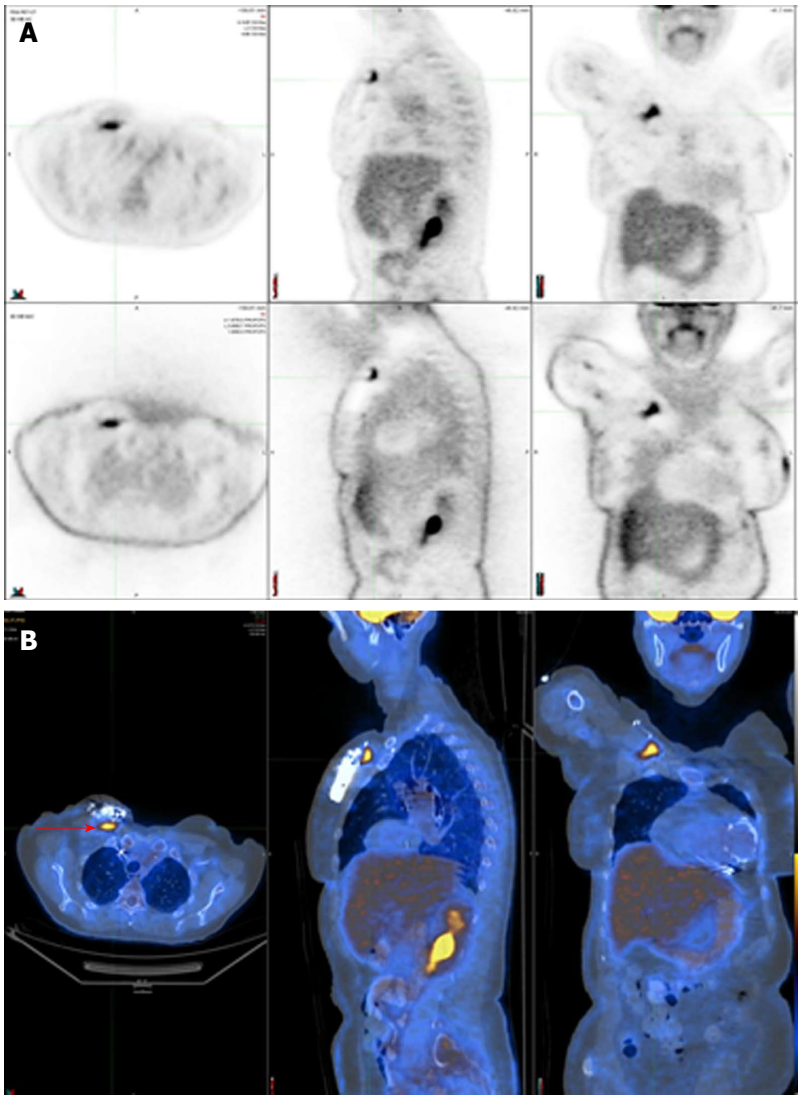

Figure 3 Positive ^{18}F-fluorodeoxyglucose positron emission tomography/computed tomography in a patient with a deep pocket infection shown by focal ^{18}F-fluorodeoxyglucose uptake just underneath the generator (red arrow). A: SPECT displayed as transverse, sagittal, and coronal attenuation corrected (top row) and uncorrected images (bottom row); B: Hybrid SPECT/CT displayed as transverse, sagittal, and coronal images. SPECT/CT: Single-photon emission computed tomography/computed tomography.

Studies using WBC SPECT/CT

The diagnostic accuracy of radiolabelled WBC scintigraphy was evaluated by Erba *et al*[29]. They obtained a sensitivity of 94% for both detection and localization of CIED infection. Two cases of false-negative scans were seen in patients with Candida and Enterococcus infection. No false-positive studies were seen, confirming the high specificity of this technique. They demonstrated the superiority of SPECT/CT over planar and SPECT alone imaging.

Based on these studies, ^{18}F-FDG PET/CT and WBC SPECT/CT might play an additional role in the diagnosis of CIED infection, but data were judged not sufficient at the moment to be incorporated into the diagnostic criteria of IE involving pacemaker or defibrillator leads in the latest European guidelines[1]. Overall, ^{18}F-FDG PET/CT seems to have an excellent sensitivity for the diagnosis of pocket infection, but a lower sensitivity in the context of lead infection.

PROSTHETIC VALVE INFECTION

Early diagnosis of PVE is also challenging. PVE is a severe form of IE and accounts for 10%-30% of all cases of IE. The diagnosis is often more difficult than in native valve endocarditis. Since the initial echocardiography is often normal or inconclusive in PVE, other imaging techniques are sometimes necessary. The use of ^{18}F-FDG PET/CT in patients with PVE has evolved as a useful tool.

Studies using ^{18}F-FDG PET/CT

Case reports have demonstrated the possible benefits of ^{18}F-FDG PET/CT in the diagnosis of prosthetic valves[30]. Saby *et al*[31] demonstrated the incremental benefit of using abnormal ^{18}F-FDG uptake as a major criterion for the modified Duke criteria in the detection of PVE. They have shown that ^{18}F-FDG PET/CT significantly increases the sensitivity of IE diagnosis from 70% to 97% (P = 0.008) on admission. They determined that ^{18}F-FDG PET/CT had an adequate diagnostic value when abnormal ^{18}F-FDG uptake is found near the prosthetic valve. They also showed that abnormal ^{18}F-FDG uptake could be seen prior to detection of valvular damage by echocardiography in multiple patients, which emphasizes the benefit of ^{18}F-FDG PET/CT to identify

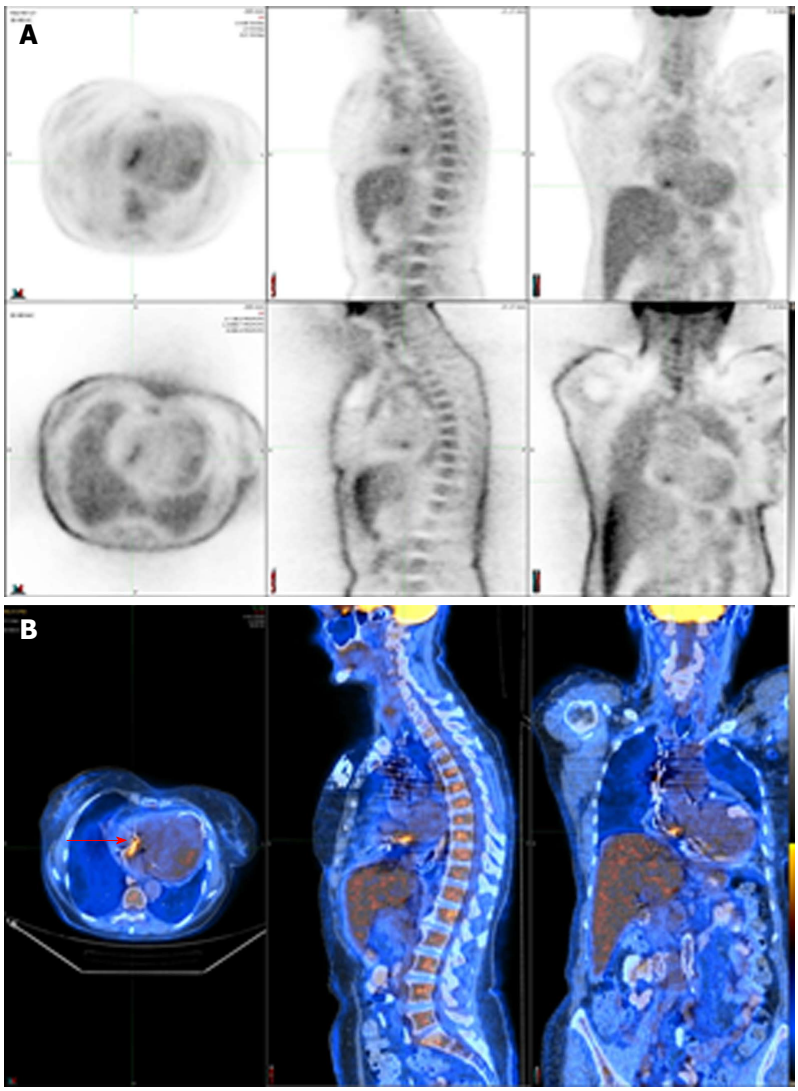

Figure 4 Positive ^{18}F-fluorodeoxyglucose positron emission tomography/computed tomography in a patient with a lead infection (red arrow). A: SPECT displayed as transverse, sagittal, and coronal attenuation corrected (top row) and uncorrected images (bottom row); B: Hybrid SPECT/CT displayed as transverse, sagittal, and coronal images. SPECT/CT: Single-photon emission computed tomography/computed tomography.

active infection before important damage has occurred.

Rouzet *et al*[32] evaluated the ability of ^{18}F-FDG PET/CT and radiolabelled WBC imaging to diagnose PVE in 39 patients with presumed PVE but inconclusive echocardiography findings. ^{18}F-FDG PET/CT had a higher sensitivity (93% *vs* 64%) but leukocyte scintigraphy had a higher specificity (100% *vs* 71%). Since it has a higher specificity for the detection of IE, it could be used in cases of equivocal ^{18}F-FDG PET/CT or within the initial two months after heart valve surgery[32].

^{18}F-FDG PET/CT can reduce the rate of misdiagnosed IE and help in the detection of peripheral events, including silent vascular phenomenon. ^{18}F-FDG PET/CT can identify lesions of clinical importance not detected by conventional work-up in one out of seven IE patients[33]. It also improves the sensitivity of the modified Duke criteria in the most difficult situations. When endocarditis on a prosthetic valve is suspected, abnormal uptake around the site of insertion identified by ^{18}F-FDG PET/CT (but more than 3 mo after prosthesis implantation) or radiolabelled WBC SPECT/CT could be considered a major diagnostic criterion. Results of ^{18}F-FDG PET/CT should always be examined together with the other conventional diagnostic tools (clinical, microbiological and echocardiographic data). In addition, ^{18}F-FDG PET/CT can be considered to monitor response to antibiotic therapy.

Studies using WBC SPECT/CT

Erba *et al*[34] assessed in another study the value of ^{99m}Tc-HMPAO leukocyte scintigraphy in 131 patients with suspected endocarditis. In these patients, 51 had a confirmed diagnosis of IE and 35 had PVE (69%). Scintigraphy had a sensitivity of 90% and a specificity of 100%. No false-positive cases were seen, including patients evaluated for IE during the first two months after their surgery. However, false-negative studies were seen with Candida and Enterococcus endocarditis. It also identified cases of septic embolism. The test could be useful in patients with a high suspicion of IE but inconclusive TEE, in differentiating between infective and sterile vegetations identified with echocardiography, when other tests are contradictory, and to exclude valve involvement in patients with sepsis and prosthetic valve. In another study, Hyafil *et al*[35] looked at the role of radiolabelled leukocyte imaging in patients with

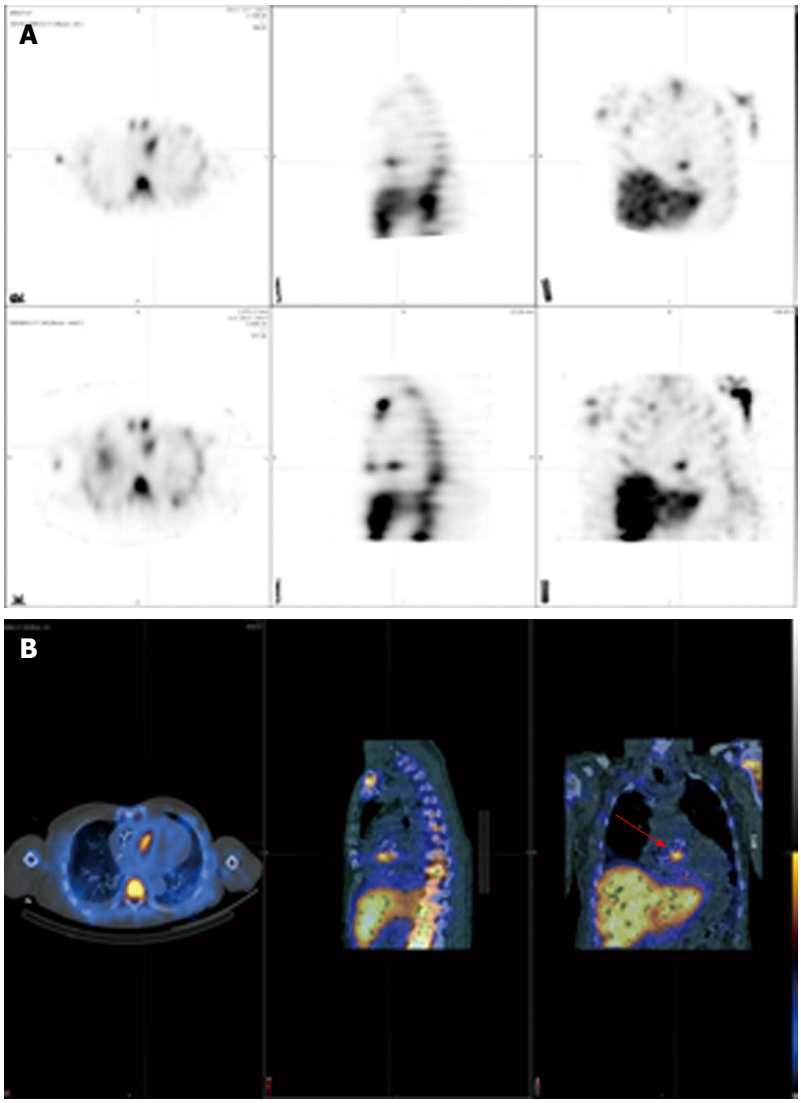

Figure 5 Positive ^{111}In white blood cell single-photon emission computed tomography/computed tomography in a patient with endocarditis following an aortic valve replacement (red arrow). A: SPECT displayed as transverse, sagittal, and coronal attenuation corrected (top row) and uncorrected images (bottom row); B: Hybrid SPECT/CT displayed as transverse, sagittal, and coronal images. SPECT/CT: Single-photon emission computed tomography/computed tomography.

presumed PVE and unconvincing echocardiography. They showed an excellent positive predictive value of intense signal with WBC scintigraphy for the presence of an abscess. Also, a negative scan predicted the absence of recurrent endocarditis in medically treated patients. Downsides of radiolabelled leukocyte scintigraphy are the necessity of blood handling, a longer procedure time, and a somewhat lower spatial resolution in contrast to ^{18}F-FDG PET/CT.

Figure 5 shows a positive ^{111}In WBC SPECT/CT in a patient with endocarditis following an aortic valve replacement.

Table 2 shows the sensitivity and specificity of both ^{18}F-FDG PET/CT and WBC SPECT/CT in the diagnosis of CIED infection and PVE.

LIMITATIONS

Despite its benefits, ^{18}F-FDG PET/CT can have false-positive and false-negative results. Postoperative inflammatory changes can lead to non-specific ^{18}F-FDG uptakes during the first several weeks after surgery, mainly following cardiac surgery or device implantation. Abnormal ^{18}F-FDG uptake could also be caused by BioGlue surgical adhesive, a combination of bovine serum albumin and glutaraldehyde, used to seal the aortic root graft at time of surgery[36]. In addition, possible uptakes can be found in active thrombi, cardiac tumours or metastasis, post-surgical inflammation, and foreign body reactions like vascular grafts. At the other end of the spectrum, ^{18}F-FDG PET/CT might be negative in patients with lower inflammation or when the test is performed after a long period of antibiotic therapy. The validity of ^{18}F-FDG PET/CT in the context of slowly evolving infections is still unknown. Because of the high glucose metabolism in the brain, ^{18}F-FDG PET/CT might not be the best test in order to detect infectious embolisms to the brain. However, an advantage of ^{18}F-FDG PET/CT is the possibility to identify non-infectious causes of fever or underlying neoplasm. As opposed to echocardiography, cardiac nuclear imaging does not evaluate hemodynamic conditions associated with IE, such as valvular regurgitation, cardiac output, pulmonary arterial pressure and ventricular function. Another important issue remains that ^{18}F-FDG PET/CT is less accessible than WBC SPECT/CT. The study quality

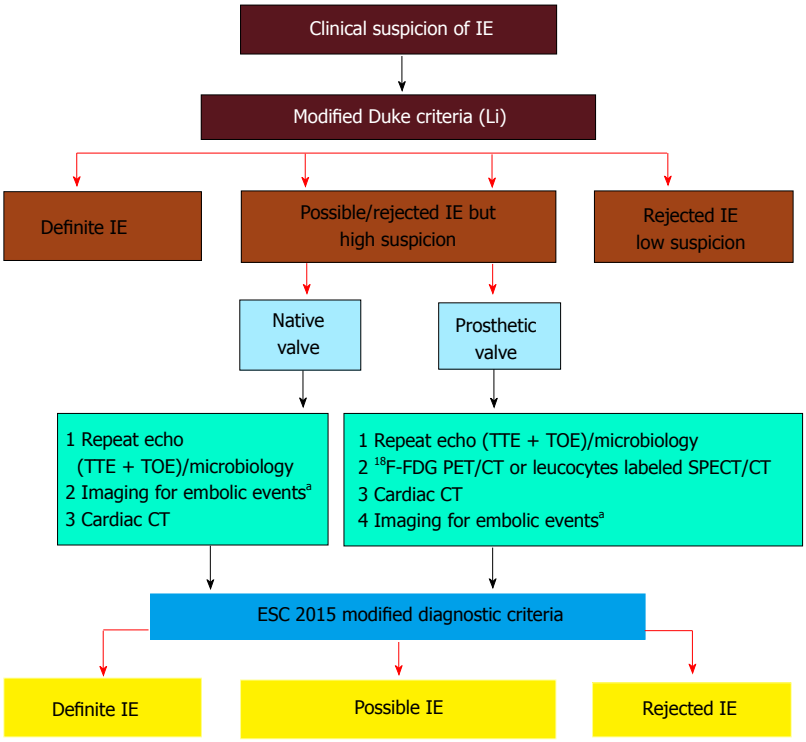

Figure 6 European Society of Cardiology 2015 algorithm for diagnosis of infective endocarditis. Reprinted from Habib G, Lancelloti P, Antunes MJ, Bongiorni MG, Casalta JP, Del Zotti F, Dulgheru R, El Khoury G, Erba PA, Iung B, Miro JM, Mulder BJ, Plonska-Gosciniak E, Price S, Roos-Hesselink J, Snygg-Martin U, Thuny F, Tornos Mas P, Vilacosta I, Zamorano JL; Document Reviewers, Erol Ç, Nihoyannopoulos P, Aboyans V, Agewall S, Athanassopoulos G, Aytekin S, Benzer W, Bueno H, Broekhuizen L, Carerj S, Cosyns B, De Backer J, De Bonis M, Dimopoulos K, Donal E, Drexel H, Flachskampf FA, Hall R, Halvorsen S, Hoen B, Kirchhof P, Lainscak M, Leite-Moreira AF, Lip GY, Mestres CA, Piepoli MF, Punjabi PP, Rapezzi C, Rosenhek R, Siebens K, Tamargo J, Walker DM. 2015 ESC Guidelines for the management of infective endocarditis: The Task Force for the Management of Infective Endocarditis of the European Society of Cardiology (ESC). Endorsed by: European Association for Cardio-Thoracic Surgery, the European Association of Nuclear Medicine. *Eur Heart J* 2015; 36: 3075-3128. Reprinted by permission of Oxford University Press (UK)© European Society of Cardiology, www.escardio.org/". This image/content is not covered by the terms of the Creative Commons license of this publication. For permission to reuse, please contact the rights holder). [a]May include cerebral MRI, whole body CT, and/or PET/CT; CT: Computed tomography; FDG: Fluorodeoxyglucose IE: Infective endocarditis; PET: Positron emission tomography; SPECT: Single-photon emission computed tomography; TTE: Transthoracic echocardiography; ^{18}F-FDG PET/CT: ^{18}F-fluorodeoxyglucose positron emission tomography/computed tomography.

could be improved by using respiratory and ECG gated techniques. This could minimize imaging artefacts, although it is technically more challenging and time-consuming. Cardiac nuclear imaging is a source of radiation. Administration of approximately 200 MBq of ^{18}F-FDG for a PET study represents an effective dose between 3 and 4 mSv, which is similar to a low-dose CT. Then the total dose for a PET/CT would be approximately 7.5 mSv[37]. A follow-up study to monitor response to antibiotic therapy would increase radiation exposure. However, an initial PET scan combined to a low-dose CT and followed by a subsequent study would be equivalent to a percutaneous coronary intervention or an atrial fibrillation ablation procedure (approximately 15 mSv)[38].

GUIDELINES

The ESC guidelines for the management of infectious endocarditis were updated in 2015[1]. The Task Force added ^{18}F-FDG PET/CT or radiolabelled WBC SPECT/CT as a new major criterion if abnormal FDG uptakes are found around the area of prosthetic valve implantation in patients with a prosthesis implanted for more than 3 mo[1]. Nuclear imaging has also been incorporated in the new algorithm for the diagnosis of IE when the diagnosis is still possible or has been dismissed but when a high index of suspicion is still present (Figure 6). However, despite data for the key role of ^{18}F-FDG PET/CT in the diagnosis of CIED infection, actual studies were judged insufficient to incorporate the results of ^{18}F-FDG PET/CT at this time as a diagnostic criterion for device infection. For the moment, ^{18}F-FDG PET/CT or radiolabelled leukocyte scintigraphy have a class IIb level of evidence C indication as an additional tool in patients with suspected CIED infection, positive blood cultures and negative echocardiography[1]. Also, the AHA scientific statement on IE judged that more clinical trials are still required to better clarify the utility of ^{18}F-FDG PET/CT for the diagnosis and management of endocarditis[9]. Since most studies on cardiac radionuclide imaging have been published in the past 5 years, the use of ^{18}F-FDG PET/CT in device infection was not discussed in the 2010 AHA scientific statement on CIED infections and their management[21].

Based on the recent ESC guidelines and previous studies, cardiac nuclear imaging could be considered in the following circumstances (Table 3): (1) accepted

Table 2 Sensibility and specificity of ^{18}F-fluorodeoxyglucose positron emission tomography/computed tomography and white blood cell single-photon emission computed tomography/computed tomography for both prosthetic valve endocarditis and cardiac device infection

	Test	Sensibility (%)	Specificity (%)	Positive predictive value (%)	Negative predictive value (%)	Accuracy (%)
Prosthetic valve endocarditis						
Saby *et al*[31]	PET/CT	73	80	85	67	76
Rouzet *et al*[32]	PET/CT	93	71	68	94	80
	WBC	64	100	100	81	86
Erba *et al*[34]	WBC	90	100	100	94	N/A
Cardiovascular implantable electronic device infection						
Bensimhon *et al*[24]	PET/CT	80	100	100	84.6	N/A
	Pocket	100	100	100	100	N/A
	Lead	60	100	100	73	N/A
Ploux *et al*[25]	PET/CT	100	93	N/A	N/A	N/A
Sarrazin *et al*[26]	PET/CT	88.6	85.7	N/A	N/A	N/A
Cautela *et al*[27]	PET/CT					
	Pocket	86.7	100	N/A	N/A	N/A
	Lead	30.8	62.5	N/A	N/A	N/A
Ahmed *et al*[28]	PET/CT					
	Pocket	97	98	N/A	N/A	N/A
Erba *et al*[29]	WBC	93.7	100	100	93.9	96.8

N/A: Not available; PET/CT: Positron emission tomography/computed tomography; WBC: White blood cell.

indication[1]: Possible or rejected IE diagnosis based on the modified Duke criteria, but persistent high clinical suspicion of infection in patients with a prosthetic valve; and (2) potential indications: Unclear diagnosis of CIED infection; Evaluation of the extent of infection when the results would affect the management of the patient, for example differentiation between superficial and deep pocket infection where device and lead extraction is recommended; Bacteremia with organisms not commonly a source of IE or fever of unknown origin in patients with CIED; High clinical suspicion of IE but negative TEE and/or negative blood cultures; Search for embolic events when it would affect the management of the patient; Monitoring the success of antibiotic therapy in medically treated patients.

FUTURE STUDIES

So far, available data on the diagnosis of CIED infection and PVE with either ^{18}F-FDG PET/CT or WBC SPECT/CT come from small studies and limited number of patients. Larger studies would be useful to confirm the preliminary data suggesting the additional benefit of cardiac nuclear imaging. Despite encouraging results, some questions need to be answered. Is the use of ^{18}F-FDG PET/CT cost-effective? Also, what is the consequence of prolonged antibiotic therapy prior to ^{18}F-FDG PET/CT? There is also a need for standardization of the imaging techniques available since the imaging and data acquisition protocols are sometimes different from one center to another. There is still a need for further prospective studies in this field of research before ^{18}F-FDG PET/CT should be systematically performed for the diagnosis of IE or used as a first line investigation. At the moment, it should be restricted to difficult cases of suspected CIED infection or PVE.

Table 3 Indications for the use of cardiac nuclear imaging in the context of cardiovascular implantable electronic device infection and prosthetic valve endocarditis

Accepted indication
Possible or rejected IE, but high suspicion of infection in patients with prosthetic valve
Potential indications
Unclear diagnosis of CIED infection
Evaluation of the extent of infection
Bacteremia or fever of unknown origin in patients with CIED
Cases with high clinical suspicion of IE but negative TEE and/or negative blood cultures
Search for embolic events
Monitoring the success of antibiotic therapy

CIED: Cardiovascular implantable electronic device; IE: Infective endocarditis; TEE: Transesophageal echocardiography.

CONCLUSION

^{18}F-FDG PET/CT appears to be a very promising imaging technique for the diagnosis of device infection and prosthetic valve endocarditis. Based on recent publications, there is growing evidence that cardiac nuclear imaging can play a key role in the diagnosis and management of patients with suspected CIED infections and PVE. This is now reflected in the most recent published guidelines. Although echocardiography remains an important initial test in the evaluation of these patients, ^{18}F-FDG PET/CT and WBC SPECT/CT have clearly demonstrated their usefulness, mainly in difficult cases. Larger prospective studies will help to confirm the benefits of ^{18}F-FDG PET/CT and clarify its role in the different algorithms of device and valve infections.

REFERENCES

1 **Habib G**, Lancellotti P, Antunes MJ, Bongiorni MG, Casalta JP, Del Zotti F, Dulgheru R, El Khoury G, Erba PA, Iung B, Miro JM, Mulder BJ, Plonska-Gosciniak E, Price S, Roos-Hesselink J, Snygg-Martin U, Thuny F, Tornos Mas P, Vilacosta I, Zamorano JL, Erol Ç, Nihoyannopoulos P, Aboyans V, Agewall S, Athanassopoulos G, Aytekin S, Benzer W, Bueno H, Broekhuizen L, Carerj S, Cosyns B, De Backer J, De Bonis M, Dimopoulos K, Donal E, Drexel H, Flachskampf FA, Hall R, Halvorsen S, Hoen B, Kirchhof P, Lainscak M, Leite-Moreira AF, Lip GY, Mestres CA, Piepoli MF, Punjabi PP, Rapezzi C, Rosenhek R, Siebens K, Tamargo J, Walker DM. 2015 ESC Guidelines for the management of infective endocarditis: The Task Force for the Management of Infective Endocarditis of the European Society of Cardiology (ESC). Endorsed by: European Association for Cardio-Thoracic Surgery (EACTS), the European Association of Nuclear Medicine (EANM). *Eur Heart J* 2015; **36**: 3075-3128 [PMID: 26320109 DOI: 10.1093/eurheartj/ehv319]

2 **Li JS**, Sexton DJ, Mick N, Nettles R, Fowler VG, Ryan T, Bashore T, Corey GR. Proposed modifications to the Duke criteria for the diagnosis of infective endocarditis. *Clin Infect Dis* 2000; **30**:

633-638 [PMID: 10770721 DOI: 10.1086/313753]
3 **Prendergast BD**. Diagnostic criteria and problems in infective endocarditis. *Heart* 2004; **90**: 611-613 [PMID: 15145855 DOI: 10.1136/hrt.2003.029850]
4 **Habib G**, Derumeaux G, Avierinos JF, Casalta JP, Jamal F, Volot F, Garcia M, Lefevre J, Biou F, Maximovitch-Rodaminoff A, Fournier PE, Ambrosi P, Velut JG, Cribier A, Harle JR, Weiller PJ, Raoult D, Luccioni R. Value and limitations of the Duke criteria for the diagnosis of infective endocarditis. *J Am Coll Cardiol* 1999; **33**: 2023-2029 [PMID: 10362209 DOI: 10.1016/S0735-1097(99)00116-3]
5 **Thuny F**, Grisoli D, Cautela J, Riberi A, Raoult D, Habib G. Infective endocarditis: prevention, diagnosis, and management. *Can J Cardiol* 2014; **30**: 1046-1057 [PMID: 25151287 DOI: 10.1016/j.cjca.2014.03.042]
6 **Vilacosta I**, Graupner C, San Román JA, Sarriá C, Ronderos R, Fernández C, Mancini L, Sanz O, Sanmartín JV, Stoermann W. Risk of embolization after institution of antibiotic therapy for infective endocarditis. *J Am Coll Cardiol* 2002; **39**: 1489-1495 [PMID: 11985912 DOI: 10.1016/S0735-1097(02)01790-4]
7 **Botelho-Nevers E**, Thuny F, Casalta JP, Richet H, Gouriet F, Collart F, Riberi A, Habib G, Raoult D. Dramatic reduction in infective endocarditis-related mortality with a management-based approach. *Arch Intern Med* 2009; **169**: 1290-1298 [PMID: 19636030 DOI: 10.1001/archinternmed.2009.192]
8 **Habib G**, Badano L, Tribouilloy C, Vilacosta I, Zamorano JL, Galderisi M, Voigt JU, Sicari R, Cosyns B, Fox K, Aakhus S. Recommendations for the practice of echocardiography in infective endocarditis. *Eur J Echocardiogr* 2010; **11**: 202-219 [PMID: 20223755 DOI: 10.1093/ejechocard/jeq004]
9 **Baddour LM**, Wilson WR, Bayer AS, Fowler VG, Tleyjeh IM, Rybak MJ, Barsic B, Lockhart PB, Gewitz MH, Levison ME, Bolger AF, Steckelberg JM, Baltimore RS, Fink AM, O'Gara P, Taubert KA. Infective Endocarditis in Adults: Diagnosis, Antimicrobial Therapy, and Management of Complications: A Scientific Statement for Healthcare Professionals From the American Heart Association. *Circulation* 2015; **132**: 1435-1486 [PMID: 26373316 DOI: 10.1161/CIR.0000000000000296]
10 **Gamelli RL**, Liu H, He LK, Hofmann CA. Augmentations of glucose uptake and glucose transporter-1 in macrophages following thermal injury and sepsis in mice. *J Leukoc Biol* 1996; **59**: 639-647 [PMID: 8656048]
11 **Fukuzumi M**, Shinomiya H, Shimizu Y, Ohishi K, Utsumi S. Endotoxin-induced enhancement of glucose influx into murine peritoneal macrophages via GLUT1. *Infect Immun* 1996; **64**: 108-112 [PMID: 8557327]
12 **Mochizuki T**, Tsukamoto E, Kuge Y, Kanegae K, Zhao S, Hikosaka K, Hosokawa M, Kohanawa M, Tamaki N. FDG uptake and glucose transporter subtype expressions in experimental tumor and inflammation models. *J Nucl Med* 2001; **42**: 1551-1555 [PMID: 11585872]
13 **Kubota R**, Yamada S, Kubota K, Ishiwata K, Tamahashi N, Ido T. Intratumoral distribution of fluorine-18-fluorodeoxyglucose in vivo: high accumulation in macrophages and granulation tissues studied by microautoradiography. *J Nucl Med* 1992; **33**: 1972-1980 [PMID: 1432158]
14 **Yamada S**, Kubota K, Kubota R, Ido T, Tamahashi N. High accumulation of fluorine-18-fluorodeoxyglucose in turpentine-induced inflammatory tissue. *J Nucl Med* 1995; **36**: 1301-1306 [PMID: 7790960]
15 **Coulden R**, Chung P, Sonnex E, Ibrahim Q, Maguire C, Abele J. Suppression of myocardial 18F-FDG uptake with a preparatory "Atkins-style" low-carbohydrate diet. *Eur Radiol* 2012; **22**: 2221-2228 [PMID: 22592807 DOI: 10.1007/s00330-012-2478-2]
16 **Persson E**. Lipoprotein lipase, hepatic lipase and plasma lipolytic activity. Effects of heparin and a low molecular weight heparin fragment (Fragmin). *Acta Med Scand Suppl* 1988; **724**: 1-56 [PMID: 2843005 DOI: 10.1111/j.1748-1716.1988.tb08452.x]
17 **Ahmed FZ**, James J, Memmott MJ, Arumugam P. Radionuclide Imaging of Cardiovascular Infection. *Cardiol Clin* 2016; **34**: 149-165 [PMID: 26590786 DOI: 10.1016/j.ccl.2015.06.004]
18 **de Vries EF**, Roca M, Jamar F, Israel O, Signore A. Guidelines for the labelling of leucocytes with (99m)Tc-HMPAO. Inflammation/Infection Taskgroup of the European Association of Nuclear Medicine. *Eur J Nucl Med Mol Imaging* 2010; **37**: 842-848 [PMID: 20198473 DOI: 10.1007/s00259-010-1394-4]
19 **Voigt A**, Shalaby A, Saba S. Rising rates of cardiac rhythm management device infections in the United States: 1996 through 2003. *J Am Coll Cardiol* 2006; **48**: 590-591 [PMID: 16875991 DOI: 10.1016/j.jacc.2006.05.016]
20 **Greenspon AJ**, Patel JD, Lau E, Ochoa JA, Frisch DR, Ho RT, Pavri BB, Kurtz SM. 16-year trends in the infection burden for pacemakers and implantable cardioverter-defibrillators in the United States 1993 to 2008. *J Am Coll Cardiol* 2011; **58**: 1001-1006 [PMID: 21867833 DOI: 10.1016/j.jacc.2011.04.033]
21 **Baddour LM**, Epstein AE, Erickson CC, Knight BP, Levison ME, Lockhart PB, Masoudi FA, Okum EJ, Wilson WR, Beerman LB, Bolger AF, Estes NA, Gewitz M, Newburger JW, Schron EB, Taubert KA. Update on cardiovascular implantable electronic device infections and their management: a scientific statement from the American Heart Association. *Circulation* 2010; **121**: 458-477 [PMID: 20048212 DOI: 10.1161/CIRCULATIONAHA.109.192665]
22 **Dundar C**, Tigen K, Tanalp C, Izgi A, Karaahmet T, Cevik C, Erkol A, Oduncu V, Kirma C. The prevalence of echocardiographic accretions on the leads of patients with permanent pacemakers. *J Am Soc Echocardiogr* 2011; **24**: 803-807 [PMID: 21493040 DOI: 10.1016/j.echo.2011.03.001]
23 **Vos FJ**, Bleeker-Rovers CP, van Dijk AP, Oyen WJ. Detection of pacemaker and lead infection with FDG-PET. *Eur J Nucl Med Mol Imaging* 2006; **33**: 1245 [PMID: 16826378]
24 **Bensimhon L**, Lavergne T, Hugonnet F, Mainardi JL, Latremouille C, Maunoury C, Lepillier A, Le Heuzey JY, Faraggi M. Whole body [(18) F]fluorodeoxyglucose positron emission tomography imaging for the diagnosis of pacemaker or implantable cardioverter defibrillator infection: a preliminary prospective study. *Clin Microbiol Infect* 2011; **17**: 836-844 [PMID: 20636421 DOI: 10.1111/j.1469-0691.2010.03312.x]
25 **Ploux S**, Riviere A, Amraoui S, Whinnett Z, Barandon L, Lafitte S, Ritter P, Papaioannou G, Clementy J, Jais P, Bordenave L, Haissaguerre M, Bordachar P. Positron emission tomography in patients with suspected pacing system infections may play a critical role in difficult cases. *Heart Rhythm* 2011; **8**: 1478-1481 [PMID: 21463705 DOI: 10.1016/j.hrthm.2011.03.062]
26 **Sarrazin JF**, Philippon F, Tessier M, Guimond J, Molin F, Champagne J, Nault I, Blier L, Nadeau M, Charbonneau L, Trottier M, O'Hara G. Usefulness of fluorine-18 positron emission tomography/computed tomography for identification of cardiovascular implantable electronic device infections. *J Am Coll Cardiol* 2012; **59**: 1616-1625 [PMID: 22538331 DOI: 10.1016/j.jacc.2011.11.059]
27 **Cautela J**, Alessandrini S, Cammilleri S, Giorgi R, Richet H, Casalta JP, Habib G, Raoult D, Mundler O, Deharo JC. Diagnostic yield of FDG positron-emission tomography/computed tomography in patients with CEID infection: a pilot study. *Europace* 2013; **15**: 252-257 [PMID: 23148119 DOI: 10.1093/europace/eus335]
28 **Ahmed FZ**, James J, Cunnington C, Motwani M, Fullwood C, Hooper J, Burns P, Qamruddin A, Al-Bahrani G, Armstrong I, Tout D, Clarke B, Sandoe JA, Arumugam P, Mamas MA, Zaidi AM. Early diagnosis of cardiac implantable electronic device generator pocket infection using ^{18}F-FDG-PET/CT. *Eur Heart J Cardiovasc Imaging* 2015; **16**: 521-530 [PMID: 25651856 DOI: 10.1093/ehjci/jeu295]
29 **Erba PA**, Sollini M, Conti U, Bandera F, Tascini C, De Tommasi SM, Zucchelli G, Doria R, Menichetti F, Bongiorni MG, Lazzeri E, Mariani G. Radiolabeled WBC scintigraphy in the diagnostic workup of patients with suspected device-related infections. *JACC Cardiovasc Imaging* 2013; **6**: 1075-1086 [PMID: 24011775 DOI: 10.1016/j.jcmg.2013.08.001]
30 **Plank F**, Mueller S, Uprimny C, Hangler H, Feuchtner G. Detection of bioprosthetic valve infection by image fusion of (18)fluorodeoxyglucose-positron emission tomography and

computed tomography. *Interact Cardiovasc Thorac Surg* 2012; **14**: 364-366 [PMID: 22180605 DOI: 10.1093/icvts/ivr107]

31 **Saby L**, Laas O, Habib G, Cammilleri S, Mancini J, Tessonnier L, Casalta JP, Gouriet F, Riberi A, Avierinos JF, Collart F, Mundler O, Raoult D, Thuny F. Positron emission tomography/computed tomography for diagnosis of prosthetic valve endocarditis: increased valvular 18F-fluorodeoxyglucose uptake as a novel major criterion. *J Am Coll Cardiol* 2013; **61**: 2374-2382 [PMID: 23583251 DOI: 10.1016/j.jacc.2013.01.092]

32 **Rouzet F**, Chequer R, Benali K, Lepage L, Ghodbane W, Duval X, Iung B, Vahanian A, Le Guludec D, Hyafil F. Respective performance of 18F-FDG PET and radiolabeled leukocyte scintigraphy for the diagnosis of prosthetic valve endocarditis. *J Nucl Med* 2014; **55**: 1980-1985 [PMID: 25453046 DOI: 10.2967/jnumed.114.141895]

33 **Asmar A**, Ozcan C, Diederichsen AC, Thomassen A, Gill S. Clinical impact of 18F-FDG-PET/CT in the extra cardiac work-up of patients with infective endocarditis. *Eur Heart J Cardiovasc Imaging* 2014; **15**: 1013-1019 [PMID: 24711514 DOI: 10.1093/ehjci/jeu054]

34 **Erba PA**, Conti U, Lazzeri E, Sollini M, Doria R, De Tommasi SM, Bandera F, Tascini C, Menichetti F, Dierckx RA, Signore A, Mariani G. Added value of 99mTc-HMPAO-labeled leukocyte SPECT/CT in the characterization and management of patients with infectious endocarditis. *J Nucl Med* 2012; **53**: 1235-1243 [PMID: 22787109 DOI: 10.2967/jnumed.111.099424]

35 **Hyafil F**, Rouzet F, Lepage L, Benali K, Raffoul R, Duval X, Hvass U, Iung B, Nataf P, Lebtahi R, Vahanian A, Le Guludec D. Role of radiolabelled leucocyte scintigraphy in patients with a suspicion of prosthetic valve endocarditis and inconclusive echocardiography. *Eur Heart J Cardiovasc Imaging* 2013; **14**: 586-594 [PMID: 23456094 DOI: 10.1093/ehjci/jet029]

36 **Schouten LR**, Verberne HJ, Bouma BJ, van Eck-Smit BL, Mulder BJ. Surgical glue for repair of the aortic root as a possible explanation for increased F-18 FDG uptake. *J Nucl Cardiol* 2008; **15**: 146-147 [PMID: 18242493]

37 **Xia T**, Alessio AM, De Man B, Manjeshwar R, Asma E, Kinahan PE. Ultra-low dose CT attenuation correction for PET/CT. *Phys Med Biol* 2012; **57**: 309-328 [PMID: 22156174 DOI: 10.1088/0031-9155/57/2/309]

38 **Picano E**, Vañó E, Rehani MM, Cuocolo A, Mont L, Bodi V, Bar O, Maccia C, Pierard L, Sicari R, Plein S, Mahrholdt H, Lancellotti P, Knuuti J, Heidbuchel H, Di Mario C, Badano LP. The appropriate and justified use of medical radiation in cardiovascular imaging: a position document of the ESC Associations of Cardiovascular Imaging, Percutaneous Cardiovascular Interventions and Electrophysiology. *Eur Heart J* 2014; **35**: 665-672 [PMID: 24401558 DOI: 10.1093/eurheartj/eht394]

P- Reviewer: Falconi M, Peteiro J, Said SAM **S- Editor**: Gong XM
L- Editor: A **E- Editor**: Wu HL

World Journal of Cardiology

Submit a Manuscript: http://www.wjgnet.com/esps/
Help Desk: http://www.wjgnet.com/esps/helpdesk.aspx
DOI: 10.4330/wjc.v8.i9.547

World J Cardiol 2016 September 26; 8(9): 547-552
ISSN 1949-8462 (online)

ORIGINAL ARTICLE

Retrospective Study

Depression risk in patients with coronary heart disease in Germany

Marcel Konrad, Louis Jacob, Michael A Rapp, Karel Kostev

Marcel Konrad, Department of Health, Fresenius University, 65510 Idstein, Germany

Louis Jacob, Department of Biology, École Normale Supérieure, 69007 Lyon, France

Michael A Rapp, Department of Social and Preventive Medicine, University of Potsdam, 14469 Potsdam, Germany

Karel Kostev, Department of Epidemiology, IMS Health, 60598 Frankfurt am Main, Germany

Author contributions: Konrad M designed and performed the research and wrote the paper; Jacob L designed the research; Rapp MA designed the research and provided clinical advice; Kostev K performed the analysis and supervised the report.

Institutional review board statement: This study was reviewed and approved by the Ethics Committee of the IMS Health.

Informed consent statement: Patients were not required to give informed consent to the study because the analysis used anonymous data.

Conflict-of-interest statement: We have no financial relationships to disclose.

Data sharing statement: Technical details and statistical methods are available with the corresponding author at kkostev@de.imshealth.com.

Manuscript source: Invited manuscript

Correspondence to: Karel Kostev, DMSc, PhD, Professor, Department of Epidemiology, IMS Health, Frankfurt am Main, Darmstädter Landstr, 60598 Frankfurt am Main, Germany. kkostev@de.imshealth.com
Telephone: +49-69-66044878
Fax: +49-69-66045878

Received: May 5, 2016
Peer-review started: May 9, 2016
First decision: June 13, 2016
Revised: July 12, 2016
Accepted: July 29, 2016
Article in press: August 1, 2016
Published online: September 26, 2016

Abstract

AIM

To determine the prevalence of depression and its risk factors among patients with coronary heart disease (CHD) treated in German primary care practices.

METHODS

Longitudinal data from nationwide general practices in Germany (n = 1072) were analyzed. Individuals initially diagnosed with CHD (2009-2013) were identified, and 59992 patients were included and matched (1:1) to 59992 controls. The primary outcome measure was an initial diagnosis of depression within five years after the index date among patients with and without CHD. Cox proportional hazards models were used to adjust for confounders.

RESULTS

Mean age was equal to 68.0 years (SD = 11.3). A total of 55.9% of patients were men. After a five-year follow-up, 21.8% of the CHD group and 14.2% of the control group were diagnosed with depression (P < 0.001). In the multivariate regression model, CHD was a strong risk factor for developing depression (HR =

1.54, 95%CI: 1.49-1.59, $P < 0.001$). Prior depressive episodes, dementia, and eight other chronic conditions were associated with a higher risk of developing depression. Interestingly, older patients and women were also more likely to be diagnosed with depression compared with younger patients and men, respectively.

CONCLUSION

The risk of depression is significantly increased among patients with CHD compared with patients without CHD treated in primary care practices in Germany. CHD patients should be routinely screened for depression to ensure improved treatment and management.

Key words: Coronary heart disease; Depression; Primary care; Risk factors; Quality of life

Core tip: This is a retrospective study to determine the prevalence of depression and its risk factors among patients with coronary heart disease (CHD) treated in German primary care practices. Fifty-nine thousand nine hundred and ninety-two patients with CHD from German primary care practices were included and matched to 59992 controls. After a five-year follow-up, 21.8% of the CHD group and 14.2% of the control group were diagnosed with depression. In the multivariate regression model, CHD was a strong risk factor for developing depression.

Konrad M, Jacob L, Rapp MA, Kostev K. Depression risk in patients with coronary heart disease in Germany. *World J Cardiol* 2016; 8(9): 547-552 Available from: URL: http://www.wjgnet.com/1949-8462/full/v8/i9/547.htm DOI: http://dx.doi.org/10.4330/wjc.v8.i9.547

INTRODUCTION

Coronary heart disease (CHD), as one of the cardiovascular diseases (CVDs), is a leading chronic medical condition worldwide, with a large number of affected patients[1,2]. CHD is characterized by the manifestation of atherosclerosis in coronary arteries, that is, narrowed coronary arteries and reduced perfusion of the heart. This can lead to a myocardial infarction[3,4]. CVD and CHD are major causes of death around the world[1], particularly in Germany, where CVD was responsible for 338056 deaths in 2014 (38.9% of the total number of deaths)[5]. In this context, the CHD-related mortality rate was approximately 20%, with a total of 69890 deaths in 2014[6].

Approximately 6 million people are affected by CHD in Germany[7]. Due to improvements in various therapies, mortality rates have decreased worldwide. Nevertheless, the prevalence of CHD is increasing, partly due to the demographic aging of the population, increased prevalence of cardiovascular risk factors, and patients' improved survival after a cardiovascular event[2]. While the lifetime prevalence of CHD among German women remained unchanged at approximately 7% between 2003 and 2012, it increased from 8% in 2003 to 10% in 2010 among German men[8].

It is known that the risk of depression is significantly increased among individuals with chronic diseases (*e.g.,* CHD), as they exhibit 2-3 times higher rates than the general population[9,10]. Depression significantly worsens the health state of patients with chronic diseases[11]. Overall, depression adversely affects the course, complications, and management of CHD[10,12]. Furthermore, depression in patients with CHD contributes to poor functional and cardiovascular outcomes, poor quality of life, and increased mortality[13-16].

Depression is frequently observed in patients with CHD[14]. Previous studies showed that up to 30% of patients with CHD suffer from depression[17]. Most published studies examined hospital patients or were based on a small number of patients[18]. Thus, little is known about the prevalence of depression among outpatients with CHD[14]. Because no relevant German data exist, the goal of this study was to estimate the prevalence and the risk factors of depression among CHD patients treated in primary care practices in Germany.

MATERIALS AND METHODS

Database

The Disease Analyzer database (IMS HEALTH) compiles drug prescriptions, diagnoses, and basic medical and demographic data obtained directly and in anonymous format from computer systems used by general practitioners[19]. IMS has monitored diagnoses (ICD-10), prescriptions (Anatomical Therapeutic Chemical (ATC) Classification System), and the quality of reported data according to a number of criteria (*e.g.,* completeness of documentation, linkage between diagnoses and prescriptions). In Germany, the sampling methods used to select physicians' practices were appropriate for obtaining a representative database of primary care practices[19]. The statistics regarding prescriptions for several drugs were very similar to data available in pharmaceutical prescription reports[19]. The age groups suffering from given diagnoses in the Disease Analyzer were also consistent with those in corresponding disease registries[19].

Study population

This study included patients between 40 and 90 years of age who were being treated in 1072 primary care practices and who received an initial CHD diagnosis (ICD 10: I25) during the index period (January 2009 to December 2013). Follow-up lasted a maximum of five years and ended in October 2015. Patients were excluded if they were diagnosed with depression

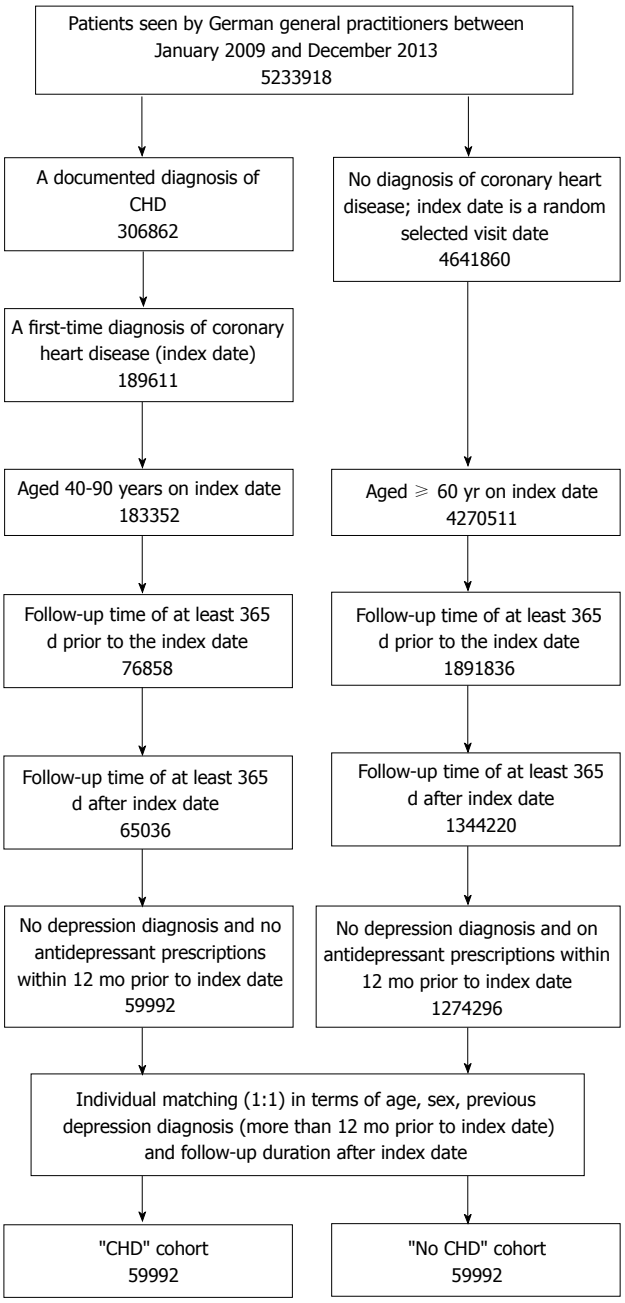

Figure 1 Selection of study patients. CHD: Coronary heart disease.

(ICD-10: F32, F33) or received any antidepressant prescription (ATC: N06A) within 12 mo prior to CHD diagnosis (index date). A total of 59992 CHD patients remained after these exclusion criteria were applied. Finally, 59992 controls without CHD, depression diagnosis or antidepressant prescriptions within 12 mo prior to index date (any randomly selected visit date) were chosen and matched (1:1) to CHD cases based on age, sex, past depression diagnosis (more than 12 mo prior to index date), and follow-up duration after the index date (Figure 1).

Study outcome

The primary outcome was the diagnosis of depression recorded in the database between the index date and the end of follow-up. Depression diagnoses were based on primary care documentation.

Table 1 Characteristics of coronary heart disease patients and matched controls treated in primary care practices in Germany

Variables	CHD group	Control group	*P* value
n	59992	59992	
Age (yr)	68.0 (11.3)	68.0 (11.3)	1
Aged ⩽ 60 (%)	26.7	26.7	1
Aged 61-70 (%)	26.5	26.5	1
Aged 71-80 (%)	32.6	32.6	1
Aged > 80 (%)	14.3	14.3	1
Males (%)	55.9	55.9	1
Follow-up time (yr)	3.6 (1.5)	3.6 (1.5)	1
Past depression diagnosis (> 12 mo prior to index date)	11.1	11.1	1
Co-diagnosis (%)			
Diabetes	35.9	23.4	< 0.001
Hypertension	78.7	59.4	< 0.001
Myocardial infarction	11.8	0.6	< 0.001
Cardiac arrhythmias	25.7	14.3	< 0.001
Heart failure	18.4	7.4	< 0.001
Stroke	9.2	5.6	< 0.001
Cancer	11.9	11.1	< 0.001
Dementia	4.9	4.5	< 0.001
Osteoarthritis	31.4	27.6	< 0.001
Osteoporosis	10.3	8.4	< 0.001

CHD: Coronary heart disease.

Independent variables

Demographic data included age and gender. Other chronic conditions that could be associated with depression risk were determined based on primary care diagnoses and included as confounders: Diabetes mellitus (E10-14), hypertension (I10), dementia (F01, F03, G30), stroke (F63, F64, G45), heart failure (I10), myocardial infarction (I21-23), cardiac arrhythmias (I46-I49), osteoporosis (M80, M81), cancer (C00-C98), and osteoarthritis (M15-19).

Statistical analysis

Descriptive statistics were obtained, and differences in patients' characteristics (CHD *vs* controls) were assessed using Wilcoxon tests for paired samples or McNemar's tests. Analyses of depression-free survival were carried out using Kaplan-Meier curves and log-rank tests. Cox proportional hazards models (dependent variable: Depression) were used to adjust for confounders. $P < 0.05$ was considered statistically significant. The analyses were carried out using SAS version 9.3.

RESULTS

Patient characteristics are displayed in Table 1. A total of 119984 patients were included in the CHD and control groups. Mean age was equal to 68.0 years (SD = 11.3 years), and 55.9% of the patients were men. The proportion of patients with a prior depression

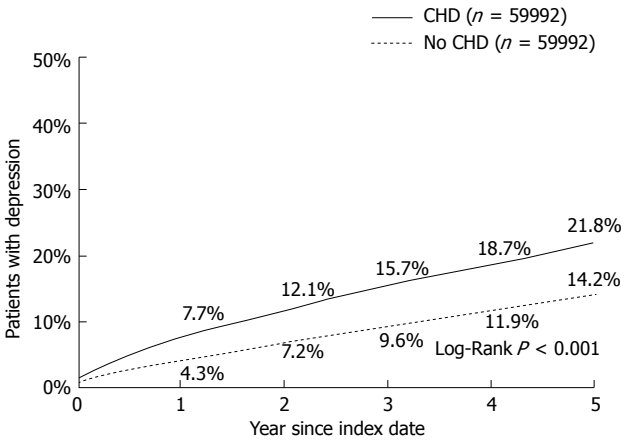

Figure 2 Kaplan-Meier curves for time to depression diagnosis in coronary heart disease patients and matched controls. CHD: Coronary heart disease.

diagnosis (> 12 mo prior to the index date) was 11.1% in both groups. All chronic conditions (*i.e.*, diabetes, hypertension, myocardial infarction, cardiac arrhythmias, heart failure, stroke, cancer, dementia, osteoarthritis and osteoporosis) occurred more frequently in the CHD group than in the control group (P < 0.001).

Kaplan-Meier curves for time to depression diagnosis in the CHD and control groups are displayed in Figure 2. Overall, 7.7% of CHD patients and 4.3% of matched controls had developed depression after one year of follow-up (P < 0.001). After a five-year follow-up period, 21.8% of the CHD group and 14.2% of the control group were diagnosed with depression (P < 0.001).

The results of the multivariate Cox regression model for depression diagnosis in CHD patients and matched controls are illustrated in Table 2. CHD was a strong risk factor for the development of depression (HR = 1.54, 95%CI: 1.49-1.59, P < 0.001). Prior depressive episodes also increased the risk of renewed depression diagnosis (HR = 3.44; 95%CI: 3.32-3.56, P < 0.001). Patients in the age group ⩽ 60 had a higher risk of depression compared with patients aged 61-70 years (HR = 1.50, 95%CI: 1.44-1.57, P < 0.001). Patients in the age groups 71-80 and > 80 years were also more likely to be diagnosed with depression than patients aged 61-70 years (HR = 1.08 (95%CI: 1.04-1.13) and 1.16 (95%CI: 1.10-1.23), respectively, both P < 0.001). Furthermore, other chronic co-diagnoses increased the risk of depression (P < 0.001). By contrast, men had a lower risk of being depressed than women (HR = 0.67; 95%CI: 0.65-0.69).

Table 2 Multivariate Cox regression model for depression diagnosis in coronary heart disease patients and matched controls chemotherapy

Variables	Hazard ratio (95%CI)	*P* value
CHD	1.54 (1.49-1.59)	< 0.001
Past depression diagnosis	3.44 (3.32-3.56)	< 0.001
Aged ⩽ 60 *vs* 61-70	1.50 (1.44-1.57)	< 0.001
Aged 71-80 *vs* 61-70	1.08 (1.04-1.13)	< 0.001
Aged > 80 *vs* 61-70	1.16 (1.10-1.23)	< 0.001
Male gender	0.67 (0.65-0.69)	< 0.001
Dementia	1.24 (1.17-1.31)	< 0.001
Stroke	1.22 (1.16-1.28)	< 0.001
Cancer	1.19 (1.14-1.24)	< 0.001
Osteoporosis	1.18 (1.13-1.24)	< 0.001
Heart failure	1.17 (1.12-1.22)	< 0.001
Osteoarthritis	1.15 (1.11-1.19)	< 0.001
Hypertension	1.10 (1.06-1.14)	< 0.001
Cardiac arrhythmias	1.08 (1.04-1.12)	< 0.001
Diabetes	1.06 (1.03-1.10)	< 0.001

CHD: Coronary heart disease.

DISCUSSION

In this retrospective study of 119984 patients treated in primary care practices in Germany, we showed that CHD was associated with an increased risk of developing depression. Moreover, prior depressive episodes and co-diagnoses such as dementia, stroke, cancer, osteoporosis, heart failure, osteoarthritis, hypertension, cardiac arrhythmias, and diabetes were also risk factors for this psychiatric disorder. Individuals aged 60 years or younger and individuals aged over 70 years were more likely to develop depression compared with patients aged 61-70 years. Finally, men were at a lower risk of being diagnosed with depression than women.

CHD is a chronic disease that has an important impact on patients' physical and psychological aspects of life. Indeed, patients affected by CHD are more likely to become depressed than those without CHD. Several studies estimated that depression affects between 17.2% and 30.6% of CHD patients[20-23] but only approximately 7% of the general population[17]. More recently, Ren *et al*[18] performed a meta-analysis on the prevalence of depression among CHD patients in hospital and community settings. In the 23 hospital-based studies (the total number of patients equalled 5236), the prevalence of depression ranged from 22.8% to 84.0%, with 0.5% to 25.44% categorized as severe forms[18]. In the four community-based studies (the total number of patients equalled 1353), depression prevalence ranged from 34.6% to 45.0%, with 3.1%-6.9% classified as major depressive disorders[18]. This meta-analysis clearly indicates that although hospital and community settings have a similar total number of patients, more hospital-based than community-based studies have been conducted and results differ between the two settings. Thus, because the findings of hospital-based studies cannot be extrapolated to the community population, new studies must be conducted outside the hospital setting. In line with previous data, we found that after five years of follow-up, 21.8% of CHD patients were depressed, whereas only 14.2% of controls exhibited this psychiatric condition. This important result underlines the fact that CHD increases the odds that patients treated in general

practices in Germany develop depression.

Interestingly, the relationship between depression and CHD is bidirectional; thus, depression is also a risk factor for CHD[17]. In 2010, Taylor *et al*[24] showed that CHD risk, which was similar at baseline to that of the general population, increased within the first two years following the diagnosis of major depressive disorders. The main hypothesis proposed to explain the bidirectional relationship between CHD and depression asserts that they share common risk factors. First, stress is known to increase the odds of developing these two diseases[24,25]. Indeed, stress has a major impact on the cardiovascular system and on psychological aspects of individuals' life and thus increases the occurrence of both disorders. Importantly, beyond the influence of stress, behavioral disorders can also lead to CHD and depression. In fact, such psychiatric preconditions are often associated with a loss of interest in daily tasks (*i.e.,* eating or engaging in physical activity)[17], which may indirectly lead to depression and disrupt the body's energetic balance. Finally, several authors suggested that CHD and depression share common genetic mechanisms that are involved in inflammation pathways and oxidative stress[17]. For example, the length of leukocyte telomeres is negatively associated with major depressive disorders and coronary artery disease[26,27].

In this study, we found that prior depressive episodes, dementia, stroke, cancer, osteoporosis, heart failure, osteoarthritis, hypertension, cardiac arrhythmias, and diabetes were additional risk factors for depression. Most of these diseases are chronic conditions that may reduce affected patients' quality of life. Of note, the strongest predictor was past depressive episodes (HR = 3.44; 95%CI: 3.32-3.56). In fact, depression is a highly recurrent disorder that is difficult for physicians to treat and manage[28]. Our data also showed that men were at a lower risk of developing this psychiatric disorder than women. In 2005, Perez *et al*[29] conducted a study of 345 patients with acute coronary syndrome and found that women were more likely to be diagnosed with depression than men (OR = 2.40, 95%CI: 1.44-4.00)[29]. Although several authors hypothesized that there are important gender differences in hormones, genes, and brain structures, our discovery may be explained by artefacts because women tend to be more emotional and are more inclined to seek medical help than men. Finally, we found that individuals aged 60 years or younger and those aged over 70 years have a higher risk of developing depression than patients aged 61-70 years. Although this finding is new and surprising, one hypothesis maintains that individuals aged 61-70 years receive optimal treatment and management. Because younger patients are less likely to develop chronic diseases, medical follow-up is difficult and they may be at higher risk of developing depression. However, very elderly patients are less compliant and may not follow the treatment prescribed by their general practitioner.

This study had several limitations. The database contained no valid information on biological markers associated with CHD. Furthermore, no detailed documentation concerning the diagnosis of depression, namely, the severity of depression, was available. Data on socioeconomic status and lifestyle-related risk factors were also unavailable. Each patient was observed retrospectively in only one practice. If a patient visited a different doctor - which is common in Germany - the visit was not documented.

In conclusion, this study showed that CHD patients were at a higher risk of developing depression than patients without CHD. Interestingly, prior depressive episodes, dementia, stroke, cancer, osteoporosis, heart failure, osteoarthritis, hypertension, cardiac arrhythmias, and diabetes were additional risk factors for this psychiatric condition. Finally, we found that individuals aged 60 years or younger and those aged over 70 years have a higher risk of developing depression than patients aged 61-70 years. Further investigations are needed to gain a better understanding of the association between depression and CHD in general practices in Germany.

COMMENTS

Background

Coronary heart disease (CHD) is a leading chronic medical condition worldwide, with a large number of affected patients. CHD is characterized by the manifestation of atherosclerosis in coronary arteries, that is, narrowed coronary arteries and reduced perfusion of the heart. This can lead to a myocardial infarction. CHD is one of the causes of death around the world. It is known that the risk of depression is significantly increased among individuals with chronic diseases. Overall, depression adversely affects the course, complications, and management of CHD.

Research frontiers

Thus, little is known about the prevalence of depression among outpatients with CHD. Because no relevant German data exist, the goal of this study was to estimate the prevalence and the risk factors of depression among CHD patients treated in primary care practices in Germany.

Innovations and breakthroughs

In this study, analyses were performed based on 119984 patients treated in primary care practices in Germany. At first, this is the first study using such large patient numbers; at second, the study cohort includes both high-risk patients and patients without CHD diagnosis.

Applications

This study showed that CHD patients were at a much higher risk of developing depression than patients without CHD, especially patients who additionally have further chronic co-diagnoses. Physicians who care for CHD patients should consider identification and treatment of depression a clinical practice.

Terminology

CHD: Coronary heart disease; ICD: International classification of disease.

Peer-review

The authors did a retrospective analysis on a German cohort of 119984 patients to examine the association between CHD and the development of depression. Strength of this study lies in the great sample size, and it is a community-based study. In this study, the author determines the prevalence of depression and its risk factors in patients with coronary heart disease. They found that CHD was a

strong risk factor for depression development in German population.

REFERENCES

1 **Nichols M**, Townsend N, Scarborough P, Rayner M. Cardiovascular disease in Europe 2014: epidemiological update. *Eur Heart J* 2014; **35**: 2929 [PMID: 25381246 DOI: 10.1093/eurheartj/ehu378]

2 **Bansilal S**, Castellano JM, Fuster V. Global burden of CVD: focus on secondary prevention of cardiovascular disease. *Int J Cardiol* 2015; **201** Suppl 1: S1-S7 [PMID: 26747389 DOI: 10.1016/S0167-5273(15)31026-3]

3 **De Hert M**, Cohen D, Bobes J, Cetkovich-Bakmas M, Leucht S, Ndetei DM, Newcomer JW, Uwakwe R, Asai I, Möller HJ, Gautam S, Detraux J, Correll CU. Physical illness in patients with severe mental disorders. II. Barriers to care, monitoring and treatment guidelines, plus recommendations at the system and individual level. *World Psychiatry* 2011; **10**: 138-151 [PMID: 21633691 DOI: 10.1002/j.2051-5545.2011.tb00036.x]

4 **Libby P**, Theroux P. Pathophysiology of coronary artery disease. *Circulation* 2005; **111**: 3481-3488 [PMID: 15983262 DOI: 10.1161/CIRCULATIONAHA.105.537878]

5 **Statistisches Bundesamt**. Todesursachen in Deutschland, 2014. Available from: URL: http//www.destatis.de/DE/ZahlenFakten/GesellschaftStaat/Gesundheit/Todesursachen/Todesursachen.html

6 **Statistisches Bundesamt**. Die 10 häufigsten Todesfälle durch Herz-Kreislauf-Erkrankungen. Sterbefälle insgesamt, 2014. Available from: URL: http// www.destatis.de/DE/ZahlenFakten/GesellschaftStaat/Gesundheit/Todesursachen/Tabellen/HerzKreislaufErkrankungen.html

7 **Hamm C**. Koronare Herzkrankheit. Was genau ist eigentlich eine KHK? 2016. Available from: URL: http://www.ukgm.de/ugm_2/deu/ugi_kar/PDF/Flyer_KHK.pdf

8 **Koch-Institut R**. Daten und Fakten: Ergebnisse der Studie "Gesundheit in Deutschland aktuell 2012". Beiträge zur Gesundheitsberichterstattung des Bundes, 2016

9 **Haddad M**, Walters P, Phillips R, Tsakok J, Williams P, Mann A, Tylee A. Detecting depression in patients with coronary heart disease: a diagnostic evaluation of the PHQ-9 and HADS-D in primary care, findings from the UPBEAT-UK study. *PLoS One* 2013; **8**: e78493 [PMID: 24130903 DOI: 10.1371/journal.pone.0078493]

10 **Katon WJ**. Epidemiology and treatment of depression in patients with chronic medical illness. *Dialogues Clin Neurosci* 2011; **13**: 7-23 [PMID: 21485743]

11 **Moussavi S**, Chatterji S, Verdes E, Tandon A, Patel V, Ustun B. Depression, chronic diseases, and decrements in health: results from the World Health Surveys. *Lancet* 2007; **370**: 851-858 [PMID: 17826170 DOI: 10.1016/S0140-6736(07)61415-9]

12 **Lichtman JH**, Froelicher ES, Blumenthal JA, Carney RM, Doering LV, Frasure-Smith N, Freedland KE, Jaffe AS, Leifheit-Limson EC, Sheps DS, Vaccarino V, Wulsin L. Depression as a risk factor for poor prognosis among patients with acute coronary syndrome: systematic review and recommendations: a scientific statement from the American Heart Association. *Circulation* 2014; **129**: 1350-1369 [PMID: 24566200 DOI: 10.1161/CIR.0000000000000019]

13 **Ruo B**, Rumsfeld JS, Hlatky MA, Liu H, Browner WS, Whooley MA. Depressive symptoms and health-related quality of life: the Heart and Soul Study. *JAMA* 2003; **290**: 215-221 [PMID: 12851276 DOI: 10.1001/jama.290.2.215]

14 **Lichtman JH**, Bigger JT, Blumenthal JA, Frasure-Smith N, Kaufmann PG, Lespérance F, Mark DB, Sheps DS, Taylor CB, Froelicher ES. Depression and coronary heart disease: recommendations for screening, referral, and treatment: a science advisory from the American Heart Association Prevention Committee of the Council on Cardiovascular Nursing, Council on Clinical Cardiology, Council on Epidemiology and Prevention, and Interdisciplinary Council on Quality of Care and Outcomes Research: endorsed by the American Psychiatric Association. *Circulation* 2008; **118**: 1768-1775 [PMID: 18824640 DOI: 10.1161/CIRCULATIONAHA.108.190769]

15 **Celano CM**, Huffman JC. Depression and cardiac disease: a review. *Cardiol Rev* 2011; **19**: 130-142 [PMID: 21464641 DOI: 10.1097/CRD.0b013e31820e8106]

16 **Sin NL**, Yaffe K, Whooley MA. Depressive symptoms, cardiovascular disease severity, and functional status in older adults with coronary heart disease: the heart and soul study. *J Am Geriatr Soc* 2015; **63**: 8-15 [PMID: 25597554 DOI: 10.1111/jgs.13188]

17 **Chauvet-Gélinier JC**, Trojak B, Vergès-Patois B, Cottin Y, Bonin B. Review on depression and coronary heart disease. *Arch Cardiovasc Dis* 2013; **106**: 103-110 [PMID: 23527914 DOI: 10.1016/j.acvd.2012.12.004]

18 **Ren Y**, Yang H, Browning C, Thomas S, Liu M. Prevalence of depression in coronary heart disease in China: a systematic review and meta-analysis. *Chin Med J* (Engl) 2014; **127**: 2991-2998 [PMID: 25131240 DOI: 10.3760/cma.j.issn.0366-6999.20140036]

19 **Becher H**, Kostev K, Schröder-Bernhardi D. Validity and representativeness of the "Disease Analyzer" patient database for use in pharmacoepidemiological and pharmacoeconomic studies. *Int J Clin Pharmacol Ther* 2009; **47**: 617-626 [PMID: 19825325]

20 **Frasure-Smith N**, Lespérance F, Talajic M. Depression and 18-month prognosis after myocardial infarction. *Circulation* 1995; **91**: 999-1005 [PMID: 7531624 DOI: 10.1161/01.CIR.91.4.999]

21 **Ziegelstein RC**, Fauerbach JA, Stevens SS, Romanelli J, Richter DP, Bush DE. Patients with depression are less likely to follow recommendations to reduce cardiac risk during recovery from a myocardial infarction. *Arch Intern Med* 2000; **160**: 1818-1823 [PMID: 10871976 DOI: 10.1001/archinte.160.12.1818]

22 **Davidson KW**, Burg MM, Kronish IM, Shimbo D, Dettenborn L, Mehran R, Vorchheimer D, Clemow L, Schwartz JE, Lespérance F, Rieckmann N. Association of anhedonia with recurrent major adverse cardiac events and mortality 1 year after acute coronary syndrome. *Arch Gen Psychiatry* 2010; **67**: 480-488 [PMID: 20439829 DOI: 10.1001/archgenpsychiatry.2010.36]

23 **Myers V**, Gerber Y, Benyamini Y, Goldbourt U, Drory Y. Post-myocardial infarction depression: increased hospital admissions and reduced adoption of secondary prevention measures--a longitudinal study. *J Psychosom Res* 2012; **72**: 5-10 [PMID: 22200515 DOI: 10.1016/j.jpsychores.2011.09.009]

24 **Taylor V**, McKinnon MC, Macdonald K, Jaswal G, Macqueen GM. Adults with mood disorders have an increased risk profile for cardiovascular disease within the first 2 years of treatment. *Can J Psychiatry* 2010; **55**: 362-368 [PMID: 20540831]

25 **Nabi H**, Kivimäki M, Batty GD, Shipley MJ, Britton A, Brunner EJ, Vahtera J, Lemogne C, Elbaz A, Singh-Manoux A. Increased risk of coronary heart disease among individuals reporting adverse impact of stress on their health: the Whitehall II prospective cohort study. *Eur Heart J* 2013; **34**: 2697-2705 [PMID: 23804585 DOI: 10.1093/eurheartj/eht216]

26 **Simon NM**, Smoller JW, McNamara KL, Maser RS, Zalta AK, Pollack MH, Nierenberg AA, Fava M, Wong KK. Telomere shortening and mood disorders: preliminary support for a chronic stress model of accelerated aging. *Biol Psychiatry* 2006; **60**: 432-435 [PMID: 16581033 DOI: 10.1016/j.biopsych.2006.02.004]

27 **Mukherjee M**, Brouilette S, Stevens S, Shetty KR, Samani NJ. Association of shorter telomeres with coronary artery disease in Indian subjects. *Heart* 2009; **95**: 669-673 [PMID: 19028761 DOI: 10.1136/hrt.2008.150250]

28 **Burcusa SL**, Iacono WG. Risk for recurrence in depression. *Clin Psychol Rev* 2007; **27**: 959-985 [PMID: 17448579 DOI: 10.1016/j.cpr.2007.02.005]

29 **Perez GH**, Nicolau JC, Romano BW, Laranjeira R. [Depression and Acute Coronary Syndromes: gender-related differences]. *Arq Bras Cardiol* 2005; **85**: 319-326 [PMID: 16358147 DOI: 10.1590/S0066-782X2005001800004]

P- Reviewer: Gao DF, Tao J **S- Editor**: Qiu S **L- Editor**: A
E- Editor: Wu HL

World Journal of Cardiology

Submit a Manuscript: http://www.wjgnet.com/esps/
Help Desk: http://www.wjgnet.com/esps/helpdesk.aspx
DOI: 10.4330/wjc.v8.i9.553

World J Cardiol 2016 September 26; 8(9): 553-558
ISSN 1949-8462 (online)

ORIGINAL ARTICLE

Observational Study

Characterization of optimal resting tension in human pulmonary arteries

Azar Hussain, Robert T Bennett, Mubarak A Chaudhry, Syed S Qadri, Mike Cowen, Alyn H Morice, Mahmoud Loubani

Azar Hussain, Robert T Bennett, Mubarak A Chaudhry, Syed S Qadri, Mike Cowen, Mahmoud Loubani, Department of Cardiothoracic Surgery, Castle Hill Hospital, Cottingham HU16 5JQ, United Kingdom

Alyn H Morice, Centre for Cardiovascular and Metabolic Research, Hull York Medical School, Castle Hill Hospital, Cottingham HU16 5JQ, United Kingdom

Author contributions: Hussain A was the principal investigator and was responsible for the design and conduct of the study; Hussain A was responsible for the acquisition, analysis and interpretation of the data and initial draft of the manuscript; Bennett RT, Chaudhry MA, Qadri SS, Cowen M, Morice AH and Loubani M supervised the study and critically reviewed the article.

Institutional review board statement: The study was reviewed and approved by the Local Research Ethics Committee and local research and development department.

Informed consent statement: All patients were consulted and consented for resected lung tissue to be studied for our research prior to their operation at the time of their consent for surgery.

Conflict-of-interest statement: There are no conflicts of interest to report.

Data sharing statement: No additional data are available.

Manuscript source: Invited manuscript

Correspondence to: Azar Hussain, MBBS, MRCS (Ed), Clinical Research Fellow, Department of Cardiothoracic Surgery, Castle Hill Hospital, Castle Road, Cottingham HU16 5JQ, United Kingdom. dr_azarhussain@hotmail.com
Telephone: +44-77-48019242

Received: May 16, 2016
Peer-review started: May 16, 2016
First decision: July 5, 2016
Revised: July 15, 2016
Accepted: July 29, 2016
Article in press: August 1, 2016
Published online: September 26, 2016

Abstract

AIM

To determine the optimum resting tension (ORT) for in vitro human pulmonary artery (PA) ring preparations.

METHODS

Pulmonary arteries were dissected from disease free sections of the resected lung in the operating theatre and tissue samples were directly sent to the laboratory in Krebs-Henseleit solution (Krebs). The pulmonary arteries were then cut into 2 mm long rings. PA rings were mounted in 25 mL organ baths or 8 mL myograph chambers containing Krebs compound (37 ℃, bubbled with 21% O_2: 5% CO_2) to measure changes in isometric tension. The resting tension was set at 1-gram force (gf) with vessels being left static to equilibrate for duration of one hour. Baseline contractile reactions to 40 mmol/L KCl were obtained from a resting tension of 1 gf. Contractile reactions to 40 mmol/L KCl were then obtained from stepwise increases in resting tension (1.2, 1.4, 1.6, 1.8 and 2.0 gf).

RESULTS

Twenty PA rings of internal diameter between 2-4 mm

were prepared from 4 patients. In human PA rings incrementing the tension during rest stance by 0.6 gf, up to 1.6 gf significantly augmented the 40 mmol/L KCl stimulated tension. Further enhancement of active tension by 0.4 gf, up to 2.0 gf mitigate the 40 mmol/L KCl stimulated reaction. Both Myograph and the organ bath demonstrated identical conclusions, supporting that the radial optimal resting tension for human PA ring was 1.61 g.

CONCLUSION

The radial optimal resting tension in our experiment is 1.61 gf (15.78 mN) for human PA rings.

Key words: Pulmonary hypertension; Pulmonary artery; Optimal resting tension; Pulmonary artery rings; Human

Core tip: Pulmonary artery (PA) vasoconstriction is an important physiological process to regulate blood flow in the lungs but it also manifests in pathological conditions. Different models have been implemented to assess the baseline molecular and cellular functions of pulmonary ailments. However, a great deal of the research was undertaken on animals with little similarity to human tissue. Isolation of human PA and measurement of pulmonary vascular tension are vital to understand the pathophysiology of human pulmonary vessels. The objective behind this research is to assess the underlying resting tension for undertaking studies of the PA rings in humans.

Hussain A, Bennett RT, Chaudhry MA, Qadri SS, Cowen M, Morice AH, Loubani M. Characterization of optimal resting tension in human pulmonary arteries. *World J Cardiol* 2016; 8(9): 553-558 Available from: URL: http://www.wjgnet.com/1949-8462/full/v8/i9/553.htm DOI: http://dx.doi.org/10.4330/wjc.v8.i9.553

INTRODUCTION

The vascular wall is constituted by three sections or layers; the tunica intima, tunica media, and tunica externa, also otherwise known as the internal, middle and outer layer, respectively[1]. Endothelial cells are located in the intima and play an important role in regulating vascular operations through reacting to neurotransmitters, hormones and vasoactive elements[2]. The endothelium and smooth muscle are the vital components for maintenance of arterial tone and blood pressure directive. The arteries main purpose is to deliver the blood to the organs with high pulse pressure. Arteries are generally classified into conducting arteries, conduit arteries (macrovasculature) and resistance arteries (microvasculature) sourced on size, anatomical position and functionality[3]. Conducting arteries are the largest in size and rich in elastic tissues which support the vessels to expand and recoil to accommodate high changes in blood pressure. The aorta, pulmonary artery (PA) and carotid arteries are the main examples of conducting arteries[4]. Conduit arteries, *e.g.*, femoral, radial and brachial arteries are the subdivisions of conducting arteries, and their role is regulating the flow of blood to particular organs and sections of the body[5]. Conduit arteries advance more through separating into resistance arteries that mainly consist of smooth muscles and are highly innervated by sympathetic nerves. Resistance vessels regulate the blood flow to tissues through constricting or dilating as reaction to sympathetic simulation or dissimulation[6].

Hypoxic pulmonary vasoconstriction (HPV) is a fundamental physiological mechanism to redirect the blood from poorly to better-aerated areas of lungs to optimize the ventilation perfusion matching[7]. Persistent hypoxia leads to increased pulmonary vascular opposition and right ventricular afterload that leads to hypoxic pulmonary hypertension[8]. HPV initially thought to be caused by alveolar hypoxia by means of local lung mechanism but recent advances suggest that PA smooth muscle cells constitute both the sensor and the transducer of the hypoxic signal as well as its contractile effector[9]. A series of experiments performed to explain the phenomenon on macroscopic and microscopic level has been reported although the underlying mechanism is not clear[10-12]. However, vast majority of experiments performed in animals with little data available from humans. Experiments performed on animals are generally inapplicable on humans so we need to adapt new methodologies for use in human to understand the human disease biology.

The objective of this research is assessing the tension in human PA to facilitate future experiments and also to provide a methodology of isolation of PA and their use in studies in the form of arterial rings.

MATERIALS AND METHODS

All patients undergoing a lung lobectomy by a Consultant Cardiothoracic Surgeon at Castle Hill Hospital were consented for resected lung tissue to be included in this study prior to their operation at the time of their consent for surgery. Patients under the age of 18 and who cannot give informed consent were excluded from the study. Local research ethics committee and local research and development department approval was obtained for the use of human tissue for this study.

Isolation of PA rings

Tissue samples were collected from patients undergoing surgical lung resection for cancer and immediately moved to the laboratory in Krebs-Henseleit solution (consisting of 113.8 mmol/L NaCl, 4.7 mmol/L KCl, 1.2 mmol/L $MgSO_4$, 25 mmol/L $NaHCO_3$, 1.2 mmol/L KH_2PO_4, 11.4 mmol/L glucose, and 2.4 mmol/L $CaCl_2$ dissolved in distilled water). Pulmonary arteries were

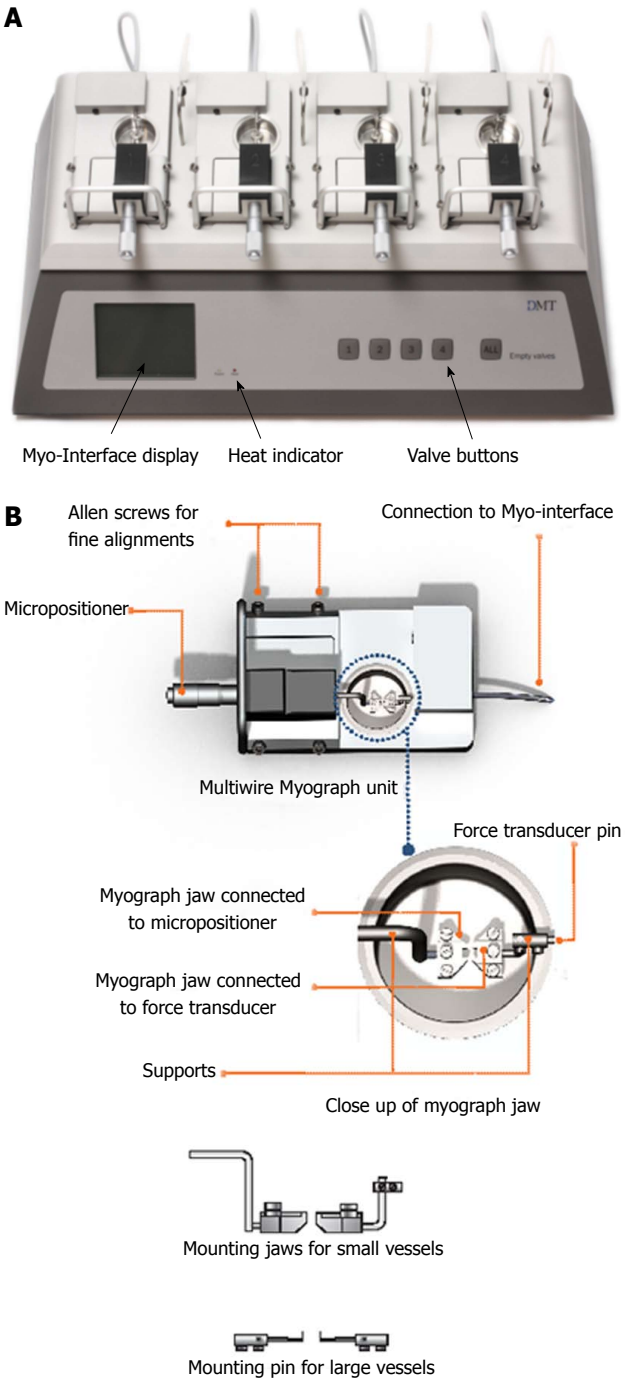

Figure 1 Multiwire Myograph System (DMT 620 M) (A) and Multiwire Myograph Unit (B).

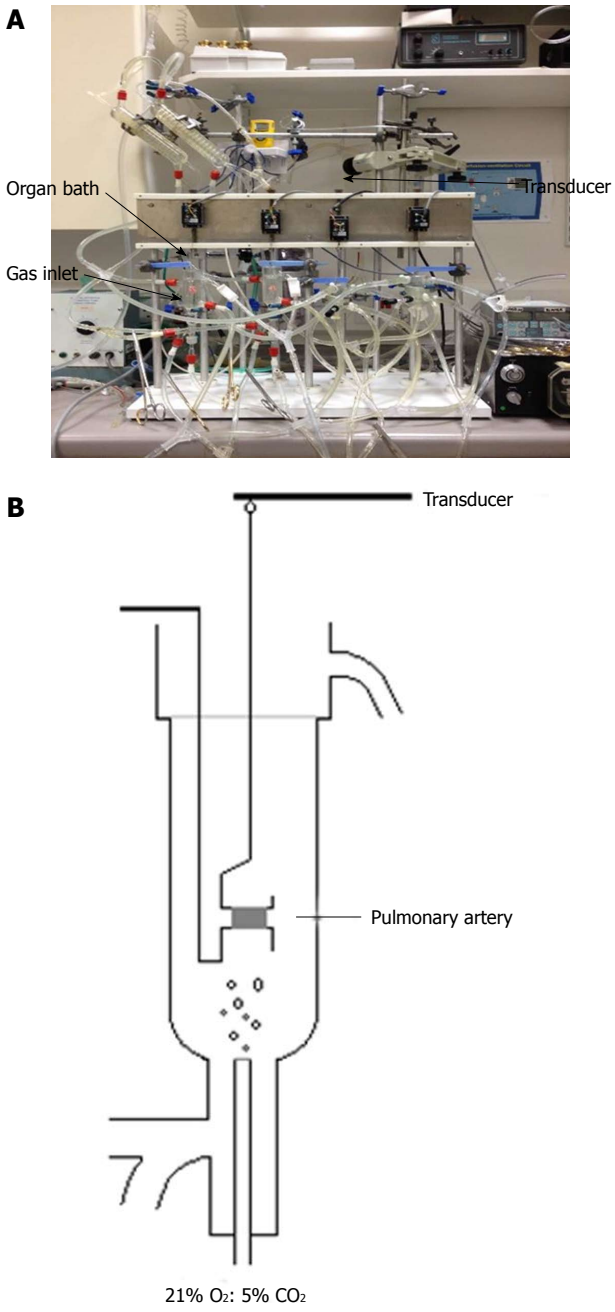

Figure 2 Radnotti (A) and Schematic (B) Organ Bath system.

dissected from disease free areas of lung resection and after careful removal of adipose and connective tissues cut into 2 mm long rings. The Internal diameter of vessels ranged between 2-4 mm.

Mounting of PA rings

A multiwire myograph system (DMT 620M) and an organ bath system (Radnotti) were used for mounting of PA rings and measurement of ORT. The Multi wire myograph system consists of 4 individual myograph units. Each unit is created with aluminum and has a centralized placement of 8 mL stainless steel chamber (Figure 1A). Pins to support the tissue were placed within the chamber, one end being connected to a force transducer whilst the other connected with a micrometer. PA rings were mounted between the pins. All units were subject to administered gas inflow and suction. Connections for vacuum and gassing, as well as heating are provided in the myograph interface, allowing for all chambers to be smoothly maintained under physiological settings (37 ℃, and bubbled with 21% O_2: 5% CO_2) (Figure 1B). The myograph system was connected to a PC *via* an amplifier (Power Lab 8/35, AD Instruments) for continuous measurement of isometric tension using data acquisition software (Lab

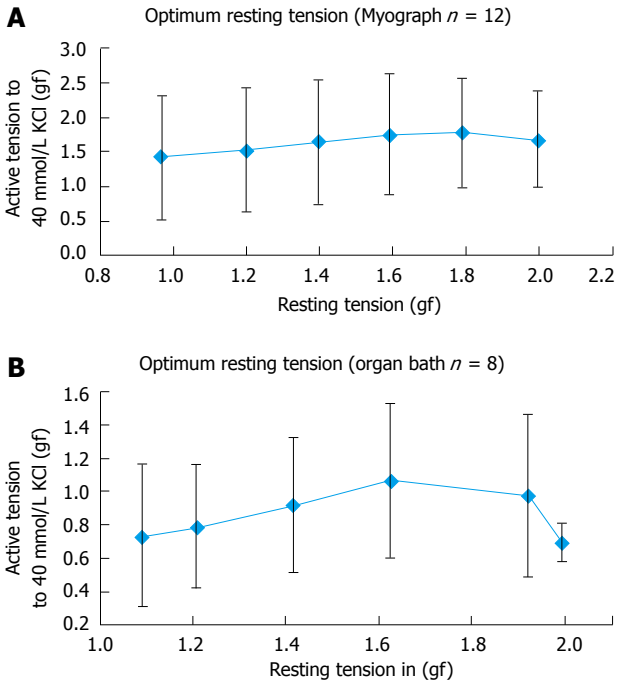

Figure 3 Measurement of Optimal Resting Tension using Multi-wire Myograph (A) and Organ Bath system (B). A: Total 12 PA rings from four patients were used to perform the experiment. Increasing the resting tension from 1.0 gf to 1.6 gf significantly augmented the 40 mmol/L KCl induced active tension. Increasing the active tension from 1.6 to 2.0 gf initially plateaued off than decreased the 40 mmol/L KCl induced response; B: Total 8 PA rings from four patients were used to perform the experiment. Increasing the resting tension from 1.0 to 1.6 gf significantly augmented the 40 mmol/L KCl induced active tension. Increasing the active tension from 1.6 to 2.0 gf either decreased the 40 mmol/L KCl induced response.

Chart Pro Version 8.0).

The organ bath system consists of 4 organ baths connected to a gas inlet where gas mixtures can be bubbled through (Figure 2A). Surrounding each bath is a heat exchanger that recreated the physiological temperatures of the human body. Each organ bath contained Krebs's solution and the PA rings were mounted between two hooks. One hook was fixed and the other connected with a force transducer (Harvard UF1), which was linked to a PC for continuous measurement of isometric tension (Figure 2B).

Determination of optimal resting tension

After mounting of PA rings the resting tension was set at 1 gf and the vessels left to equilibrate under 21% O_2: 5% CO_2 at 37 ℃ for 60 min. When a stable resting tension was achieved the vessels were contracted to 40 mmol/L KCl by direct addition to the organ bath. The maximum contraction to KCl was recorded when the contractile response reached a plateau. Active tension was calculated as maximum tension at plateau (gf) - resting tension (gf). Vessels were then washed for 30 min by rapidly replacing the Krebs solution in the chambers with fresh solution three times every five minutes. When a stable resting tension was achieved a repeat reaction with 40 mmol/L KCl was obtained and the vessels again washed before obtaining a third

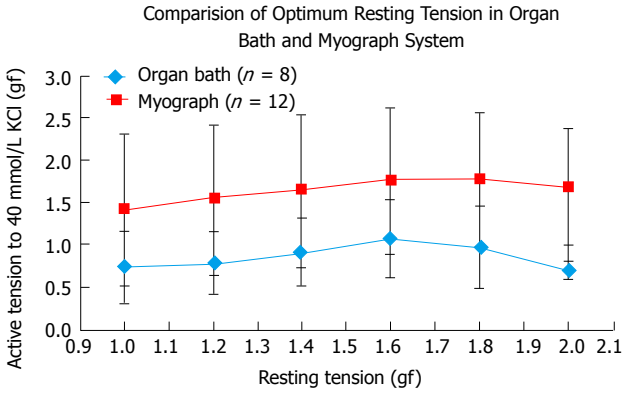

Figure 4 Comparison of Optimal Resting Tension measurement in Organ Bath and Myograph system. Total 20 PA rings from four patients were used to perform the experiment. Increasing the resting tension from 1.0 to 1.6 gf significantly augmented the 40 mmol/L KCl induced active tension. Increasing the active tension from 1.6 to 2.0 gf either decreased or plateaued off the 40 mmol/L KCl induced response. Both organ bath and myograph shows similar result and confirmed that radial optimal resting tension for human pulmonary artery ring was 1.61 g.

reaction to 40 mmol/L KCl for the purpose of confirming reproducibility in the response. When a reproducible response was obtained the maximum contraction to 40 mmol/L KCl had been established from increasing resting tensions of 1.2, 1.4, 1.6, 1.8 and 2.0 gf with the vessels being washed for 30 min between responses.

At the end of each experiment the integrity of endothelium was confirmed by the addition of 1 umol/L acetylcholine. Rings that did not contract to KCl were excluded from the study.

Chemicals and reagents

Five percent of carbon dioxide/balance air (10 lt cylinders) was sourced from BOC Limited. All reagents were obtained from Fischer Scientific and acetylcholine from Sigma Aldrich.

Statistical analysis

Data are presented as mean ± SD and n represents the number of PA rings used.

RESULTS

Twenty PA rings (internal diameter 2-4 mm) were obtained from 4 patients. Results showed that in human PA rings increasing the basal tension from 1.0 to 1.6 gf significantly augmented the 40 mmol/L KCl induced active tension. Increasing the active tension from 1.6 to 2.0 g mitigate the 40 mmol/L KCl induced response (Figure 3). The myograph and organ bath demonstrated identical conclusions (Figure 4), confirming that the most efficient resting tension for human PA rings is 1.61 gf (Figure 5).

DISCUSSION

The pulmonary circulation carries deoxygenated blood from right section of heart towards lungs, under which

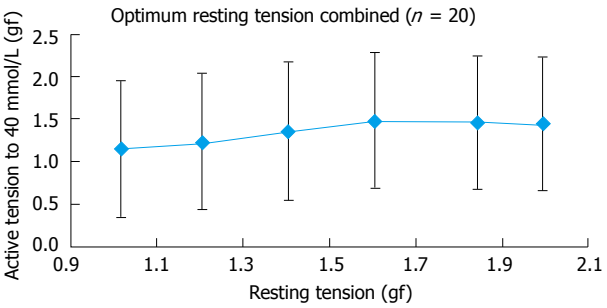

Figure 5 Combined result of optimal resting tension measurement. Total 20 PA rings from four patients were used to perform the experiment. Increasing the active tension from 1.6 to 2.0 gf decreased the 40 mmol/L KCl induced response. The radial optimal resting tension for human pulmonary artery ring measured was 1.61 g. PA: Pulmonary artery.

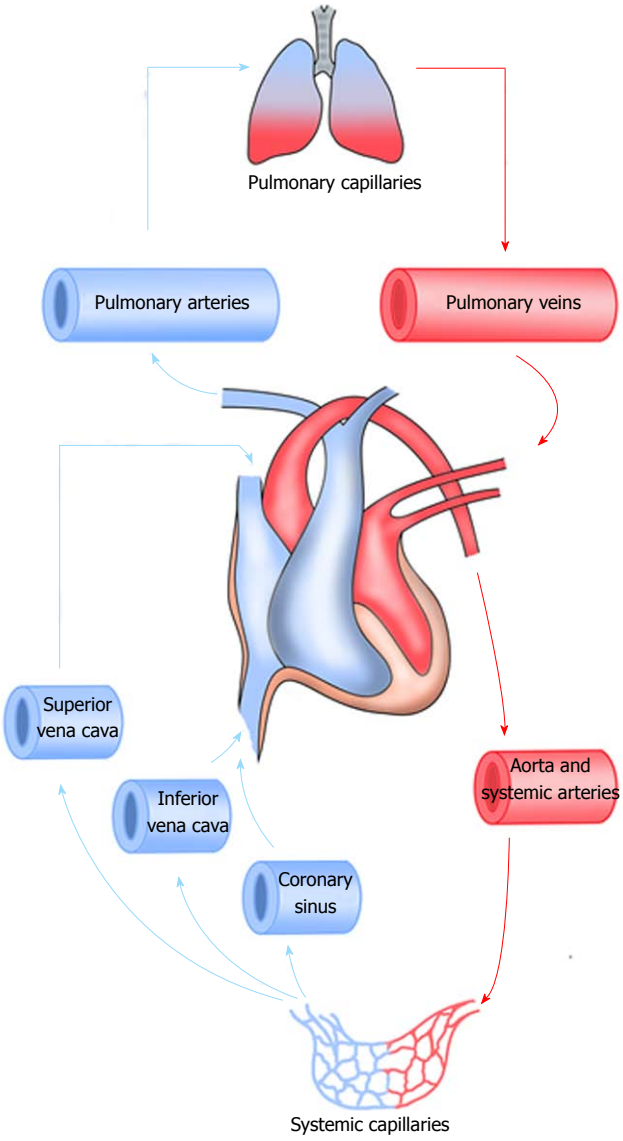

Figure 6 Schematic representation of pulmonary circulation.

it is subject to oxygenation while carbon dioxide is filtered, thereafter returning the clean blood onto the left section of the heart prepared for dissemination[13] (Figure 6). The pulmonary circulation is in series and reliant not only on the systemic blood flowing to right section of the heart, rather also the outflow from the left section[14]. Therefore, in case of an increment under the left atrium pressure or increase in afterload like in aortic stenosis, greater pressure will be observed in the PA[15]. PA vasoconstriction is an important physiological process to regulate blood flow in lungs but it also results in pathologies. Various models are utilized for assessing the baseline molecular and cellular functions of lung ailments, particularly pulmonary vascular affliction. However, a great deal of researches is undertaken on animals with little similarity to humans. Few centers have the luxury to utilize human tissue to study this phenomenon. Isolation of human PA and measurement of pulmonary vascular tension are vital to understand the pathophysiology of human pulmonary vessels. The objective behind this research is to assess the optimal resting tension for undertaking studies on human PA rings.

COMMENTS

Background

Pulmonary artery (PA) vasoconstriction is an important physiological process to regulate blood flow in the lungs but it also manifests in pathological conditions. Isolation of human PA and measurement of pulmonary vascular tension are vital to understand the human pulmonary vessels disease especially pulmonary hypertension.

Research frontiers

Further research is required to confirm the conclusion of this research, and also to evaluate if whether the optimum tension varies between various sizes of pulmonary arteries.

Innovations and breakthroughs

The authors yields the base optimal resting tension (ORT) for conducting studies on human PA rings and the ORT measured was 1.61 gf (15.78 mN) for vessels with internal diameter ranged between 2-4 mm.

Applications

This study provides a baseline ORT to facilitate future experiments on human PA rings and also provide a methodology of isolation of PA and their use in studies in the form of arterial rings.

Terminology

Pulmonary hypertension is a hemodynamic state elaborated by defined by a resting mean PA pressure at or above 25 mmHg.

Peer-review

It is a valuable paper for physiology and pathology pulmonary arteries. The system will provide a basic for further research about pulmonary arteries and its-related diseases.

REFERENCES

1 **Levick JR**. An introduction to cardiovascular physiology. 4th ed. London: Arnold; New York: Distributed in the United States of America by Oxford University Press, 2003
2 **Galley HF**, Webster NR. Physiology of the endothelium. *Br J Anaesth* 2004; **93**: 105-113 [PMID: 15121728 DOI: 10.1093/bja/aeh163]
3 **O'Brien SF**, McKendrick JD, Radomski MW, Davidge ST, Russell JC. Vascular wall reactivity in conductance and resistance arteries:

differential effects of insulin resistance. *Can J Physiol Pharmacol* 1998; **76**: 72-76 [PMID: 9564552 DOI: 10.1139/y97-186]
4 **McEniery CM**, Wilkinson IB, Avolio AP. Age, hypertension and arterial function. *Clin Exp Pharmacol Physiol* 2007; **34**: 665-671 [PMID: 17581227 DOI: 10.1111/j.1440-1681.2007.04657.x]
5 **Pugsley MK**, Tabrizchi R. The vascular system. An overview of structure and function. *J Pharmacol Toxicol Methods* 2000; **44**: 333-340 [PMID: 11325577 DOI: 10.1016/S1056-8719(00)00125-8]
6 **Baumbach GL**, Heistad DD. Effects of sympathetic stimulation and changes in arterial pressure on segmental resistance of cerebral vessels in rabbits and cats. *Circ Res* 1983; **52**: 527-533 [PMID: 6851007 DOI: 10.1161/01.RES.52.5.527]
7 **Ward JP**, McMurtry IF. Mechanisms of hypoxic pulmonary vasoconstriction and their roles in pulmonary hypertension: new findings for an old problem. *Curr Opin Pharmacol* 2009; **9**: 287-296 [PMID: 19297247 DOI: 10.1016/j.coph.2009.02.006]
8 **Maggiorini M**, Mélot C, Pierre S, Pfeiffer F, Greve I, Sartori C, Lepori M, Hauser M, Scherrer U, Naeije R. High-altitude pulmonary edema is initially caused by an increase in capillary pressure. *Circulation* 2001; **103**: 2078-2083 [PMID: 11319198 DOI: 10.1161/01.CIR.103.16.2078]
9 **Wang L**, Yin J, Nickles HT, Ranke H, Tabuchi A, Hoffmann J, Tabeling C, Barbosa-Sicard E, Chanson M, Kwak BR, Shin HS, Wu S, Isakson BE, Witzenrath M, de Wit C, Fleming I, Kuppe H, Kuebler WM. Hypoxic pulmonary vasoconstriction requires connexin 40-mediated endothelial signal conduction. *J Clin Invest* 2012; **122**: 4218-4230 [PMID: 23093775 DOI: 10.1172/JCI59176]
10 **Ariyaratnam P**, Loubani M, Morice AH. Hypoxic pulmonary vasoconstriction in humans. *Biomed Res Int* 2013; **2013**: 623684 [PMID: 24024204 DOI: 10.1155/2013/623684]
11 **Swenson ER**. Hypoxic pulmonary vasoconstriction. *High Alt Med Biol* 2013; **14**: 101-110 [PMID: 23795729 DOI: 10.1089/ham.2013.1010]
12 **Lumb AB**, Slinger P. Hypoxic pulmonary vasoconstriction: physiology and anesthetic implications. *Anesthesiology* 2015; **122**: 932-946 [PMID: 25587641 DOI: 10.1097/ALN.0000000000000569]
13 **Comroe JH**. The main functions of the pulmonary circulation. *Circulation* 1966; **33**: 146-158 [PMID: 5322600 DOI: 10.1161/01.CIR.33.1.146]
14 **Guazzi M**, Arena R. Pulmonary hypertension with left-sided heart disease. *Nat Rev Cardiol* 2010; **7**: 648-659 [PMID: 20924360 DOI: 10.1038/nrcardio.2010.144]
15 **Hunt JM**, Bethea B, Liu X, Gandjeva A, Mammen PP, Stacher E, Gandjeva MR, Parish E, Perez M, Smith L, Graham BB, Kuebler WM, Tuder RM. Pulmonary veins in the normal lung and pulmonary hypertension due to left heart disease. *Am J Physiol Lung Cell Mol Physiol* 2013; **305**: L725-L736 [PMID: 24039255 DOI: 10.1152/ajplung.00186.2013]

P- Reviewer: Landesberg G, Tang JM **S- Editor**: Ji FF
L- Editor: A **E- Editor**: Wu HL

Published by **Baishideng Publishing Group Inc**
8226 Regency Drive, Pleasanton, CA 94588, USA
Telephone: +1-925-223-8242
Fax: +1-925-223-8243
E-mail: bpgoffice@wjgnet.com
Help Desk: http://www.wjgnet.com/esps/helpdesk.aspx
http://www.wjgnet.com